Molecular mechanisms of Ca2+-dependent neuropeptide secretion

van Westen-Erbrink, Rhode Mirjam

2021

document version
Publisher's PDF, also known as Version of record

Molecular Mechanisms of Ca^{2+}-dependent Neuropeptide Secretion

RHODÉ VAN WESTEN-ERBRINK

The research described in this thesis was conducted at the department of Functional Genomics, Center for Neurogenomics and Cognitive Research, Neuroscience Campus Amsterdam, VU University Amsterdam, The Netherlands

Illustrations and cover: S. Kloppenburg, Glitterende Eenhoorn
Printed by: Studio Proefschrift

Printing of this thesis was financially supported by the CNCR.

VRIJE UNIVERSITEIT

Molecular mechanisms of Ca^{2+}-dependent neuropeptide secretion

ACADEMISCH PROEFSCHRIFT

ter verkrijging van de graad Doctor of Philosophy aan
de Vrije Universiteit Amsterdam,
op gezag van de rector magnificus
prof.dr. V. Subramaniam,
in het openbaar te verdedigen
ten overstaan van de promotiecommissie
van de Faculteit der Geneeskunde
op donderdag 9 september 2021 om 9.45 uur
in de aula van de universiteit,
De Boelelaan 1105

door

Rhodé Mirjam van Westen-Erbrink

geboren te Renkum

promotor:	prof.dr. M. Verhage
copromotor:	dr. R.F.G. Toonen

Doctorate board: prof.dr. P. Burbach
prof.dr. H. Mansvelder
prof.dr. J. Sørensen
dr. C. Dean
dr. S. Groffen

CONTENTS

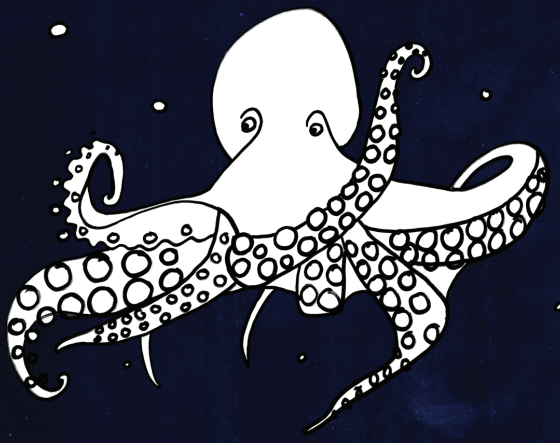

Chapter 1

General introduction

GENERAL INTRODUCTION

Fast and slow neuronal communication

We navigate through a complicated and demanding environment by using our sophisticated ability to perceive and integrate sensory information on a millisecond time-scale. This is powered by a fine-tuned network of billions of neurons in our brain, which receive, integrate and propagate information. Neuronal communication relies on the release of fast signaling molecules, neurotransmitters, from synaptic vesicles (SVs). In addition virtually all neurons release neuropeptides and express a variety of neuropeptide receptors (Smith et al., 2019). Neuropeptides, which include neurotrophins and neuromodulators, are slow signaling molecules that control neuronal communication. Will a neuron propagate an action potential, grow a new neurite, or make new connections? Neuropeptides contribute to all of these processes. Hereby, neuropeptides significantly alter neuronal circuitry output (for review, see Marder, 2012), and contribute to information processing in the brain. Neuropeptides are involved in a large variety of physiological conditions, such as reward, food intake, learning and memory, social behaviors, reproduction and metabolism. Moreover, they are implicated in pathological states, such as obesity, addiction, PTSD, autism, depression, and schizophrenia (for reviews, see Koob and Volkow, 2010; Meyer-Lindenberg et al., 2011; Schwartz et al., 2000; Tasan et al., 2016). Despite their indisputable importance, neuropeptide secretion remains understudied and secretory mechanisms are poorly understood. The research presented in this dissertation aims to contribute to the understanding of the molecular mechanisms that underlie the regulated secretion of neuropeptides.

Neuropeptide functions

From an evolutionary perspective, neuropeptides have an early origin and precede synaptic neurotransmission (for review, see Grimmelikhuijzen et al., 1999). Neuropeptide precursors are already present in the neuronless organism *Trichoplax adhaerens* (Jékely, 2013), and in lower animals such as corals and sea anemones intercellular communication is peptidergic (for review, see Grimmelikhuijzen et al., 1996). Neuropeptide signaling is not only ancient, but also highly diverse: the term 'neuropeptides' denotes a large (>100) group of peptidergic signaling molecules, secreted from large dense-core vesicles (DCVs) in mammals (for an overview, visit the neuropeptide database www.neuropeptides.nl or see Burbach, 2011). Neuropeptides typically consist of 3-40 amino acid residues (the product of proteolytic processing of larger precursor molecules) and are aggregated into

an electron-dense core, after which a DCV is named. Upon release, neuropeptides act on a time scale of seconds, which can be partially explained by the fact that nearly all neuropeptides engage G-protein coupled receptors (GPCRs) (Hewes and Taghert, 2001). Neuropeptides can target multiple GPCRs, e.g., neuropeptide Y activates a total of 5 different receptors, each having different kinetics, interactions and signaling cascades (for review, see Holliday et al., 2004). The diversity of both neuropeptides and neuropeptide receptors affords a large functional diversity, and neuropeptide signaling cascades are only beginning to be understood. To illustrate their importance, some examples will be highlighted in the following sections.

Modulators of neurotransmission

One of the most well-known and important actions of neuropeptide signaling, is their neuromodulatory action. Neuromodulators do not necessarily transfer an excitatory or inhibitory signal from one neuron to another, but rather alter cellular and synaptic properties, thereby modulating neurotransmission. For example, NPY activates Y2 receptors in the hippocampus, which attenuate the glutamate release probability by suppressing Ca^{2+} influx via N- and P/Q-type Ca^{2+} channels (see for a review Tasan et al., 2016). Lower Ca^{2+} levels result in a dampened response to incoming input. Hereby, NPY substantially reduces neuronal excitability. The functional relevance of this mechanism becomes clear during seizures, which lead to NPY upregulation (Dubé, 2007). NPY-deficient mice have a kainic acid-induced seizure mortality rate of 93%, whereas death is rarely observed in WT littermates (Baraban et al., 1997). The phenotype could be fully rescued by pre-exposure to NPY (Baraban et al., 1997). Therefore, NPY regulates neuronal excitability, a property that is important for survival. This action of NPY is one of many examples where the neuromodulatory role of neuropeptides is key for maintaining a healthy excitatory/inhibitory balance.

Neurotrophic factors

Neurotrophins are implicated in neuronal proliferation, differentiation, survival and outgrowth, and include nerve growth factor (NGF), brain-derived neurotrophic factor (BDNF), and neurotrophin-3. These neurotrophins act on Trk receptors: TrkA, TrkB and TrkC, respectively. BDNF, for example, is known for its role in neuronal development, survival and synaptic plasticity (for reviews, see Miranda et al., 2019; Vicario-Abejón et al., 2002). Mood disorders, such as major depression, are linked to a reduction in BDNF levels and BDNF/TrkB signaling, and treatment with antidepressants increases BDNF levels (Nibuya et al., 1995). Moreover, double knockout (DKO) of TrkB receptor subunits

Gαi1 and Gαi3 reduces TrkB signaling, dendritic branching, and synapse numbers, and induces depressive behaviors in mice (Marshall et al., 2018). These results suggest that neurotrophin signaling cascades are essential for maintaining the healthy neuronal architecture necessary for promoting mental health.

Long range hormones

Upon release, neuropeptides can act locally or over long distances. Long-range signaling may occur in the brain by means of volume transmission (for review, see van den Pol, 2012), although the actual distance is under debate (e.g. see Chini et al., 2017 for review). Long-range signaling is evident in cases where neuropeptides are released into the bloodstream, acting as hormones. One well-studied example of a neuropeptide hormone is oxytocin (OXT). OXT is produced in the paraventricular nucleus (PVN) and supraoptic nucleus (SON), from which axons project to the pituitary to release OXT into the bloodstream to induce labour, among others (Brownstein et al., 1980). Additionally, OXT acts locally when released in the supraoptic nucleus, where it is released during parturition and facilitates its own release via a receptor-mediated positive feedback loop (Neumann et al., 1996). Therefore, neuropeptides can act locally and as long-range hormones depending on their release site.

Protein delivery to cell surface

In addition to vesicle cargo release, DCVs are hypothesized to deliver GPCRs, ion channels, and other transmembrane proteins to the plasma membrane upon fusion. This is supported by the discovery that in dorsal root ganglia at least, the membranes of DCVs contain a variety of GPCRs and ion channels (Zhao et al., 2011). Although GPCR sorting and delivery has been studied (Hanyaloglu and von Zastrow, 2008), GPCR delivery by DCV fusion specifically has not received a lot of attention in the field, and experimental evidence is currently sparse.

Neuropeptides as neurotransmitters

Although the vast majority of neuropeptides act on GPCRs, neuropeptides can also act on ionotropic receptors (for review, see DeLaney et al., 2018). For example, the invertebrate neuropeptide Phe-Met-Arg-Phe-NH2 (FMRFamide) binds to a Na^+-gating ion channel, resulting in an inward Na^+ current, independent of GPCR signaling (Lingueglia et al., 1995). Therefore, neuropeptides can act as transmitter molecules that directly contribute to neurotransmission.

There is considerable cross-regulation between neurotransmitters and neuropeptides. For example, NPY modulates neurotransmission via presynaptic Y2 receptors,

which inhibit release of the neurotransmitter norepinephrine (NE) (see for a review Bartfai et al., 1988; Westfall et al., 2006). As NPY requires a stronger stimulation for release than NE, this cross-regulation is of physiological significance to put a ceiling to NE release at higher frequencies (for review, see Bartfai et al., 1988). In other examples of cross-regulation, neuropeptides can modulate the affinity or availability of neurotransmitter receptors, or inhibit endopeptidases that degrade neuropeptides in the extracellular space (for review, see Bartfai et al., 1988). Importantly, neurotransmitter/neuropeptide cross-regulation can be a therapeutic target, but also a suspect for the side-effects of monoamine antidepressants, such as clozapine (for review, see Bartfai et al., 1988).

Neuromodulators and disease

Disruptions in neuropeptide systems are associated with many pathological states, such as addiction, stress, major depression, schizophrenia, obesity and anorexia, antisocial behaviors and anxiety (for reviews, see Kormos and Gaszner, 2013; Kovac and Walker, 2013; Ogren et al., 2010; van den Pol, 2012). Expectedly, several neuropeptides receive considerable attention as therapeutic targets, including neuropeptide Y to treat PTSD (NIH Clinical Trial ID number NCT01533519), mood disorders (NCT00748956) and Type II diabetes mellitus (NCT02639637), and oxytocin as treatment of autism (i.e. NCT01944046, NCT01788072, NCT01908205, NCT01256060), alcohol dependence (i.e. NCT03046836, NCT03339024), migraine (NCT01839149), depression (i.e. NCT03566069), and many others.

Taken together, neuropeptide actions are diverse, complex, of great physiological relevance and are therapeutic targets for a variety of diseases. However, neuropeptides remain relatively understudied and their release mechanisms are poorly understood. Increasing our knowledge about neuropeptide signaling pathways and release mechanisms contributes to development of new drug targets and may increase success rates of clinical trials.

Dense-core vesicles

Biogenesis and maturation

An average cultured hippocampal neuron is estimated to contain between 1.400 – 18.000 DCVs (Persoon et al., 2018). To achieve this, DCVs are *de novo* synthesized at the Golgi. Here, neuropeptide precursor proteins (pre-pro-neuropeptides) are sorted and packaged into large DCVs of ~70 nm diameter. Notably, DCVs can also contain neurotransmitters and monoamine transmitters, such as acetylcholine

(ACh), norepinephrine (NE), dopamine (DA), and serotonin (5-HT) (for review, see Merighi, 2018).

DCVs bud from the trans-Golgi network (TGN) as immature organelles (see for a review Kim et al., 2006). Maturation of DCVs includes processing of the immature pre-pro-neuropeptides into one or multiple biologically active neuropeptides by prohormone convertases (see Burbach, 2011 for review of cleavage products per precursor). An acidic vesicle lumen (pH 5.0-6.0) is required for enzymatic processing, which is accommodated by proton pumps in the vesicle membrane, the V/H ATPases (e.g. Helwig et al., 2011; Saw et al., 2011). Additional DCV maturation may involve reorganization of its membrane. This is supported by the observation that Secretogranin, a DCV marker protein, distributes to heavier sucrose fractions over time in density gradients of PC12 cell subcellular fractionations, suggesting post-Golgi budding processing of DCVs (Tooze et al., 1991). This processing may happen via (1) homotypic fusion, a process that may involve Synaptotagmin-4 (Ahras et al., 2006), (2) heterotypic fusion with endosomes (Topalidou et al., 2016), and/or (3) clathrin-mediated removal of proteins and lipids (for review, see Kim et al., 2006). However, as most experiments are performed *ex vivo* and in non-neuronal cell types, it remains uncertain whether these maturation mechanisms occur in (intact) neurons as well.

Trafficking

A hippocampal neuron contains approximately 2-3 DCVs per synapse (Persoon et al., 2018). To achieve this, DCVs travel back and forth throughout the axons and dendrites along microtubule tracks. This is an energy demanding process, requiring ATP hydrolysis for motor proteins such as axonal KIF1A and dynein to conduct anterograde and retrograde transport, respectively (for review, see Hoogenraad and Akhmanova, 2016; Lo et al., 2011). DCVs that approach a synaptic bouton reduce trafficking speed, possibly promoting synaptic capture (Knabbe et al., 2018). The continuous flow of DCVs with low-probability capture by synaptic boutons is suggested to ensure an even distribution of vesicles throughout the axon (Wong et al., 2012), similar to a conveyer belt in a sushi restaurant (for review, see Moughamian and Holzbaur, 2012).

Trigger for fusion

A presynapse contains several hundreds of SVs, whereas they contain only a few DCVs (Persoon et al., 2018). DCVs often reside outside the active zone, at the periphery of the synaptic vesicle cluster (Verhage et al., 1991). SVs fuse in response to a single action potential. DCV fusion typically requires a stronger physiological

trigger, such as a tetanic burst or prolonged high frequency stimulation (Dutton and Dyball, 1979; Gainer et al., 1986; Persoon et al., 2018). High-frequency trains of action potentials with spaced intervals are most efficient in triggering DCV fusion, whereas application of a single action potential does not efficiently trigger DCV fusion (Balkowiec and Katz, 2000; Hartmann et al., 2001; Matsuda et al., 2009; Persoon et al., 2018). Related, a single action potential elicits a transient increase in intracellular Ca^{2+}, whereas methods capable of triggering DCVs fusion – high-frequency

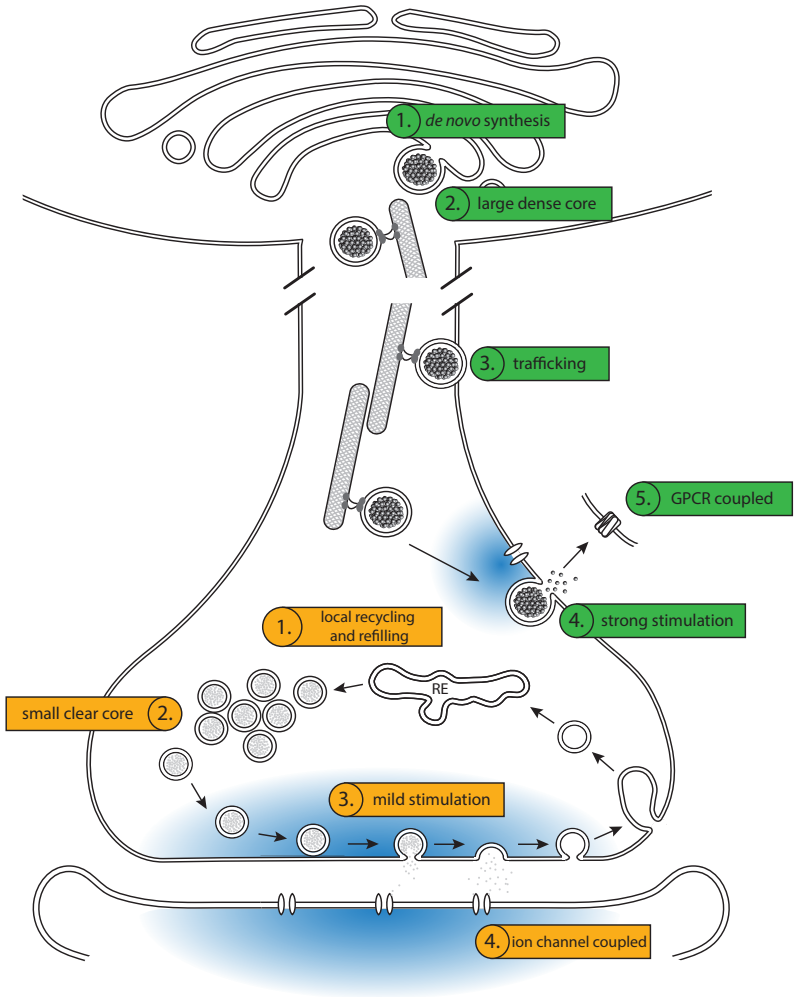

Figure 1: DCV biogenesis and fusion vs. SV recycling and fusion. DCVs differ from SVs with respect to their morphology, de novo biogenesis, active axonal and dendritic trafficking, target receptors, and required stimulation, as highlighted by the green and orange boxes for DCVs and SVs, respectively.

burst stimulation, bath application of potassium chloride or ionomycin – increase Ca^{2+} levels for a sustained period of time (Persoon et al., 2018).

In response to intense high-frequency stimulation, only several hundreds of DCVs fuse per neuron, which is a small number compared to SV fusion. In addition to a smaller DCV pool – a thousand to several thousands per neuron (Persoon et al., 2018), the low DCV release numbers may be a consequence of a more distant localization from Ca^{2+} channels compared to SVs. Despite equal distribution among dendrites and axons, fusion occurs predominantly in axons (Persoon et al., 2018), where they can fuse in- and outside synapses (Wit et al., 2009). In comparison with neurotransmitters, relatively few neuropeptides are released. Released neuropeptides are degraded by circulating or membrane-bound endopeptidases (Rose et al., 2009). However, neuropeptides bind to GPCRs with nanomolar affinities, whereas neurotransmitters bind to their ion channels with relatively low affinity (i.e. ~10-100 μM for ACh receptors) (Purohit and Grosman, 2006). Therefore, neuropeptides can be potent modulators of network activity even at low quantities.

This, together with the above described differences in *de novo* biogenesis, vesicle morphology and cargo, and target receptors, shows that DCV fusion is a fundamentally different mode of neuronal communication than SV fusion (Figure 1).

Cellular Ca^{2+} gradient and Ca^{2+} effectors

Neurons invest a considerable amount of energy in the maintenance of a 20.000-fold Ca^{2+} gradient across the plasma membrane. This gradient allows cells to use transient increases in intracellular Ca^{2+} as signals to regulate a large range of cellular functions, including neurotransmitter and neuropeptide release. A low intracellular Ca^{2+} concentration of 50-100 nM is maintained through Ca^{2+} cellular ion pumps (Ca^{2+} pumps and Na^{+}/Ca^{2+}-exchangers) (Helmchen et al., 1997; Maravall et al., 2000), sequestering free Ca^{2+} into mitochondria, the endoplasmic reticulum (ER), and in lysosomes, and through binding to Ca^{2+}-buffering proteins, such as calmodulin, calbindin, calretinin and parvalbumin. Cytosolic Ca^{2+} can increase through opening of voltage-gated Ca^{2+} channels (VGCCs) and receptor-operated channels with Ca^{2+} permeability, such as N-methyl-D-aspartate receptors (NMDARs) and Ca^{2+} permeable α-amino-3-hydroxy-5-methyl-4-isoxazolepropionic acid receptor (AMPARs). Moreover, Ca^{2+} can enter the cytosol via release of intracellular stores through ryanodine receptors and inositol-3-phosphate receptors.

In the presynaptic terminal, Ca^{2+} levels in close vicinity of Ca^{2+} channels (10-100 nm, called a nanodomain), can quickly rise from 50-100 nM to 100 μM after a single action potential. Outside the nanodomain, the global Ca^{2+} levels can increase up

to 1.5 µM during a 100 Hz stimulus train (for review, see Neher and Sakaba, 2008). The residual Ca^{2+} concentration, which is Ca^{2+} remaining after buffering and VGCCs closure, is low (10-100 nM) but can remain up to a second, and contributes to short-term plasticity (for review, see Regehr, 2012).

Ca^{2+} binding proteins are abundant in the presynapse, and neuronal activity activates an array of sensors that trigger downstream signaling pathways. Three major classes of calcium sensors are Annexins, EF-hand Ca^{2+} sensors, and C2 domain proteins. Annexins, also known as Lipocortins, possess Ca^{2+} dependent lipid binding domains, and regulate membrane structure. Annexin A2, for example, is recruited to membranes upon Ca^{2+} binding (for review, see Rescher and Gerke, 2004). Here, it serves as F-actin assembly platform and may stabilize lipid rafts (for review, see Rescher and Gerke, 2004). Another group of calcium sensors are the EF-hand proteins. EF-hand proteins are involved in a variety of functions, such as buffering (e.g. Calbindin) and cell signaling (e.g. Calmodulin) (for review, see Yáñez et al., 2012). A particularly large family of Ca^{2+} sensors is the family of C2-domain proteins. In addition to Synaptotagmins, this family includes Protein Kinase C, phospholipase C, Synaptotagmin-like proteins (SLPs), extended Syts (E-Syts), and many others. Moreover, C2 domains are present on Munc13 which may facilitate bridging of membranes (Brose et al., 1995; Liu et al., 2020), and on CAPS - a vesicle priming protein for which the Ca^{2+} dependent function is currently unknown (for review, see Martin, 2015). C2 domains often contain negative aspartate residues that together can bind up to three Ca^{2+} ions (Ubach et al., 1998). Upon Ca^{2+} binding, some C2 domains get embedded into negatively charged phospholipids, such as phosphatidylserine and phosphatidylinositol, resulting in lipid splaying and membrane curvature (for review, see McMahon et al., 2010). The combination of lipid splaying and Ca^{2+} sensing makes C2-domain containing proteins perfect candidates for the regulation of membrane fusion. The following sections focus on calcium sensors that are directly related to exocytosis: Synaptotagmin (Syt) and Double-C2 domain proteins (Doc2).

The fusion machinery

The SNARE complex and Sec/Munc proteins

Fusion of the vesicle membrane with the plasma membrane is an energetically demanding process due to the repulsive electrostatic forces between the two membranes and other factors, such as water molecules trapped between the two bilayers. Vesicle fusion is driven by the coordinate action of a set of proteins, called the fusion machinery.

The main components of the fusion machinery are Soluble NSF attachment receptor (SNARE) proteins. In neurons, SNARE proteins for synchronous SV fusion are SNAP-25, VAMP2 and Syntaxin-1 (for reviews, see Jahn and Fasshauer, 2012; Südhof and Rothman, 2009), and SNAP-25 and VAMP2 are also identified as regulators of DCV fusion (Arora et al., 2017; Hoogstraaten et al., 2020; Shimojo et al., 2015). SNARE proteins form a parallel four-helix bundle, which generates energy that is most likely used for fusion of the two membranes (Figure 2) (Gao et al., 2012; Min et al., 2013; Sørensen et al., 2006).

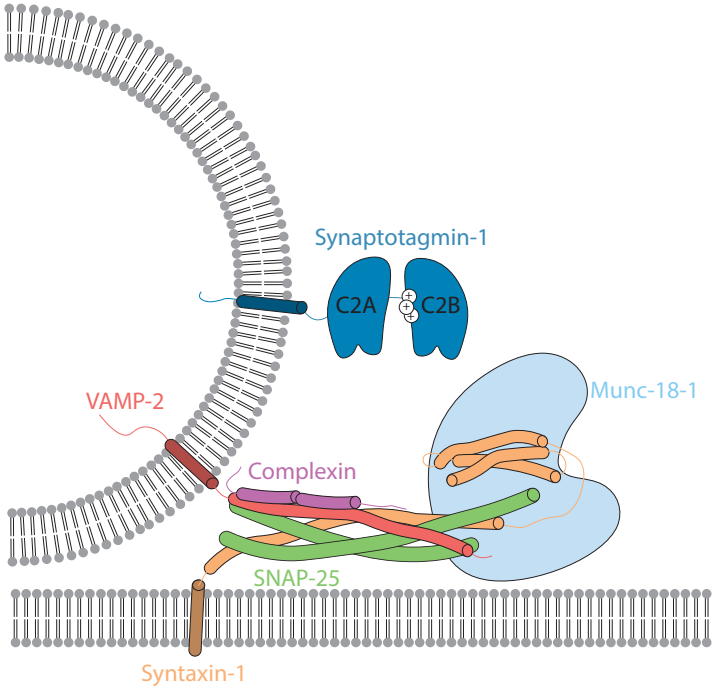

Figure 2: representation of the molecular machinery for vesicle fusion. The SNARE complex is formed by Syntaxin-1 (orange), SNAP-25 (green) and VAMP-2 (red). The SNARE complex is formed with the help of priming factor Munc18-1 (light blue) and Munc13-1 (not depicted). Complexin (purple) facilitates priming and prevents fusion in absence of Ca^{2+}. The two Ca^{2+} binding domains of Syt-1, C2A and C2B, the latter containing a poly-lysine stretch (white pluses), bind to the SNARE complex and the plasma membrane upon Ca^{2+} influx.

The N-terminal region of Syntaxin-1 folds back onto the SNARE motif, thereby preventing SNARE complex assembly (Dulubova et al., 1999). The Sec/Munc protein Munc18-1, as essential docking and priming factor, maintains Syntaxin-1 in its closed conformation (Dulubova et al., 1999). Sec/Munc protein Munc13-1 open up Synaxtin-1, and, together with Munc18, support SNARE complex assembly (Lai et al., 2017; Ma et al., 2013; Rich-

mond et al., 2001). Munc13-1 and Munc18-1 furthermore prevent the SNARE complex from N-ethylmaleimide sensitive factor (NSF)-mediated disassembly (He et al., 2017a).

Complexin

Complexin is another crucial molecular player in vesicle fusion. Complexin functions as a priming factor for SNARE complexes and clamps SNARE complex formation, possibly through steric or electrostatic repulsion (Trimbuch et al., 2014). Complexin-deficient neurons present a similar but milder phenotype as Syt1-KO neurons: loss of synchronous SV fusion and increased spontaneous release (Reim et al., 2001). For this reason, Complexin's role is therefore both stimulatory and inhibitory, and is regarded as an essential co-factor for Syt1.

Synaptotagmin fusion mechanisms

The fusion to two electrostatically repulsive membranes depends on an increase of intracellular calcium (Ca^{2+}), sensed by the calcium sensor Synaptotagmin. Synaptotagmin-1 (Syt1), the first Syt-isoform described (Matthew et al., 1981), is the main Ca^{2+} sensor for synchronous SV fusion (Geppert et al., 1994). Syt1 stimulates fusion by the Ca^{2+} dependent binding to phospholipids and SNARE proteins. Syt1 is suggested to regulate fusion via several non-mutually exclusive mechanisms. First, Ca^{2+} binding to Syt1 dislodges the Complexin clamp, possibly through a direct interaction with the Syt1-SNARE complex, in which Complexin and Syt1 compete for SNARE complexes (Tang et al., 2006). Second, Ca^{2+} binding to the C2 domains of Synaptotagmin neutralizes the negative charges between two otherwise electrostatically repulsive membranes, and thereby functions as an 'electrostatic switch' (Shao et al., 1997; Zhang et al., 1998). Third, Ca^{2+} binding to the negatively charged pockets of the C2 domains allows Synaptotagmin's Ca^{2+} binding loops to perturbate the lipid bilayer. Syt thereby bends the plasma membrane (Lynch et al., 2008) and creates shear and lowers the energy barrier for fusion. Finally, Syt1 has been implicated in linking membranes with its two C2-domains, bringing the vesicle into closer vicinity of the plasma membrane (Araç et al., 2006; Chang et al., 2018).

Synaptotagmins

Family members

The coupling of Ca^{2+} influx to vesicle exocytosis is primarily regulated by Synaptotagmins. Syts are specialized Ca^{2+} sensitive proteins that are named after the discovery of the synaptic vesicle localization of Syt1, at the time named p65, which

is the first Syt paralog described (Matthew et al., 1981). Since then, Syt paralogs are found in multicellular organisms (*Arabidopsis, Caenorhabditis, Drosophila, Mus, Homo,* and others) (Craxton, 2004). In mammals, 17 paralogs are described (Craxton, 2004, 2007), named Syt1-Syt17. Syts are generally characterized by a transmembrane domain (TMD) that is flanked by the N-terminal intraluminal fragment, and a cytosolic linker of variable length that connects to the Ca^{2+} binding C2A and C2B domains at the C-terminus (Figure 3).

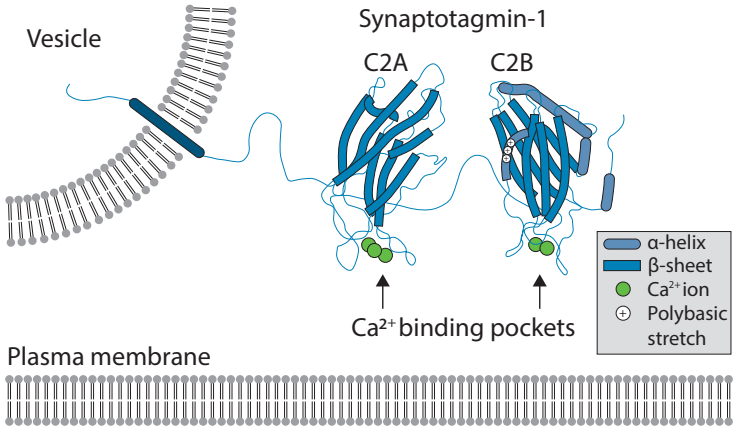

Figure 3: model of Synaptotagmin-1. Left part represents the SV membrane, in which Syt1 is anchored by its transmembrane domain (TMD). The TMD is flanked by the intraluminal fragment and a cytosolic linker that connects to the Ca^{2+} binding C2A and C2B domains. The C2 domains consist of two beta-sandwiches of two antiparallel four-stranded beta sheets. The C2A and C2B domain contain aspartate residues that form a Ca^{2+} binding pocket and allow 3 and 2 Ca^{2+} ions (green dots) to bind, respectively. Figure based on crystal structures of C2A and C2B domains (Fernandez et al., 2001; Sutton et al., 1995); linker domains and intraluminal domain are artistic impressions.

Within the C2 domains, Ca^{2+} is bound to aspartate residues that form a negatively charged Ca^{2+} binding pocket for ~2 or 3 Ca^{2+} ions to bind. However, of the 17 Syt paralogs, about half lack the aspartates that are required for Ca^{2+}- binding: Syt4, Syt8, Syt11 – Syt17 (Bhalla et al., 2008; Sugita et al., 2002), broadly dividing the Synaptotagmin family into Ca^{2+}-dependent and Ca^{2+}-independent sensors. Of the Ca^{2+} binding Synaptotagmins, Syt1 and Syt2 bind Ca^{2+} with a considerably lower affinity than Syt7, which is considered a high-affinity Ca^{2+} sensor (Sugita et al., 2002). Syt3, Syt5 and Syt10 have intermediate Ca^{2+} binding affinity, broadly dividing the sensors in high, medium and low affinity sensors, although the Ca^{2+} binding affinity also depends on the presence of phospholipids (Sugita et al., 2002). Other classifica-

tions rely on protein characteristics, such as the presence of disulfide bonds at the N-terminus (Syt3, 5, 6, and 10), or N-glycosylation sites at the N-terminus (Syt1 and Syt2) (Fukuda et al., 1999; Geppert et al., 1994; Perin et al., 1991).

As Synaptotagmins bind fusion proteins, such as SNARE complexes and Syntaxin-1, and to phospholipids, Syts are generally considered a class of membrane trafficking proteins (Fernandez et al., 2001; Fernández-Chacón et al., 2001; Li et al., 1995). However, to date, the function of most of the Synaptotagmins paralogs remains unknown.

Synaptotagmin-1

Ca^{2+} levels quickly rise and trigger fusion of synaptic vesicles within in a timescale of 75-100 ms after the action potential (Sabatini and Regehr, 1996), referred to as synchronous SV fusion. Syt1 is the calcium sensor responsible for this ultrafast fusion (Geppert et al., 1994), together with Syt2 and Syt9 (Xu et al., 2007). This is consistent with its low Ca^{2+}- affinity, which confines Syt1's Ca^{2+} binding to the Ca^{2+} peak of the action potential (Sugita et al., 2002). Moreover, Syt1 has fast Ca^{2+}/membrane unbinding kinetics, and tight coupling to Ca^{2+} nanodomains (for reviews, see Eggermann et al., 2011; Jackman and Regehr, 2017), further contributing to Syt1's role in synchronous SV fusion.

Syt1 is also required for the fast phase of secretory granule fusion in chromaffin cells. As most secretory granule fusion is slow, Syt1 null mutation results in a partial effect (~20% reduction) on overall exocytosis (Voets et al., 2001). Taken together, Syt1 is generally regarded as a sensor for the fast phase of secretion.

In addition to its role in synchronous/fast fusion, it is well-established that Syt1 exerts an inhibiting effect on spontaneous, action-potential independent ('mini's') release. Spontaneous fusion occurs during stochastic opening of Ca^{2+} channels or release from internal stores, resulting in fusion of a single synaptic vesicle. In addition, some spontaneous fusion events are probably Ca^{2+}-independent. In Syt1-deficient neurons, mini release increases 10-fold, possibly by outcompeting or unclamping of another Ca^{2+} sensor (Maximov and Südhof, 2005; Walter et al., 2011; Xu et al., 2009).

Syt1 deficiency leads to postnatal death in mice within 48 hours (Geppert et al., 1994). *De novo* Syt1 missense mutations in the C2B domain in human are linked to several neurological/developmental phenotypes, such as severe cognitive impairments, severe to profound speech/language impairments, hyperkinetic movement disorder, sleeping/eating/breathing difficulties and EEG abnormalities (Baker et al., 2018).

Synaptotagmin-7

Asynchronous fusion occurs after a longer, variable delay upon the action potential (> 10 ms), and can last up to 200 ms (Kaeser and Regehr, 2014)). Under most physiological conditions, asynchronous fusion is absent in most synapses, but becomes apparent after repetitive stimulation. However, in some cell types, such as CCK+ interneurons, asynchronous release is the primary mode of fusion (Hefft and Jonas, 2005). Although synchronous release is absent in Syt1-deficient hippocampal neurons, some SV fusion remains, although highly asynchronized (Fig. 4) (Geppert et al., 1994). Additional ablation of Syt7 in Syt1KO neurons almost completely abolishes asynchronous fusion, suggesting Syt7 is the calcium sensor that drives asynchronous SV fusion (Fig. 4) (Bacaj et al., 2013).

Asynchronous fusion mediated by Syt7 becomes apparent in absence of Syt1, or after repetitive stimulation (Bacaj et al., 2013; Chen et al., 2017; Luo and Südhof, 2017; Luo et al., 2015; Turecek and Regehr, 2018; Turecek et al., 2017; Wen et al., 2010). Syt-7's role in asynchronous release is in line with its a higher Ca^{2+} affinity (Sugita et al., 2002), allowing Syt7 to bind Ca^{2+} beyond the peak Ca^{2+} of an action potential. Moreover, Syt7 has exceptionally slow Ca^{2+} and phospholipid binding and unbinding kinetics (Brandt et al., 2012; Hui et al., 2005), characteristics that correspond to the role of Syt7 in slower types of vesicle fusion. However, the role of Syt7's extends beyond regulation of asynchronous release. In some synapses, Syt7 is required for synaptic facilitation (Jackman et al., 2016), possibly by binding residual Ca^{2+} (for review, see Jackman and Regehr, 2017). Moreover, Syt7 is required for SV pool replenishment (Liu et al., 2014). Finally, Syt7 overexpression is able to reduce the increase in spontaneous SV release that is observed in Syt1KO neurons (Bacaj et al., 2013), suggesting that Syt7 can substitute for Syt1's clamping function at increased expression levels. The increase of spontaneous fusion in Syt1KO neurons cannot be rescued by knockdown of Syt7, indicating it is not a Ca^{2+} sensor for spontaneous SV fusion under physiological conditions (Bacaj et al., 2013).

Syt7 is also a major calcium sensor for the slow/ phase of neuroendocrine secretion (Schonn et al., 2008). However, loss of Syt7 in Syt1KO cells also reduces the fast component of secretory granule fusion with >50%, and therefore also partially mediates fast burst of secretory granule exocytosis in chromaffin cells, possibly through a role in vesicle priming (Schonn et al., 2008; Tawfik et al., 2020). Moreover, Syt7 regulates insulin and glucagon secretion in pancreatic cells (Gao et al., 2000; Gauthier et al., 2007; Gustavsson et al., 2008) - the latter phenotype relates to the glucose intolerance observed in Syt7KO animals (Gustavsson et al., 2008, 2009). Moreover, Syt7 regulates lysosomal fusion in fibroblasts (Martinez et al., 2000, but

also see Jaiswal et al., 2004) and likely does so in neurons as well (Padamsey et al., 2017). Syt7KO animals present inflammation and fibrosis in skin and skeletal muscle (Chakrabarti et al., 2003), an effect probably related to the function of lysosomal fusion in plasma membrane repair regulated by Syt7 (Reddy et al., 2001).

The changes in neuronal communication in Syt7-deficient neurons, together with the disturbed glucose metabolism in Syt7KO animals, may contribute to the manic- and depressive-like bipolar behaviors that are observed in Syt7KO mice (Shen et al., 2020; Wang et al., 2020). This is supported by the reduced expression levels of Syt7 in both plasma and in IPSC-derived neurons of patients with bipolar disorder (BD), and high (~40%) glucose/insulin comorbidities in BD patients (Shen et al., 2020).

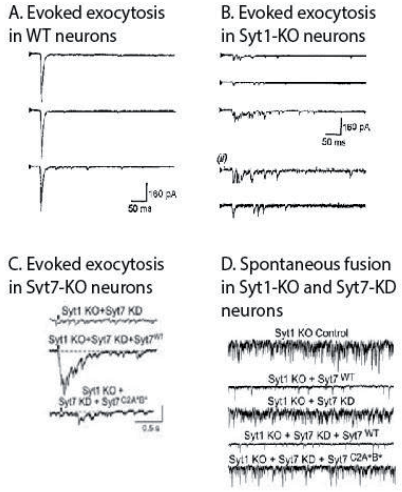

Figure 4: evoked exocytosis of SVs in mouse neurons. A) Synchronous evoked response in WT neurons. B) Evoked response in Syt1-KO neurons is desynchronized. C) Syt1KO/Syt7KD neurons abolish synchronous and asynchronous exocytosis. D) Spontaneous fusion can be rescued by overexpression, but not by knockdown of Syt7. Figure adjusted from Bacaj et al., 2013a; Geppert et al., 1994**.**

Role of Synaptotagmin in fusion pore stability

After fusion pore opening, full fusion pore expansion may lead to complete DCV cargo release ('full fusion') followed by cargo diffusion in extracellular space (Wit et al., 2009). Alternatively, the fusion pore may close, followed by vesicle reacidification, resulting in partial cargo release ('kiss-and-run'). Therefore, fusion pore expansion or re-closure may regulate DCV cargo release.

The exocytotic fusion pore consists of the mix of membrane lipids and proteins, such as SNAREs and Synaptotagmins (Bao et al., 2016). Fusion pore dilation requires Syt1 and its interaction with SNAREs, PIPs and Ca^{2+} (Wu et al., 2019). Mathematical modelling suggests that Syt1 Ca^{2+} binding and membrane insertion reorients the SNARE complex in a way that it acts as a lever that increases the fusion pore size (Wu et al., 2019). In line with these observations, a Syt1 mutant with a gain-of-function for membrane insertion showed increased fusion pore expansion and cargo release (Lynch et al., 2008). Summarized, Syt1 requires its membrane interaction to support fusion pore dilation and subsequent cargo release.

In PC12 cells, a neuroendocrine cell line, a Syt1 Ca^{2+} binding mutant reduces the amount of secretory granule fusion events, and additionally also shortens the event duration of the remaining fusion events (Lynch et al., 2008), suggesting Syt1 contributes to fusion pore kinetics. Similar conclusions were drawn from patch-amperometry experiments assessing the pre-spike foot (PSF) duration of secretory granule fusion. The pre-spike foot represents a fusion pore that leaks small amounts of norepinephrine (NE) prior to full expansion of the fusion pore, generating the amperometric spike. Changes in the PSF therefore reflect changes in fusion pore stability. A Syt1 mutant with an increased linker length between the C2A and C2B domain shortened the PSF duration, suggesting fusion pore stability was reduced (Bai et al., 2004a). In line with these observations, overexpression of Syt1 increases the PSF (Wang et al., 2001), suggesting pore stability increased. Taken together, these experiments suggest that Syt1 promotes fusion pore duration/stability and facilitates pore dilation in neuroendocrine cells.

Similar observations have been reported for SV fusion. SV fusion events, reported by VGlut1-pHluorin dequenching, are more short-lived in Syt1KO neurons (Li et al., 2016), possibly reflecting a reduced pore stability. However, the shortened duration of SV events may also be explained by enhanced endocytosis. Syt1 binds AP-2 (Zhang et al., 1994), a protein that is essential for clathrin-mediated endocytosis (CME) (Boucrot et al., 2010). CME is Ca^{2+} dependent, but becomes Ca^{2+}-independent and slower in Syt1 deficient neurons (Li et al., 2016; Poskanzer et al., 2003) and neuroendocrine cells (Yao et al., 2012b). Similarly, Syt1-photoinactivation upon fusion slows down endocytosis of SVs, suggesting Syt1 indeed supports endocytosis after SV fusion (Poskanzer et al., 2003). This effect seems to oppose Syt1's role on stabilization on the fusion pore, which prolongs fusion events. However, single vesicle fusion event duration and (possibly bulk-) endocytosis are two mechanistically distinct phenomena that don't necessarily correlate (Li et al., 2016).

Synaptotagmin expression

Expression in brain

Among all Synaptotagmin isoforms, only Syt1, Syt4 and Syt7 are expressed in all metazoans (Craxton, 2010). Synaptotagmins are differentially expressed throughout the brain. Syt1 and Syt7 are relatively abundant in mammals, whereas other Synaptotagmins, such as Syt2, Syt9 and Syt10 expression levels are highly restricted. Syt8 expression is typically not detected in brain (Figure 5) (Mittelsteadt et al., 2009; Zeisel et al., 2015), although some expression may be restricted to hippocampal somata (Monterrat et al., 2006). Due to the abundant expression of Syt1 and Syt7 in brain, their Ca^{2+}-dependent lipid binding capacity and the established roles in secretion (as will be discussed below), these sensors are good candidates for DCV fusion. Therefore, the following sections primarily focus on these two Ca^{2+} sensors.

Splice variants

Alternative splicing may in- or exclude specific protein domains. Among all Syt paralogs, Syt7 is most extensively alternatively spliced, and at least 8 splice variants have been detected in rat ((Craxton and Goedert, 1999; Sugita et al., 2001) Ensembl Rat Syt7). Splice variants differ with respect to their linker domain, which separates the transmembrane domain from the C2 domains (Figure 6). Exon 5 contains an in-frame stop codon, resulting in a truncated splice variant (Syt7T) that lacks the C2 domains (Figure 6). The remaining splice variants include the two Ca^{2+} binding domains, but have a variable linker length, resulting in proteins ranging from ~45 kDa (Syt7S) to ~76 kDa (Syt7L) (Sugita et al., 2001). Long and short splice variants of Syt7 are expressed in the brain, whereas insulin secreting and neuroendocrine cells mainly express short splice variants (Monterrat et al., 2007; Sugita et al., 2001). Alternative splicing of Syt7 is developmentally and regionally regulated; the longer isoforms are expressed later in development (during the first postnatal week and later), whereas short isoforms are continuously present in the mouse brain (Han et al., 2004; Sugita et al., 2001). The role of these splice variants is currently unknown. However, Syt7L rescues asynchronous SV fusion in Syt1KD/Syt7KO hippocampal neurons (Bacaj et al., 2015), indicating that the longer linker does not interfere with its functionality in synaptic transmission. The truncated variant, Syt7T, in contrast, does not rescue SV fusion (Bacaj et al., 2015). However, its overexpression slows down SV endocytosis ((Li et al., 2016) but also see (Virmani et al., 2003)), but full-length Syt7 did as well (Li et al., 2016; Virmani et al., 2003), indicating that this effect is not specific to the splice variant.

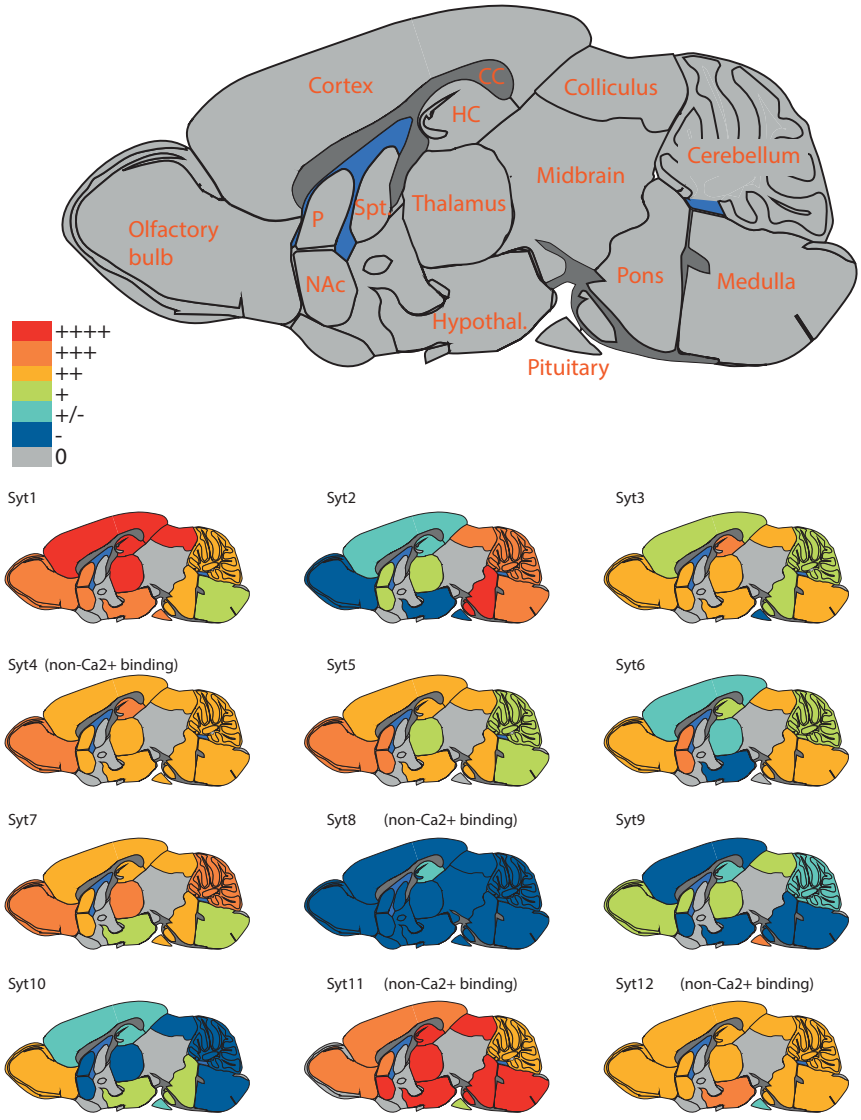

Figure 5: Synaptotagmin expression in mouse/rat brain. Overview based on in situ hybridization and immunoblot data presented in Marquhze et al.; Mittelsteadt et al., 2009; Roper et al., 2015. The non-Ca^{2+} binding Syt13 - Syt17 have been excluded from this overview.

Syt1, in contrast, has no alternative spliced linker, and only two splice variants are reported. Syt1 contains an alternative exon entry that can lead to inclusion or exclusion of three amino acids ('wobble splicing') at the juxtamembrane region (McAdam et al., 2015). However, the functional relevance of this splice variant remains unknown.

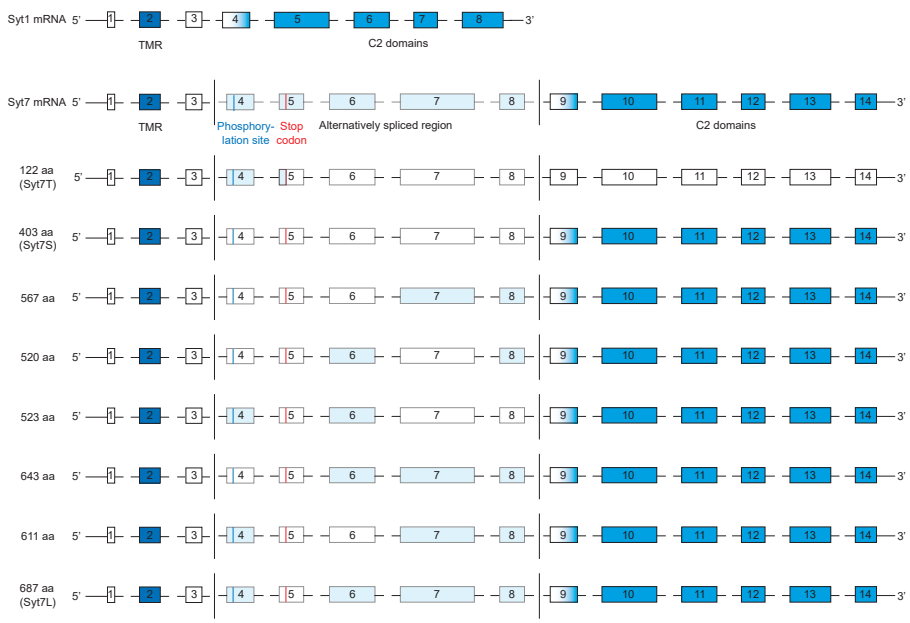

Figure 6: Syt exons and splice variants. Syt1 and Syt7 are alike, but only the linker domain of Syt7 is extensively alternatively spliced, resulting in at least 9 slice variants with differential in- or exclusion of exons 4-8. Syt7T is a truncated slice variant lacking both C2 domains due to inclusion of exon 5, which contains a stop codon. Syt7S is the short splice variants of Syt7, Syt7L the long variant. TMR = exon encoding the transmembrane region. C2 domains are localized at the 3' site (encoding the C-terminus) and are included in all splice variants with exception of Syt7T. Splice variants adapted from Ensembl rat Syt7 (entry number ENSRNOG00000026432).

Cellular localization of Synaptotagmins

Synaptotagmin paralogs differ with respect to their localization. Syt1 is targeted to SVs (Brose et al., 1992; Matthew et al., 1981; Takamori et al., 2006), is present on DCVs (Walch-Solimena et al., 1993), and travels together with lysosomes (Vukoja et al., 2018). In contrast, Syt7 is not detected on SVs but instead is present on the plasma membrane (Sugita et al., 2001; Takamori et al., 2006). Syt1 and Syt7 are probably both localized to secretory granules in neuroendocrine cells, maybe to partially separate populations (Rao et al., 2014).

Targeting of Syt1 to SVs depends on an N-terminal N-glycosylation site, which is present in Syt1 but not in Syt7 (Han et al., 2004). Substitution of the N-terminal sequence of Syt7 with the N-glycosylation sequence of Syt1 is sufficient to target Syt7 to vesicular structures in neuroendocrine (PC12) cells. *Vice versa*, replacement of the Syt1 N-terminal sequence for the Syt7 sequence results in plasma membrane targeted Syt1 (Han et al., 2004), indicating that the N-terminus regulates Syt target-

ing. Syt1 engineered without a TMD, resulting in a cytosolic C2AB fragment, is still functional in liposome fusion assays (Wang et al., 2011). However, expression of C2AB in neurons does not restore synchronous SV fusion (Díez-Arazola et al., 2020; Lee and Littleton, 2015). In contrast, re-targeting of Syt1 to the plasma membrane by replacing the TMD for a palmitoylation sequence of GAP43 fully rescued synchronous synaptic vesicle fusion, suggesting Syt1 requires membrane anchoring to mediate fusion (Hui et al., 2009; Yao et al., 2012a). However, GAP43-Syt1 does not restore endocytosis (Yao et al., 2012a). This suggests that the N-glycosylation site and the TMD are required for vesicular targeting and endocytosis, but not for vesicle fusion *per se*.

Other Ca^{2+} sensors

Double C2 (Doc2) proteins

Doc2 is a Synaptotagmin-like protein, and possesses two C2 domains that are homologous to Synaptotagmin. Three isoforms have been reported: Do2α, Doc2β and Doc2γ. Of these isoforms, Doc2α and Doc2β bind to phospholipids and to Ca^{2+} with high affinity (Groffen et al., 2010). Doc2γ lacks phospholipid binding, is localized to the nucleus (Fukuda and Mikoshiba, 2000; Fukuda et al., 2001), and will not be further discussed in this thesis.

Doc2β is abundant in brain, but also expressed in most other tissues, whereas Doc2α is exclusively expressed in the brain. Doc2α/β are complementarily expressed in brain (Korteweg et al., 2000; Verhage et al., 1997). Both are expressed in the hippocampus (Bacaj et al., 2013; Zeisel et al., 2015). Doc2α/β lack a transmembrane domain, resulting in cytosolic localization, but translocate to the plasma membrane upon stimulation along with Munc13 (Duncan et al., 1999; Groffen et al., 2004). In neurons, Doc2 facilitates spontaneous SV transmission (Courtney et al., 2018; Groffen et al., 2010; Pang et al., 2011). It has been suggested that Doc2α and Doc2β regulate glutamatergic and GABAergic spontaneous events (mini events), respectively (Courtney et al., 2018). However, they are functionally redundant as both isoforms rescue inhibitory and excitatory mini's (Courtney et al., 2018). Additionally, it is reported that Doc2α/β regulate asynchronous vesicle fusion in some (Xue et al., 2015; Yao et al., 2011) but not all studies (Groffen et al., 2010; Pang et al., 2011).

In neuroendocrine cells, Doc2 facilitates priming of adrenal secretory granules (Houy et al., 2017). In line with this, Doc2β enhances insulin secretion from MIN6 β-cells (Ke et al., 2007) and catecholamine secretion from chromaffin cells (Friedrich et al., 2008). Taken together, these data show that Doc2α/β facilitate neuroendocrine secretion and SV exocytosis.

Other Syts

In addition to Syt1, two other low affinity Ca^{2+} sensors, Syt2 and Syt9, mediate synchronous SV fusion in brain stem/cerebellum/striatum and limbic system/striatum, respectively (Fernández-Chacón et al., 2001; Geppert et al., 1994; Pang et al., 2006; Xu et al., 2007). Although all three mediate synchronous SV fusion, there are differences in kinetics: Syt2 has a fast onset and decline, whereas Syt9 onset and decline is slower (Xu et al., 2007). This fits well Syt2's expression in synapses that require ultrafast signaling, such as the auditory system and neuromuscular junctions.

The role of other sensors remains much more elusive. Syt3 is predominantly localized postsynaptically and drives AMPA receptor endocytosis, and Syt3-KO mice show impaired LTD and memory extinction (Awasthi et al., 2018). Syt4 negatively regulates BDNF (Dean et al., 2009; Wong et al., 2015) and oxytocin release (Zhang et al., 2011a), in line with its Ca^{2+}-independency. No function has been described for Syt5. Syt6 mediates secretion of endocytosed BDNF-quantum dots, but not endogenously produced BDNF (Wong et al., 2015). Syt9, in addition to its role in synchronous SV fusion, regulates follicle stimulating hormone (FSH) secretion from anterior pituitary cells (Roper et al., 2015), and Syt10 controls insulin-like growth factor (IGF-1) secretion in the olfactory bulb (Cao et al., 2011). However, Syt9 and Syt10 expression is highly restricted in the brain (Figure 5) (Mittelsteadt et al., 2009; Xu et al., 2007; Zeisel et al., 2015). Therefore, the calcium sensors that trigger neuronal DCV fusion remain largely elusive.

AIM AND OUTLINE OF THIS THESIS

Neuropeptides, secreted from DCVs, are essential signaling molecules in brain, regulating brain development, neurogenesis and synaptic plasticity. Neuronal activity and subsequent rises in Ca^{2+} levels are essential for DCV fusion. However, the molecular machinery that senses Ca^{2+} and triggers DCV fusion remains unclear. The general aim of this thesis is to identify and study the calcium sensors that regulate DCV fusion. For this purpose, the effect of genetic ablation of four candidate calcium sensors on DCV fusion was investigated in **Chapter 2**. Syt1 and Syt7 were both identified as required, but redundant Ca^{2+} sensors for DCV fusion. **Chapter 3** focused on the localization of these two sensors in neurons, and reports whether Syt1 and Syt7 are present on trafficking and fusing DCVs. In **Chapter 4**, the kinetics of individual fusion events in Syt1 and Syt7 KO neurons were studied. Finally, the

main findings of this thesis are summarized and discussed in the light of existing literature in **Chapter 5**.

In **Chapter 2**, we investigated the role of four candidate calcium sensors on DCV fusion, Doc2α/β, Syt1 and Syt7, which were of particular interest due to their identified roles in vesicle fusion and their high expression levels in brain. For this purpose, DCV fusion was quantified in Doc2α/β, Syt1 and Syt7 *null* mutant mice. In mouse hippocampal neurons, DCV fusion is strongly and equally reduced in Syt1- or Syt7-deficient neurons, but combined Syt1/Syt7 deficiency did not reduce fusion further, suggesting the two sensors operate in the same pathway. Cross-rescue, expression of Syt1 in Syt7-deficient neurons, or *vice versa*, completely restored fusion, indicating redundant functions of these two sensors and suggesting that their endogenous expression levels are rate-limiting to compensate for each other's loss. Overexpression of either sensor in WT neurons confirmed this and increased fusion. Hence, two calcium sensors together drive neuromodulator secretion in an expression-dependent and functionally-redundant manner.

As these results suggest that Syt1 and Syt7 operate in the same pathway, we addressed the localization of both Syts in **Chapter 3**. Specifically, we show that Syt1, and to lesser extent Syt7, are present on traveling and fusing DCVs. Moreover, Syt7 has a higher plasma membrane localization than Syt1. These localization analyses suggest that Syt1 mediates fusion while being present on the DCV, whereas Syt7 functions elsewhere, possibly the plasma membrane.

As both Syts are required for the majority of DCV fusion events, we next tested whether Syt1 and Syt7 differentially contribute to the kinetics of fusion events. In **Chapter 4**, the kinetics of individual DCV fusion events in Syt1-KO and Syt7-KO neurons were studied and reports that the duration of single DCV fusion events was reduced in Syt1-deficient neurons, but not in Syt7-deficient neurons. Syt7 did not rescue event duration in Syt1-deficient neurons, suggesting that Syt1 but not Syt7 regulates fusion pore stability. Finally, the transmembrane domain of Syt1 is required for fusion pore stability, but not for fusion pore opening.

Chapter 5 discusses these findings, provides a model of the molecular mechanism of DCV fusion and presents suggestions of future directions for further research.

Chapter 2

Two calcium sensors are required for neuromodulator release in neurons in a functionally redundant manner

Rhodé van Westen[1,2], Ruud F. Toonen[1*], Matthijs Verhage[1,2*]

[1] Department of Functional Genomics, Center for Neurogenomics and Cognitive Research, Neuroscience Campus Amsterdam, Vrije Universiteit (VU) Amsterdam

[2] Department of Clinical Genetics, UMC Amsterdam, the Netherlands

Parts of this chapter are accepted for publication in *Proceedings of the National Academy of Sciences of the United States of America* (PNAS) together with Chapter 3 and 4.

ABSTRACT

Neuropeptides and neurotrophic factors secreted from dense-core vesicles (DCVs) control many brain functions, but the calcium sensors that trigger their secretion remain unknown. Here, we show that in mouse hippocampal neurons DCV fusion is strongly and equally reduced in Synaptotagmin-1 (Syt1) - or Syt7-deficient neurons, but combined Syt1/Syt7 deficiency did not reduce fusion further. Cross-rescue, expression of Syt1 in Syt7-deficient neurons, or *vice versa*, completely restored fusion. Overexpression of either sensor in WT neurons confirmed this and increased fusion. In conclusion, two functionally redundant calcium sensors drive neuromodulator secretion in an expression-dependent manner.

INTRODUCTION

To date, over 100 genes encoding neuropeptides and neurotrophic factors, together referred to as neuromodulators, are identified and most neurons express neuromodulators and neuromodulator receptors (Smith et al., 2019). Neuromodulators travel through neurons in dense core vesicles (DCVs) and upon secretion regulate neuronal excitability, synaptic plasticity, and neurite outgrowth (van den Pol, 2012; Poo, 2001; Zaben and Gray, 2013). Dysregulation of DCV secretion is linked to many brain disorders, including epilepsy, anxiety disorder, and cognitive deficits (Kormos and Gaszner, 2013; Kovac and Walker, 2013; Ogren et al., 2010). However, the molecular mechanisms that regulate neuromodulator secretion remain largely elusive.

Neuromodulator secretion, like neurotransmitter secretion from neurons and signaling molecules from neuroendocrine cells, is a tightly controlled process triggered by Ca^{2+}. The Ca^{2+} sensors that regulate secretion have been described for these secretory pathways, but not for neuromodulator secretion. Synaptotagmin (Syt) and Doc2a/b are good candidate sensors, due to their interaction with SNARE complexes, phospholipids and Ca^{2+} (Geppert et al., 1994; Li et al., 1995; Perin et al., 1990; Poser et al., 1997). The Syt family consists of 17 paralogs (Craxton, 2004, 2007). Eight show Ca^{2+}-dependent lipid binding: Syt1-3, Syt5-7, Syt9 and 10 (Bhalla et al., 2008; Sugita et al., 2002). Syt1 mediates synchronous fusion of synaptic vesicles (SVs) (Geppert et al., 1994), consistent with its low Ca^{2+}-dependent lipid affinity (Hui et al., 2005; Sugita et al., 2002) and fast Ca^{2+}/membrane dissociation kinetics (Hui et al., 2005; Jackman and Regehr, 2017). Syt1 is also required for the fast fusion in chromaffin cells, resulting in a partial effect of Syt1 null mutation on overall exocytosis (Voets et al., 2001) and fast striatal dopamine release (Banerjee et al., 2020). Synaptotagmin-7 (Syt7), in contrast, drives asynchronous SV fusion (Bacaj et al., 2013), in line with its a higher Ca^{2+} affinity (Sugita et al., 2002) and slower dissociation kinetics (Hui et al., 2005). Syt7 is also a major calcium sensor for neuroendocrine secretion (Schonn et al., 2008), and for insulin and glucagon secretion in pancreatic cells (Gao et al., 2000; Gauthier et al., 2007; Gustavsson et al., 2008). Other sensors include Syt4, which negatively regulates BDNF (Dean et al., 2009) and oxytocin release (Zhang et al., 2011a), in line with its Ca^{2+}-independency. Syt9 regulates follicle stimulating hormone secretion in anterior pituitary (Roper et al., 2015) and, together with Syt1, secretion from PC12 cells (Fukuda et al., 2002; Lynch and Martin, 2007). Syt10 controls insulin-like growth factor secretion (Cao et al., 2011). However, Syt9 and Syt10 expression is highly restricted in the brain (Mittelsteadt et al., 2009; Xu et al., 2007; Zeisel et al., 2015). Hence, the calcium sensors for neuronal DCV fusion remain largely elusive. Because DCVs are generally not located close to

Ca^{2+} channels (Persoon et al., 2018), we hypothesized that DCV fusion is triggered by high affinity Ca^{2+} sensors. Due to their important roles in vesicle secretion, their Ca^{2+} binding ability, and high expression levels in brain (Bacaj et al., 2013; Groffen et al., 2010; Mittelsteadt et al., 2009; Pang et al., 2011; Verhage et al., 1997; Yao et al., 2011), we addressed the roles of Doc2a/b, Syt1 and Syt7 in neuronal DCV fusion.

In this study, we used primary hippocampal Doc2a/b-, Syt1- and Syt7-null (KO) neurons expressing a DCV fusion reporter (Bospoort et al., 2012; Emperador-Melero et al., 2018; Persoon et al., 2018; Wit et al., 2009) to obtain real-time single-vesicle resolution of DCV fusion events. We show that both Syt1 and Syt7, but not Doc2a/b, are required for ~60-90% of DCV fusion events. Deficiency of both Syt1 and Syt7 did not produce an additive effect, suggesting that both Syts function in the same pathway. Overexpression of Syt1 (Syt1-OE) rescued DCV fusion in Syt7-null mutant neurons, and *vice versa*, indicating that the two proteins compensate for each other in the DCV secretory pathway. Moreover, overexpression of Syt1 or Syt7 in WT neurons increased DCV fusion rates, suggesting that the two Syts are rate-limiting for DCV fusion. We conclude that DCV fusion requires two calcium sensors, Syt1 and Syt7, that act in a single/serial pathway, and that both sensors regulate fusion in a rate-limiting and dose-dependent manner.

RESULTS

Doc2a/b are dispensable for DCV fusion

To identify the calcium sensor(s) for DCV fusion in neurons, we used single hippocampal neurons cultured on glia micro-islands expressing the DCV fusion reporter

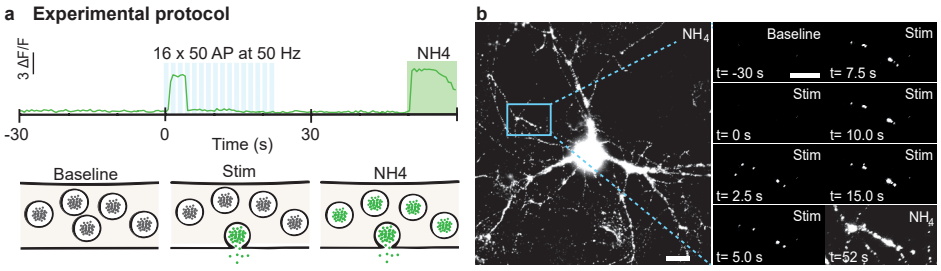

Figure 1: experimental protocol.

a. Stimulation paradigm with a single vesicle fluorescence intensity trace.

b. Large image: representative image of NPY-SEP infected neuron during Tyrode's-NH_4 application. Scale bar = 20 µm. Zoom: neurite before (baseline) and during (16x50AP at 50 Hz) stimulation and during NH_4 application (NH_4). Scale bar = 10 µm.

NPY-Super Ecliptic pHluorin (SEP) (Fig.1A, B) to quantify DCV fusion at single-vesicle resolution (Bospoort et al., 2012; Emperador-Melero et al., 2018; Persoon et al., 2018). Vesicle fusion was triggered by bursts of action potentials at 50 Hz (Fig.1A). The total number of DCVs per neuron was quantified upon brief NH_4 superfusion to dequench NPY-SEP in all acidic compartments (DCVs, Fig.1A, 1B).

Doc2a/b are soluble high-affinity calcium sensors reported to trigger spontaneous and asynchronous SV fusion (Groffen et al., 2010; Pang et al., 2011; Yao et al., 2011). Due to their high Ca^{2+} affinity and plasma membrane translocation upon stimulation (Groffen

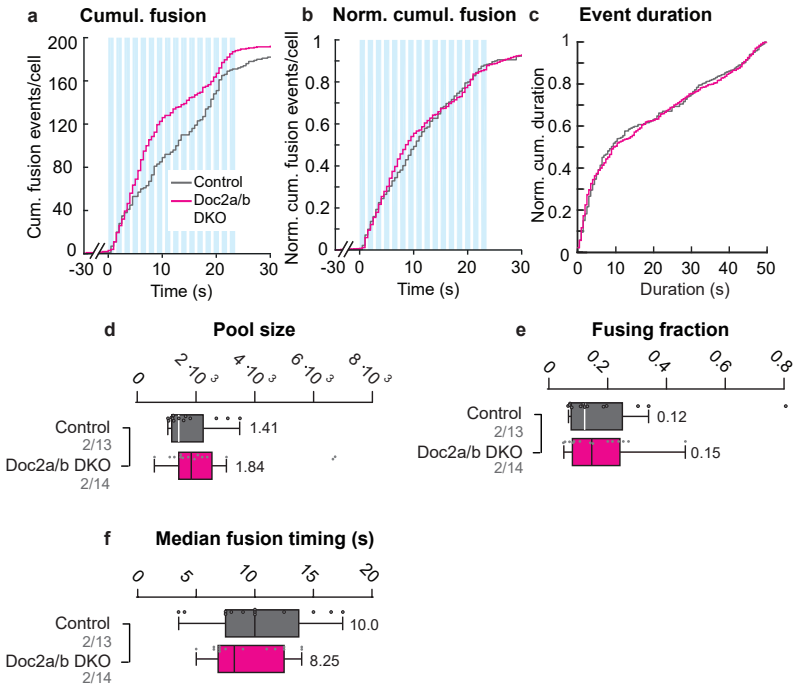

Figure 2. DOC2a/b DKO does not affect DCV fusion

a. Median number of neuropeptide vesicle fusion events in control (DHZ), and Doc2a/b DKO neurons in a cumulative plot (n_{HZHZ}=13, n_{DKO}=14).

b. Normalized median cumulative fusion of DCVs per neuron in control and DKO neurons.

c. Normalized median cumulative DCV fusion event duration per neuron in control and DKO neurons.

d. Total number of DCVs per neuron is not significantly different between control and DKO neurons (Mann Whitney $U = 67$, $p = .26$).

e. Fusing fraction in control and DKO neurons is similar (Mann Whitney $U = 91.0$, $p > .99$).

f. Fusion timing in control and DKO neurons is not significantly different ($t(25) = 48.6$, $p = 0.63$).

Number before and after dash represents number of independent experiments and number of neurons, respectively.

et al., 2006), we hypothesized that Doc2a/b are suitable Ca^{2+}-sensors for DCV fusion. To test this, DCV fusion was quantified in Doc2a/b double-null (DKO) neurons and double-heterozygous (DHZ) littermate controls (n_{HZHZ}=13, n_{DKO}=14). DCV fusion upon high frequency stimulation, visualized by rapid dequenching of NPY-SEP puncta (Figure 1A, B, Fig. S1A), was abundant in DHZ neurons, and occurred almost exclusively during stimulation (Figure 2A). Doc2a/b deficiency did not alter the number of DCV fusion events nor the total number of DCVs per neuron (Figure 2A, D). In line with these findings, the released fraction of DCVs, defined as the number of fusing vesicles divided by the total DCV pool, was not affected by Doc2a/n deficiency (Figure 2E). Moreover, no difference in fusion kinetics, either timing or event duration, was observed (Figure 2B, C, F).

DCV fusion requires both Syt1 and Syt7

Due to their established roles in synaptic- and neuroendocrine vesicle secretion, and high brain expression levels (Bacaj et al., 2013; Mittelsteadt et al., 2009; Zeisel et al., 2015), we next tested the role of Syt1 and Syt7 in DCV fusion using Syt1 knock-down (Syt1-KD, (Xu et al., 2012)), Syt7-null mutant (Syt7-KO, (Maximov et al., 2008)), and Syt1-KD/Syt7-KO hippocampal neurons. Immunoblotting of Syt1 from hippocampal cultures confirmed Syt1-KD efficiency in Syt1-KD neurons, as shown before (Supplementary Figure 1B, (Xu et al., 2012)). Wild-type (WT) neurons showed many fusion events in response to high frequency stimulation. However, in Syt1-KD or Syt7-KO

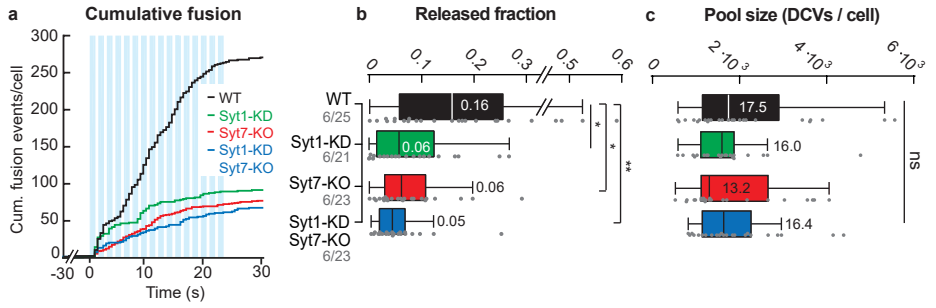

Figure 3. Synaptotagmin-1 and Synaptotagmin-7 are required for neuropeptide vesicle fusion.

a. Median number of neuropeptide vesicle fusion events per neuron in a cumulative plot in Syt1-KD, Syt7-KO and Syt1-KD/Syt7-KO neurons, respectively.

b. Box plot of fusing fraction ($X^2(4) = 14.05$, $p = .0028$), defined as the number of fusion events divided by total number of vesicles per neuron measured during Tyrode's-NH_4 superfusion.

c. Deficiency of Syt1 or Syt7 does not affect the total number of DCVs per neuron ($X^2(4) = 1.233$, $p = .75$).

Median value is presented in or next to the box plot. Number before and after dash represents number of independent experiments and number of neurons, respectively. *$p < .05$, **$p < .01$, ns p>.05.

neurons the number of DCV fusion events was reduced by 64% and 69%, respectively (Figure 3A, Supplementary Figure 1D). Strikingly, loss of both Syt1 and Syt7 did not produce additive effects, but a similar reduction in fusion events (76% reduction) as in single mutant neurons (Figure 3A, Supplementary Figure 1D). The absence of Syt1 and/or Syt7 did not significantly alter the timing of the remaining DCV fusion events (Supplementary Figure 1E, F), or the total number of DCVs per neuron (Fig. 3B). The released fraction, defined as the number of fusing vesicles divided by the total DCV pool, showed a 3-fold reduction in Syt1-KD, Syt7-KO and Syt1-KD/Syt7-KO neurons (Supplementary Figure 3C). Hence, DCV fusion in hippocampal neurons requires both Syt1 and Syt7, and loss of both sensors does not produce additive effects, suggesting that the two sensors function in a single pathway.

Syt1 and Syt7 cross-rescue DCV fusion

We next asked whether Syt1 and Syt7 are essential for DCV fusion, or whether the absence of one sensor can be by-passed by overexpressing the other ('cross-rescue'). To test this, Syt1 or Syt7 was overexpressed in Syt7-KO or Syt1 null mutant (Syt1-KO) (Geppert et al., 1994) neurons, respectively.

We first confirmed that in Syt1-KO neurons DCV fusion was reduced to a similar extent as in Syt1-KD neurons (Figure 4A). Furthermore, Syt1 expression in Syt1-KO neurons fully rescued DCV fusion, as well as the released fraction (Figure 4A, B). Strikingly, over-expression of Syt7 in Syt1-KO neurons also rescued DCV fusion (Figure 4C) and fusing fraction (Figure 4D) similar to Syt1 expression in Syt1-KO neurons. Conversely, overexpression of Syt1 in Syt7-KO neurons also rescued DCV fusion event numbers and fusing fraction (Figure 4E, F), to a comparable extent as Syt7 rescue (Figure 4E, F). Cross-expression of either Syt1 or Syt7 did not affect the total number of DCVs nor fusion timing (Supplementary Figure 2A-C). Hence, Syt1 and Syt7 are functionally redundant in supporting DCV fusion upon overexpression.

Fusion timing, defined as the latency to fusion onset relative to the onset of stimulation, was not significantly different between all groups tested (Supplementary Figure 1). However, small changes in fusion timing may occur in the initial phase of the stimulation. To test this, we compared the percentage of vesicles that fused during the first 50 AP, or during the first 150 AP, and found no difference between groups of either condition (Supplementary Figure 3A-C and D-F, respectively). The number of fusion events after the end of the stimulation burst was also compared. While the absolute number of fusion events was severely reduced in Syt1KO neurons (Fig. 3, Fig. 4), the relative number of delayed fusion events, after the end of the stimulation, was also not significantly different (Supplementary Figure 4A-F). Hence, Syt1 and Syt7 do not affect the overall timing of DCV fusion, nor the fusion timing in the initial bursts of release.

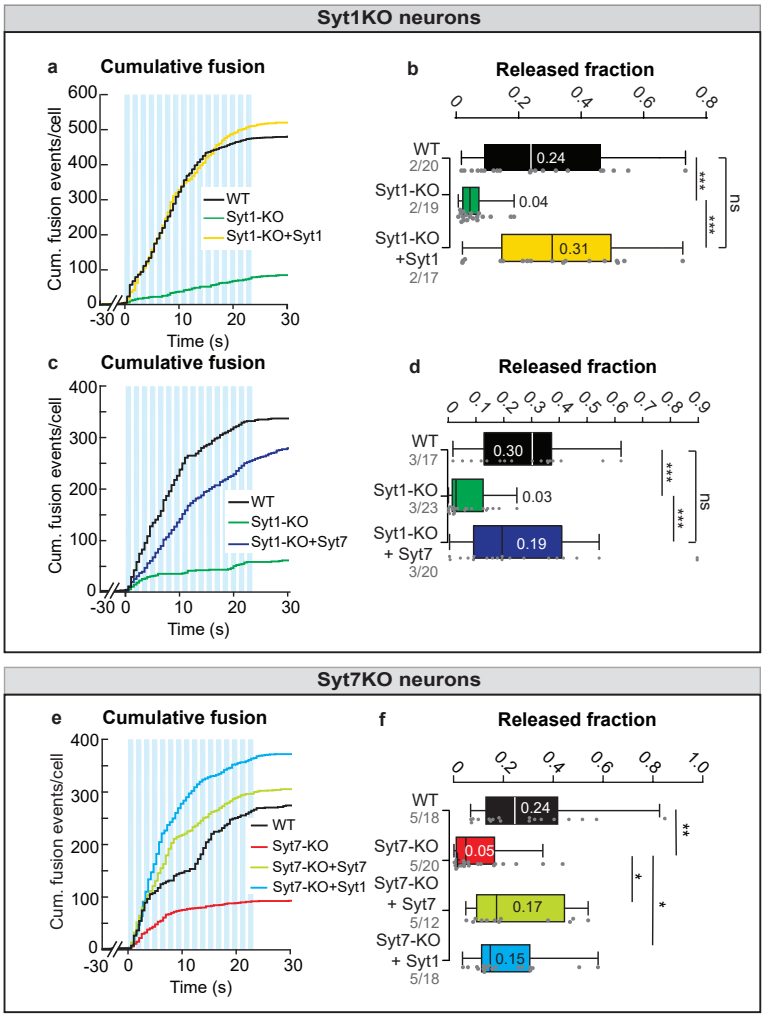

Figure 4: Synaptotagmin-1 and Synaptotagmin-7 can cross-rescue neuropeptide vesicle fusion.

a. Median number of neuropeptide vesicle fusion events in WT, and Syt1-KO neurons with and without Syt1-OE in a cumulative plot.

b. Fusing fraction in Syt1-KO neurons is rescued by Syt1-OE ($X^2(3) = 19.28$, $p < .0001$). For lentiviral infection, 2 µl of lentivirus was used. For the effects of different volumes of lentivirus, see Supplementary Figure 5.

c, d. Same as A-C, but with Syt7-OE. Fusing fraction in Syt1-KO neurons is rescued by Syt7-OE ($X^2(3) = 20.96$, $p < .0001$).

e, f. Same as A-C, but with Syt7-KO neurons with Syt7-OE. Fusing fraction in Syt7-KO neurons is rescued by Syt7-OE and Syt1-OE ($X^2(4) = 15.96$, $p = .0012$). Median value is presented in or next to the box plot. Number before and after dash represents number of independent experiments and number of neurons, respectively. *$p < .05$, **$p < .01$, ***$p < .001$, ns p>.05.

Overexpression of Syt1 and Syt7 in WT neurons increases DCV fusion

Because excess of Syt1 cross-rescued Syt7-deficient neurons, and *vice versa*, (Fig. 4), whereas physiological levels were not sufficient (Fig. 3), we conclude that endogenous Syt levels are rate-limiting in their regulation of DCV fusion. To confirm this, Syt1 and Syt7 were overexpressed in WT neurons. Overexpression resulted in a 50% and 100% increase in Syt1 and Syt7 immunostaining intensity, respectively, without affecting the expression of the other sensor (Supplementary Fig. 6C, D). Total DCV pool sizes were unaffected (Fig. S6A, B). Overexpressing Syt1 (Figure 5A, Supplementary Figure 6) or Syt7 (Figure 5C, Supplementary Figure 6) in WT neurons

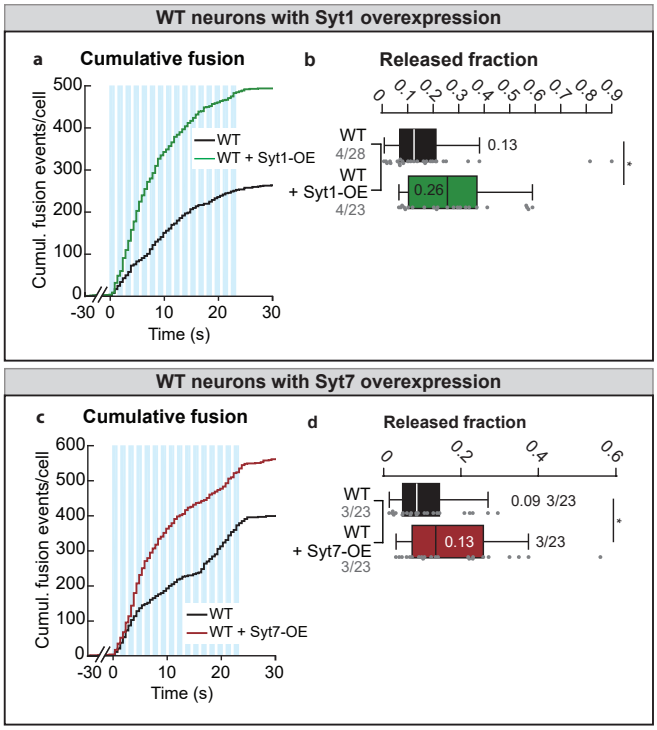

Figure 5: Overexpression of Syt1-OE and Syt7-OE in WT neurons increases neuropeptide vesicle fusion.

a. Median number of neuropeptide vesicle fusion events in WT neurons with and without Syt1-OE in a cumulative plot.

b. Fusing fraction is increased in WT neurons with Syt1-OE ($U = 193$, $p < .05$). Neurons with a fusing fraction above 0.9 were plotted at 0.9 for visualization purposes.

c, d Same as a, b, but with Syt7-OE (Fusing fraction $U = 174$, $p < .05$). Median value is presented in or next to the box plot. Number before and after dash represents number of independent experiments and number of neurons, respectively. *$p < .05$, ns $p > .05$.

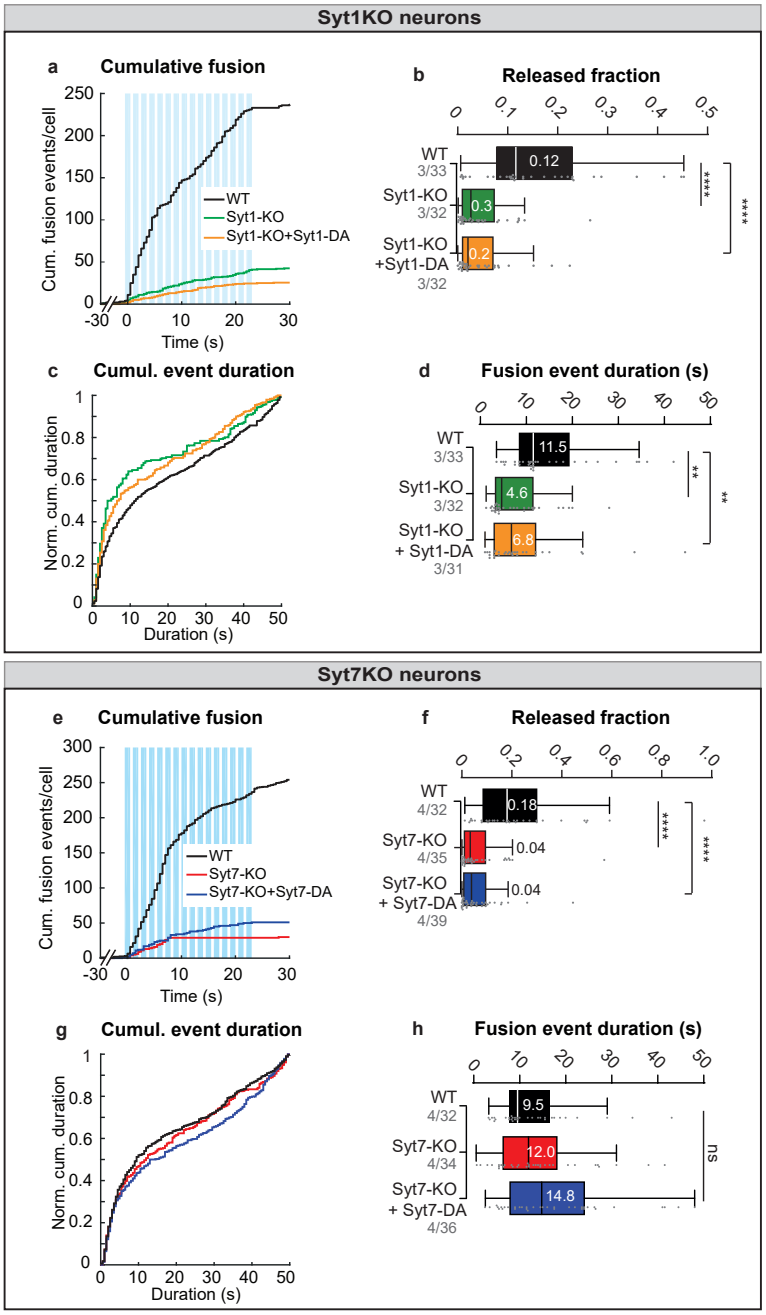

Figure 6. Caption on next page ⇢

significantly increased DCV fusion 2-fold and 1.5-fold, respectively. Additionally, both Syt1-OE and Syt7-OE increased the fraction of fused DCVs (Figure 5B, D). These data suggest that endogenous levels of Syt1 and Syt7 are rate-limiting for DCV fusion in neurons.

DCV fusion requires the Ca^{2+}-binding capacity of Syt1- and Syt7

To confirm whether Syt1 and Syt7 are indeed Ca^{2+} sensors for DCV fusion, we expressed Syt1 and Syt7 variants that cannot bind Ca^{2+} (Syt1-DA and Syt7-DA (Bacaj et al., 2013)) in Syt1KO or Syt7KO neurons. Overexpression of Syt1-DA and Syt7-DA did not restore DCV fusion (Fig. 6A, B, E, F) in Syt1KO or Syt7KO neurons, respectively. Similarly, the shorter event duration observed in Syt1-KO neurons was not rescued by overexpression of Syt1-DA (Fig. 6C, D). These data suggest that Ca^{2+} binding is indeed required for Syt1/7-dependent DCV fusion and both Syt1 and Syt7 are main Ca^{2+}-sensors for DCV fusion.

DISCUSSION

Calcium sensors have been identified for fusion of SVs (Bacaj et al., 2013; Geppert et al., 1994), lysosomes (Martinez et al., 2000), secretory granules in pancreatic α- and β-cells (Gao et al., 2000; Gauthier et al., 2007; Gustavsson et al., 2009; Iezzi et al.,

Figure 6. Syt1- and Syt7-mediated DCV fusion require Ca^{2+}-binding

a. Median number of neuropeptide vesicle fusion events in WT and Syt1-KO neurons with and without Syt1-DA expression in a cumulative plot. See Fig. 4A,B for Syt1-KO neurons rescued with Syt1.

b. Fusing fraction in Syt1-KO neurons is not rescued by Syt1-DA expression ($X^2(3) = 25.01$, $p < .0001$).

c. Normalized cumulative median event duration per neuron in WT, Syt1-KO and Syt1-KO neurons with Syt1-DA expression.

d. Event duration in Syt1-KO neurons is not rescued by Syt1-DA expression ($X^2(3) = 15.29$, $p = .0005$).

e. Median number of neuropeptide vesicle fusion events in WT and Syt7-KO neurons with and without Syt7-DA expression in a cumulative plot. See Fig. 4E,F for Syt7-KO neurons rescued with Syt7.

f. Fusing fraction in Syt7-KO neurons is not rescued by Syt7-DA expression ($X^2(3) = 28.23$, $p < .0001$).

g. Normalized cumulative median event duration per neuron in WT, Syt1-KO and Syt1-KO neurons with Syt1-DA expression.

h. Event duration in Syt7-KO neurons with and without Syt7-DA expression is not significantly different from WT neurons ($X^2(3) = 2.94$, $p = .23$).

Box plots are plotted with 25% (Q1) and 75% (Q3) interquartile range and Tukey whiskers. Number before and after dash represents number of independent experiments and number of neurons, respectively. Please note that the difference in n-numbers between release probability and fusion duration originates from non-releasing neurons having no event duration. * $p < .05$, ** $p < .01$, *** $p < .001$, **** $p < .0001$ ns $p > .05$.

2004), and in neuroendocrine cells (Schonn et al., 2008; Voets et al., 2001). However, the calcium sensors responsible for neuromodulator release in neurons have remained largely unknown. In this study, we show that Syt1 or Syt7 deficiency, but not DOC2A/B deficiency, each reduced DCV fusion by 60-90% in hippocampal neurons (Fig. 2A, E, 3A, B, 4A-F, 6A, B, E, F). Syt1 or Syt7 deficiency did not selectively affect specific components of DCV fusion (Fig. S2D-F, S3A-F, S4), affected fusion equally (Fig. 3A, C) and did not produce an additive effect (Fig. 3C, Supplementary Figure 1D). This indicates that, in hippocampal neurons, Syt1 and Syt7 together drive fusion of the same vesicle pool with the same kinetics in a single secretory pathway. Overexpression of Syt1 in Syt7-KO or Syt7 in Syt1-KO neurons cross-rescued DCV fusion (Fig. 4A-F), indicating that the two proteins compensate for each other in the secretory pathway. Overexpression of Syt1 or Syt7 in WT neurons increased DCV fusion by 2-fold and 1.5-fold, respectively (Fig. 5), suggesting that both proteins are rate-limiting for DCV fusion.

Loss of Syt1 or Syt7 expression led to the loss of most DCV fusion events (60-90% reduction). However, due to the mixed nature of hippocampal cultures, this effect may still be an underestimation. A small fraction of hippocampal neurons expresses Syt2 (García-Junco-Clemente et al., 2010), or Syt9 (Dean et al., 2012; Mittelsteadt et al., 2009; Xu et al., 2007). These paralogs also bind Ca^{2+} and have similar properties as Syt1 and Syt7 and may therefore compensate for the loss of Syt1 or Syt7 expression in a fraction of neurons in our cultures. Consistent with this, we observed that a small subset of neurons still released many DCVs in the absence of Syt1 and/or Syt7 (Supplementary Figure 1D). Hence, the true importance of Syt1 and Syt7 for neuromodulator release in most neurons may still be partially masked by expression of other Ca^{2+} sensors in a few other neurons.

Syt1 or Syt7 deficiency did not selectively affect DCV fusion timing (Supplementary Figure 2D-F, 3A-F, 4A-G), affected fusion equally (Fig. 3A, C, Fig. 4A-F) and deficiency of both did not produce additive effects (Fig. 3). This indicates that in hippocampal neurons Syt1 and Syt7 together drive fusion of the same vesicle pool with the same kinetics in a single secretory pathway. This situation is very different from the best studied systems so far, where sensors have specialized functions and drive fusion of distinct release phases: Syt1 drives synchronous SV fusion in neurons and fast secretory granule fusion in chromaffin cells, while Syt7 primarily drives asynchronous and slow fusion in these two systems (Bacaj et al., 2013; Geppert et al., 1994; Schonn et al., 2008; Voets et al., 2001), and may be involved in vesicle priming (Bacaj et al., 2013; Schonn et al., 2008) and activity-dependent pool replenishment (Liu et al., 2014). Syt7 overexpression does not restore (Syt1-driven)

synchronous SV release in Syt1-KO neurons (Bacaj et al., 2013) and combined deficiency of Syt1 and Syt7 reduces both phases, producing clear additive effects (Bacaj et al., 2013; Schonn et al., 2008). Hence, while Syt1 and Syt7 have clearly specialized functions in SV and chromaffin granule exocytosis, they do not for DCVs. This may be explained by evolutionary adaptations, optimizing chromaffin granule and SV exocytosis for fast and ultrafast kinetics, respectively, while there may not be an evolutionary advantage for optimizing neuromodulator signaling further. Syt1 and Syt7 most likely emerged by gene duplication of an ancestral Syt. Our data suggest that this duplication happened first, making secretory pathways more efficient and stimulus-dependent, and that Syt1 and Syt7 subsequently became more specialized to drive different phases of fast or ultrafast vesicle fusion in highly specialized secretory pathways, but not in the DCV pathway.

Although Syt1 and Syt7 have specialized functions in synaptic transmission, but not in the DCV secretory pathway, the two sensors appear to act on a single pool of vesicles in both situations. Functional redundancy among Syts has been shown for the maintenance of the readily releasable vesicle pool (Bacaj et al., 2015), and Syt7 overexpression inhibits the increase of spontaneous SV fusion in Syt1-deficient neurons (Bacaj et al., 2013). Hence, with or without specialized functions, the two sensors do not act in parallel pathways, but drive fusion of a single pool of vesicles in a single pathway for SVs and DCVs alike.

Syt1 and Syt7 were shown to act as redundant Ca^{2+}-sensors for Ca^{2+}-dependent AMPA receptor exocytosis during the induction of long-term potentiation (Wu et al., 2017a). While loss of either Syt1 or Syt7 was sufficient to lose most DCV fusion events (Fig. 3A, C, Fig. 4A-F, Supplementary fig. 5D-H), AMPA receptor insertion was lost only after losing both (Wu et al., 2017a). Hence, native Syt1/7 expression levels are probably more rate limiting for DCV fusion than for AMPA receptor insertion, as WT neurons do not express enough of one Syt to compensate for the loss of the other in single null mutant neurons (Fig. 3C). This conclusion is further supported by the fact that either Syt1 or Syt7 overexpression produced substantial increase in DCV fusion in WT neurons (Fig. 5A-D).

Syt1 mRNA levels were not affected after Syt7KD, nor did Syt1 levels differ between Syt7 null mutant neurons with and without Syt7 overexpression (Bacaj et al., 2013), suggesting neurons do not compensate for the loss of one sensor by increasing expression of the other. Similarly, WT neurons overexpressing either Syt did not result in altered expression of the other (Fig. S6C, D). Because Syt1 and Syt7 cellular expression levels are rate-limiting for DCV fusion (Fig. 5A-D), at least in hippocampal

neurons, transcription regulation of either of the two genes may be a powerful way to regulate neuromodulation.

Neuromodulator signaling is a slow process relative to synaptic transmission and DCV fusion requires prolonged stimulation with very few DCVs fusing upon single action potential stimulation (Persoon et al., 2018) and during the onset of high frequency stimulation (Supplementary Figure 3A-C). The key determinants of these slow kinetics remain incompletely understood, but one relevant observation is that DCVs, unlike SVs, do not typically cluster at the active zone (Bospoort et al., 2012; Imig et al., 2014), where Ca^{2+}-channel accumulation produces rapid local Ca^{2+}-transients (Llinás et al., 1992; Zucker and Fogelson, 1986). Hence, it will take longer before Ca^{2+}-transients spread through the terminal or axon and activate Ca^{2+}-sensors on DCVs. Since Syt1 is among the Ca^{2+}-sensors with the lowest Ca^{2+}-sensitivity (Sugita et al., 2002), Ca^{2+} must rise to high micromolar level before this sensor is activated. This reasoning contributes to an explanation for the slow DCV-release onset. However, previous studies indicate a considerable delay between the peak of (bulk) Ca^{2+}-increase in axons and the onset of DCV fusion (Persoon et al., 2018). Therefore, additional factors probably contribute to the slow DCV-release onset. For instance, DCVs are transported through neurites on molecular motor complexes (kinesins, dyneins, (Hoogenraad and Akhmanova, 2016; Lo et al., 2011)) and may need time to dissociate from these motors and translocate to a fusion site (Bharat et al., 2017; Stucchi et al., 2018).

ACKNOWLEDGEMENTS

We thank Robbert Zalm for cloning and producing viral particles; Frank den Oudsten, Lisa Laan and Desiree Schut for producing glia feeders and primary culture assistance; Joke Wortel for animal breeding; Jurjen Broeke for technical assistance; Jurjen Broeke and Alessandro Moro for Matlab programming; Ingrid Saarloos for protein chemistry; Frank den Oudsten and Joost Hoetjes for genotyping assistance; and members of the CNCR DCV project team for fruitful discussions. This work is supported by an ERC Advanced Grant (322966) of the European Union (to M.V.).

AUTHOR CONTRIBUTIONS

R.v.W, R.F.T. and M.V. designed the experiments. R.v.W. collected and analyzed experimental data, R.v.W., R.F.T. and M.V. designed the figures and wrote the manuscript.

SUPPLEMENTARY FIGURES

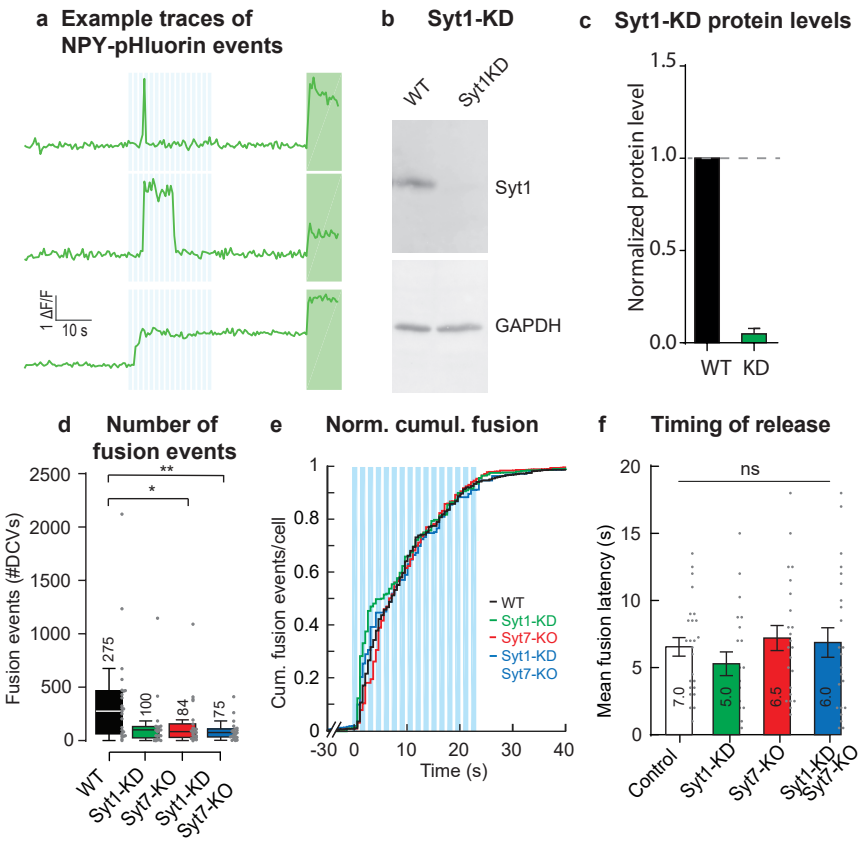

Supplementary Figure 1: Syt1 protein levels in Syt1-KD neurons, and DCV fusion in Syt1-KD, Syt7-KO and Syt1-KD/Syt7-KO neurons.

a. Representative examples of NPY-SEP fluorescence traces. Blue shading represents stimulation of 16 x 50 AP at 50 Hz. Green shadings represent NH4 bath application. Green lines are example fluorescence traces of single DCV fusion events.

b. Syt1-KD efficiently reduces Syt1 protein levels. Upper lanes: WT and Syt1-KD neurons blotted for Syt1. Lower lanes: WT and Syt1-KD neurons blotted for GAPDH as loading control.

c. Quantification of Syt1 protein levels in WT and Syt1-KD neurons.

d. Number of DCV fusion events per neuron is significantly reduced in absence of Syt1 and/or Syt7 ($X^2(4) = 11.69$, $p = .01$). Box plots are plotted with 25% (Q1) and 75% (Q3) interquartile range and Tukey whiskers. Numbers before and after dash represents number of independent experiments and number of neurons, respectively.

e. Normalized median cumulative fusion of DCVs per neuron.

f. Mean timing of DCV fusion events per neuron ($F(3,88) = .80$, $p = .50$).

Bar plots are plotted as mean ± SEM. ns = $p > .05$, *$p < .05$, **$p < .01$.

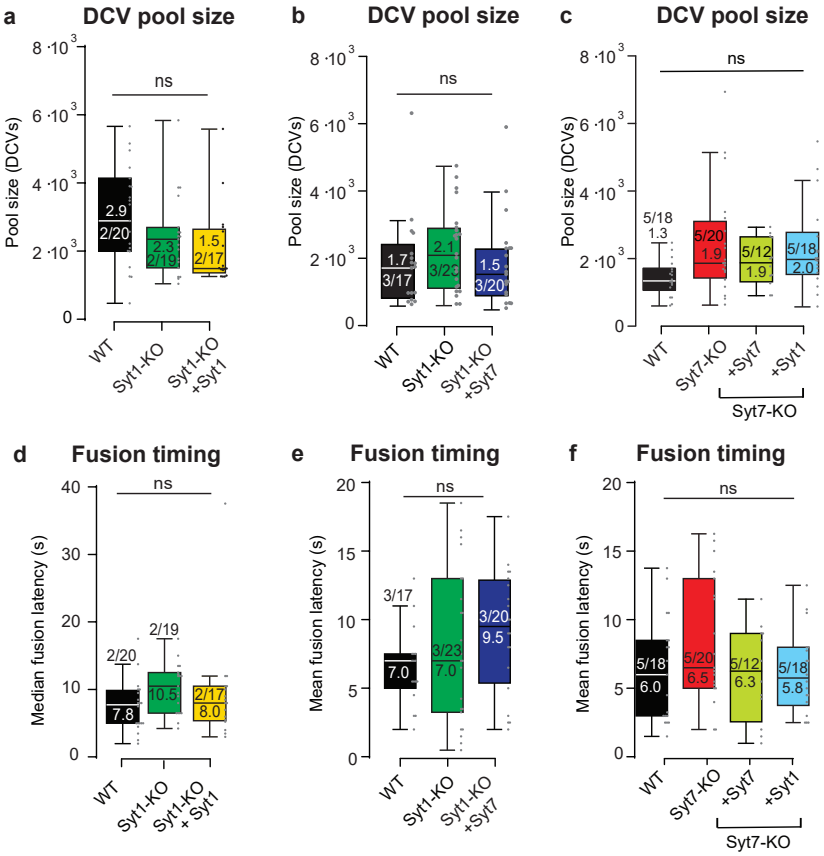

Supplementary Figure 2: DCV pool sizes and fusion timing of (cross-)rescued neurons

a. Total number of DCVs present in a neuron (pool size) is not different between WT, Syt1-KO and Syt1-KO with Syt1-OE. ($X^2(3) = 4.59$, $p = .10$).

b. Same as a, but with Syt7-OE ($X^2(3) = 2.02$, $p = .36$)

c. Same as a and b, but with Syt7-KO neurons overexpressing Syt7 or Syt1 ($X^2(4) = 10.31$, $p = .05$).

d. Median timing of DCV fusion events per neuron ($X^2(3) = 5.65$, $p = .06$).

e. Median timing of DCV fusion events per neuron ($F(2, 57) = 1.435$, $p = .25$).

f. Median timing of DCV fusion events per neuron ($F(3, 65) = 1.294$, $p = .28$).

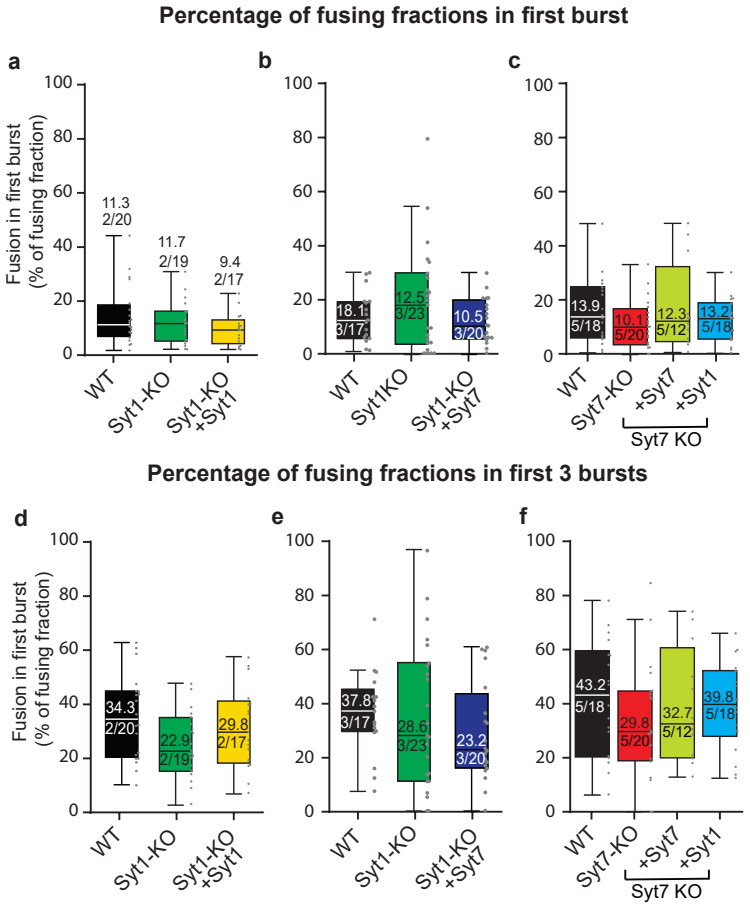

Supplementary Figure 3: Percentage of fusing fraction that occurs in the early phase of stimulation is not affected.

a, b, c. The percentage of the fusing fraction that fuses in the first 50 AP (first burst) of stimulation is unaffected between genotypes ($X^2(3) = 1.891$, $p = .38$; $X^2(3) = 0.547$, $p = .76$; $F(4, 80) = 0.8177$, $p = .52$, respectively).

d, e, f. The percentage of the fusing fraction that fuses in the first 150 AP (3 bursts of 50 AP) of stimulation is unaffected between genotypes ($X^2(3) = 3.655$, $p = .17$; $X^2(3) = 1.296$, $p = .52$; $F(4, 80) = 0.4299$, $p = .79$, respectively)

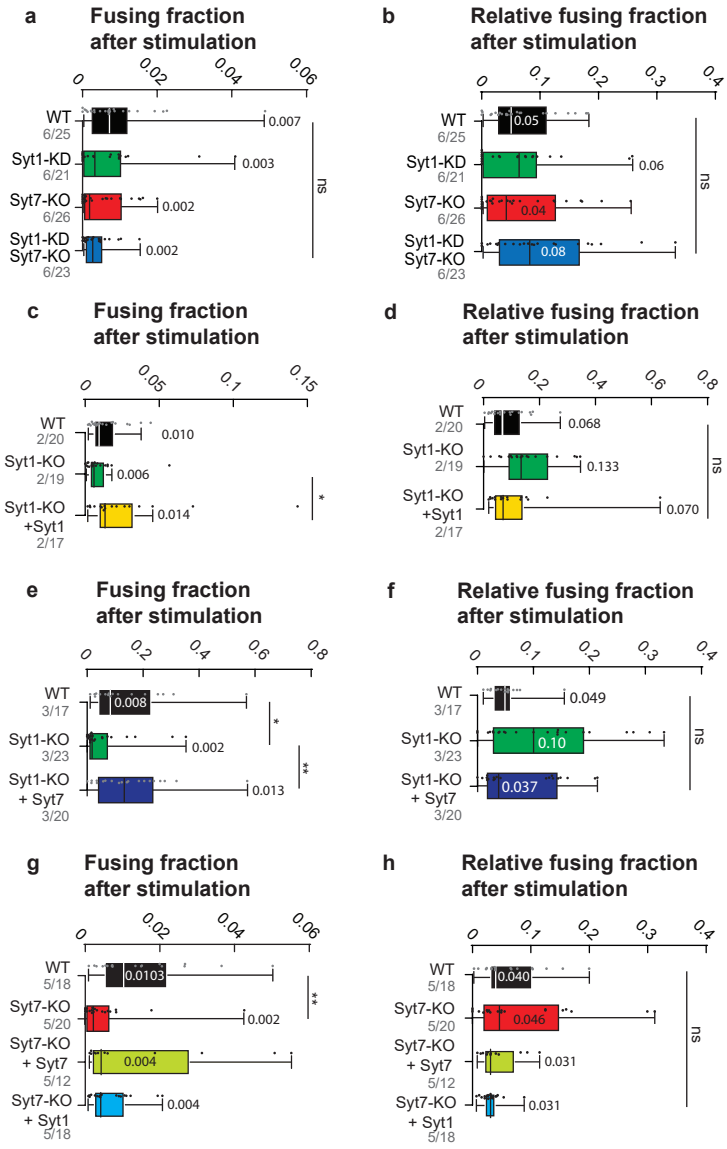

Supplementary Figure 4: Fusing fraction after stimulation

a. Fusing fraction of events that fuse after the 16 x 50 AP stimulation bursts is not significantly different in Syt1-KD neurons compared to Syt1-KD/Syt7-KO neurons ($X^2(4) = 5.29$, $p = .15$).

b. The relative amount of fusion (fraction of fusion events after stimulation / total fusing fraction) is not significant different ($X^2(4) = 3.34$, $p = .34$).

c. Fusing fraction of events that fuse after the 16 x 50 AP stimulation bursts is significantly reduced in Syt1-KO neurons compared to Syt1-KO + Syt1 neurons ($X^2(3) = 7.64$, $p = .022$).

d. The relative amount of fusion is not significantly higher in Syt1-KO neurons compared to WT neurons ($X^2(3) = 5.4$, $p = .07$).

e. Fusing fraction of events that fuse after the 16 x 50 AP stimulation bursts is significantly reduced in Syt1-KO neurons compared to WT and Syt1-KO + Syt7 neurons ($X^2(3) = 12.65$, $p = .0018$).
f. The relative amount of fusion is not significant different ($X^2(3) = 2.643$, $p = .27$).
g. Fusing fraction of events that fuse after the 16 x 50 AP stimulation bursts is significantly different between WT and Syt7-KO ($X^2(4) = 10.22$, $p = .017$).
h. The relative amount of fusion is not significant different ($X^2(4) = 3.969$, $p = .026$).

→

Supplementary Figure 5: DCV fusion and DCV event duration in neurons infected with variable amounts of Syt1-expressing lentivirus.

a. Representative images of WT and Syt1-KO neurons infected with variable amounts of Syt1-expressing lentivirus, immunostained for Syt1 (red) and VGluT1 (green). Scale bar = 10 µm.
b. Syt1 intensity in neurons. Multiple comparisons to WT neurons shown exclusively for clarity purposes ($F(7,82) = 25.66$, $p < .0001$). Numbers of neurons included in analyses: $n_{WT} = 13$; $n_{KO} = 9$; $n_{KO + 0.5\ µl} = 8$; $n_{KO + 1\ µl} = 10$; $n_{KO + 1.5\ µl} = 13$; $n_{KO + 2\ µl} = 14$; $n_{KO + 3\ µl} = 12$; $n_{KO + 4\ µl} = 11$.
c. Syt1 intensity in VGluT1+ synapses. Multiple comparisons to WT neurons shown exclusively for clarity purposes ($F(7,82) = 24.22$, $p < .0001$). Number of neurons equal to panel b.
d. Median number of neuropeptide vesicle fusion events in WT and Syt1-KO neurons with and without different volumes of Syt1 expression in a cumulative plot.
e. Event duration of DCV fusion events in WT and Syt1-KO neurons with and without different volumes of Syt1 expression in a normalized cumulative plot.
f, g. Same as D, but with higher amounts of lentivirus. Note that data presented in Fig D-E and F-G are gathered in a single experiment, distributed over two panels, presenting the WT data twice. Panels were splitted for clarity purposes.
h. Number of DCV fusion events per neuron. All volumes significantly increase DCV fusion ($X^2(8) = 32.88$, $p < .0001$).
i. Median event duration in WT and Syt1-KO neurons with and without different volumes of Syt1 expression ($X^2(8) = 22.84$, $p = .0018$).

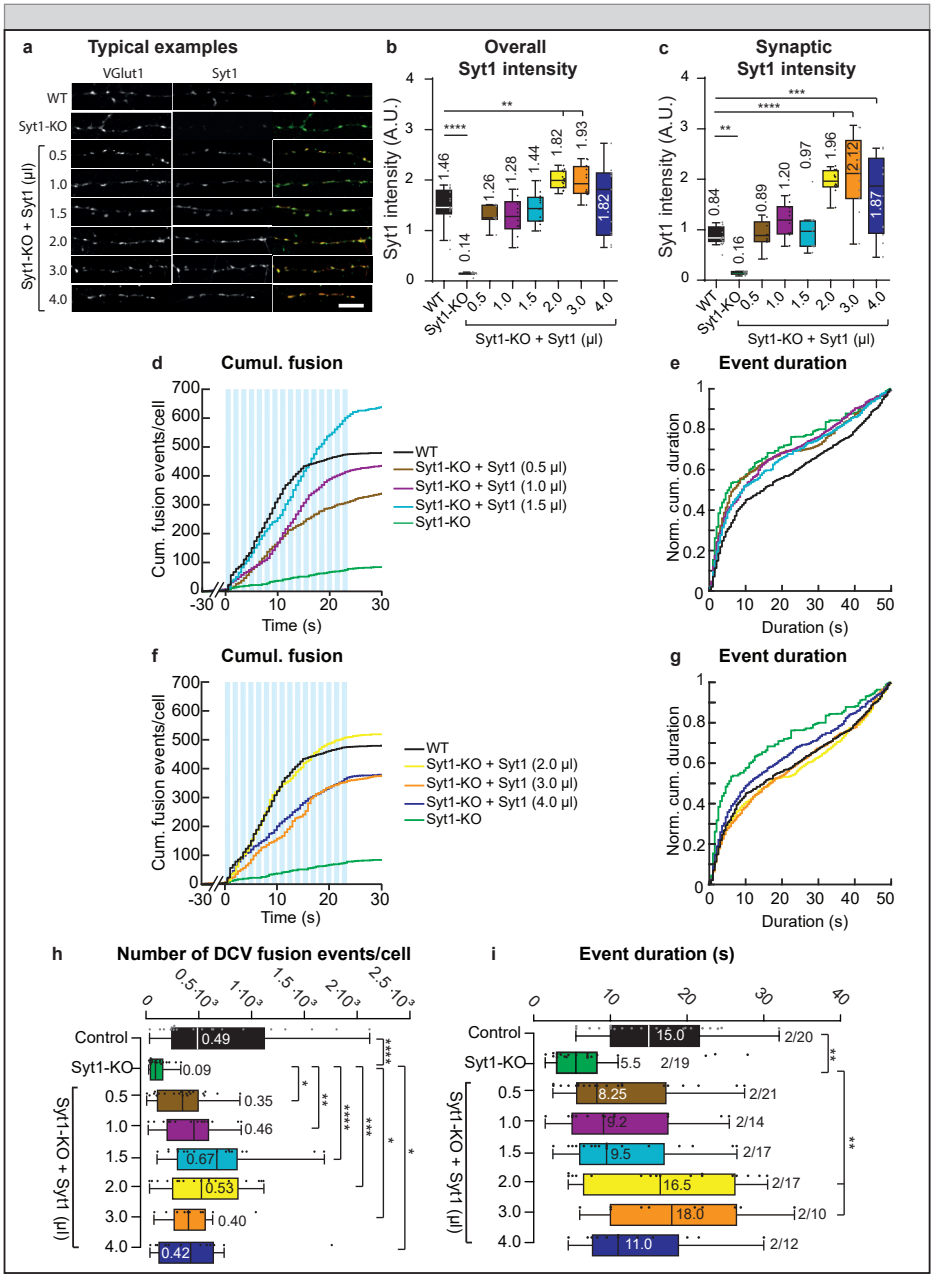

Supplementary Figure 5. Caption on previous page

←···

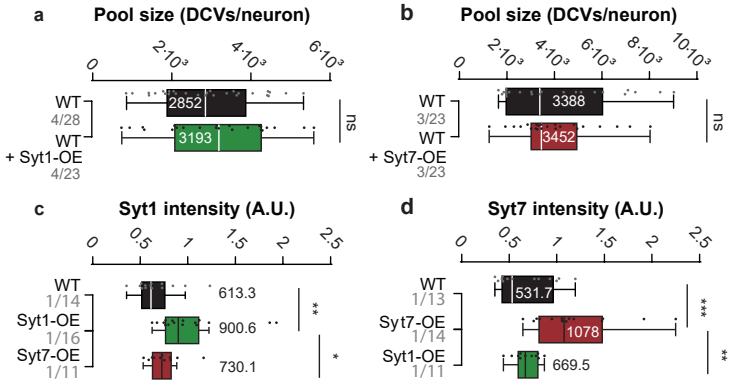

Supplementary Figure 6: Syt1 and Syt7 overexpression in WT neurons increases the fusing fraction of DCVs.

a. Fusing fraction as presented in Fig. 3C, but with individual neurons plotted.

b. Fusing fraction as presented in Fig. 3F, but with individual neurons plotted.

c. Fluorescence intensity of WT neurons overexpressing Syt1 ($U = 35.00$, $p = .0009$)

d. Fluorescence intensity of WT neurons overexpressing Syt7 ($F(2,35) = 10.35$, $p = .0003$).

Chapter 3

Synaptotagmin-1 and to lesser extent Synaptotagmin-7 co-travel and co-fuse with dense-core vesicles

Rhodé van Westen[1,2], Josse Poppinga[1], Ruud F. Toonen[1*], Matthijs Verhage[1,2*]

[1] Department of Functional Genomics, Center for Neurogenomics and Cognitive Research, Neuroscience Campus Amsterdam, Vrije Universiteit (VU) Amsterdam

[2] Department of Clinical Genetics, UMC Amsterdam, The Netherlands

Parts of this chapter are accepted for publication in *Proceedings of the National Academy of Sciences of the United States of America* (PNAS) together with Chapter 2 and 4.

ABSTRACT

Syt1 and Syt7 are both involved in the secretion of neuropeptides and neuromodulators from dense core vesicles (DCV) in neurons (chapter 2). However, where in the DCV secretory pathway both Syts operate remains unclear. In this study, we assessed the cellular localization of Syt1 and Syt7 in mouse hippocampal neurons, and addressed whether they are present on traveling and fusing DCVs. DCVs, labeled by expression of NPY-super ecliptic pHluorin (SEP), highly colocalized with endogenous Syt1, and to lesser extent with endogenous Syt7. Expression of Syt7-SEP, but not Syt1-SEP, combined with bath application of acid/NH4 washes, shows that Syt7, and to lesser extent Syt1, localized to the plasma membrane. In contrast, Syt1-SEP mainly localized to intracellular acidic compartments. Syt1-SEP traveled with DCVs in neurites and was present on fusing DCVs, but Syt7-SEP to a much lesser extent. Additionally, Syt7-SEP traveled with lysosomes, Syt1 less so. These results suggest that Syt1 and Syt7 localize to largely distinct subcellular compartments. Syt1 supports DCV fusion while localized on fusing DCVs, whereas Syt7's supports DCV fusion primarily from another location, possibly the plasma membrane.

INTRODUCTION

Synaptotagmins are a family of transmembrane proteins that are involved in a variety of membrane trafficking events in neurons (for review, see Wolfes and Dean, 2020). 17 Synaptotagmin paralogs are identified, of which most are expressed in the brain (Mittelsteadt et al., 2009). Syt paralogs have different subcellular localizations and variable responses to stimulation (Dean et al., 2012). Syt1 is present on synaptic vesicles (Brose et al., 1992; Matthew et al., 1981; Takamori et al., 2006), and supports synchronous SV fusion (Geppert et al., 1994). Moreover, Syt1 possibly localizes to lysosomes (Vukoja et al., 2018), but may not regulate lysosomal fusion (Martinez et al., 2000). Syt1 is also present on at least a subpopulation of DCVs in the brain, as shown by immunocapture of DCVs (Pons-Vizcarra, 2020), and by subcellular fractionation and immunogold labeling (Walch-Solimena et al., 1993). Vesicular targeting of Syt1 depends on an N-glycosylation site at the N-terminal of the protein (Han et al., 2004). A Syt1 mutant that lacks the N-glycosylation site is directed to the plasma membrane and reduces the readily-releasable pool (RRP) of SVs (Han et al., 2004). GAP43-Syt1, a mutant that is also located on the plasma membrane, supports SV fusion but not endocytosis (Hui et al., 2009; Yao et al., 2012b). This suggests that Syt1 localization is a key factor in supporting its diverse biological functions.

Syt7, in contrast to Syt1, localizes mostly to the plasma membrane in neurons (Sugita et al., 2001). In synaptic boutons, hemagglutinin-tagged Syt7 locates to a distance of ~100 nm from the active zone, but is not present in the active zone itself (Wang et al., 2020). Syt7 may also be present on SVs (Sugita et al., 2001; Taoufiq et al., 2020), but is not detected by all studies/methods, possibly because Syt7 levels on SVs are low and require high sensitivity methods for detection (Takamori et al., 2006; Taoufiq et al., 2020). Stimulation triggers increased Syt7-pHluorin fluorescence in axons exclusively (Dean et al., 2012), suggesting that vesicular Syt7 localization of fusogenic vesicles is restricted to axons. In neurons, Syt7 regulates asynchronous SV fusion, SV pool replenishment, synaptic facilitation, RRP maintenance and endocytosis (Bacaj et al., 2013, 2015; Jackman et al., 2016; Li et al., 2016; Liu et al., 2014; Virmani et al., 2003). Syt7 is also present on lysosomes and regulates lysosomal fusion in fibroblasts (Martinez et al., 2000), and possibly in neurons as well (Padamsey et al., 2017). In line with these observations, Syt7KO animals present inflammation and fibrosis in skin and skeletal muscle (Chakrabarti et al., 2003), an effect possibly related to the function of lysosomal fusion in plasma membrane repair regulated by Syt7 (Reddy et al., 2001).

In neuroendocrine cells, Syt1 and Syt7 support fast and slow secretion respectively (Schonn et al., 2008; Voets et al., 2001). The two sensors are targeted to vesicles with different diameters, although a subset of secretory granules carry both sensors (Bendahmane et al., 2020; Rao et al., 2014; Tawfik et al., 2020; Zhang et al., 2011b). In line with their different Ca^{2+} affinities (Sugita et al., 2002), Syt7 triggers granule fusion at lower Ca^{2+} concentrations than Syt1 and with different fusion kinetics (Bendahmane et al., 2020; Rao et al., 2014, 2017).

The lack of additive effect (Chapter 2) together with the functional redundancy of Syt1 and Syt7 as mediators of fusion (Chapter 2) suggest that the sensors operate in the same pathway, and possibly at the same location. It is currently unknown to what extent Syt1 and Syt7 localize to DCVs. Our aim in the current study was to address where in the neuron Syt1 and Syt7 are located, and specifically whether Syt1 and Syt7 are both present on DCVs. We report that Syt7 is abundant on the plasma membrane, whereas Syt1 mainly localizes to acidic intracellular compartments. Syt1, and to a lesser extent Syt7, co-travels with DCVs and co-localizes with fusing DCVs. In addition, Syt7, and to a lesser extent Syt1, co-travels with lysosomes. Together, these data suggest that Syt1 is present on and necessary for DCV fusion, while Syt7 regulates DCV fusion while being largely on the plasma membrane.

RESULTS

Syt1, and to lesser extent Syt7, are present on DCVs

The lack of additive effect in Syt1-KD/Syt7-KO neurons (Chapter 2) suggests that Syt1 and Syt7 operate in a single pathway. To address where in the neuron Syt1 and Syt7 are located, and specifically whether Syt1 and Syt7 are both present on DCVs, we first tested the co-localization in neurites of endogenous Syt1/7 with the DCV marker NPY-SEP and synapse marker VGluT1. Colocalization was expressed by the Manders M1/M2 coefficient, which reports the co-occurring fraction of color 1 with color 2, and ranges from 0 (no overlap) to 1 (complete overlap). Syt1 and VGluT1 immunostaining largely colocalized (Manders coefficient VGlut1:Syt1 = 0.83 and Syt1:VGluT1 = 0.70) (Supplementary Fig. S1), in line with Syt1's established localization on synaptic vesicles (Brose et al., 1992; Matthew et al., 1981; Takamori et al., 2006). However, at higher laser power, Syt1 puncta were observed extrasynaptically (Fig. 1A, Supplementary Fig. S1), and highly colocalized with NPY-SEP (Manders NPY:Syt1 = 0.72, Syt1:NPY = 0.62) (Fig. 1A, B). The colocalization between NPY:Syt1 was significantly higher than NPY:VGluT1 (Fig. 1B, Manders NPY:VGlut1 = 0.40 and

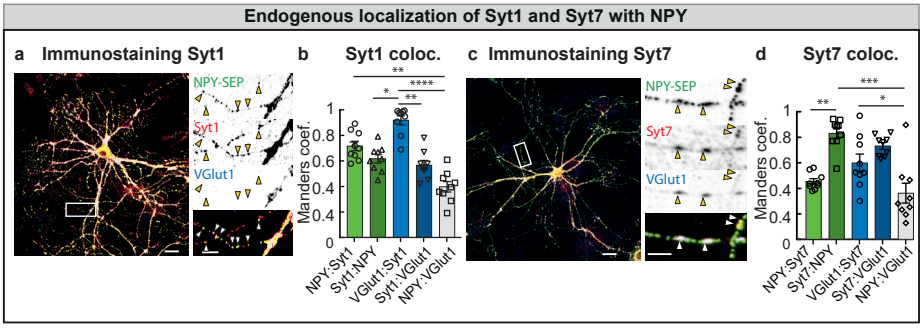

Figure 1: Syt1, and to lesser extent Syt7, co-localizes with NPY-mCherry.

a. Representative image of neuron immunostained for Syt1, NPY-SEP and VGluT1. Scale bar of large image =20 µm. Scale bar of zoomed image = 5 µm.

b. Quantification of colocalization between Syt1, NPY-SEP and VGluT1 ($X^2(5) = 31.74$, $p < .0001$).

c. Representative image of neuron immunostained for Syt7, NPY-SEP and VGluT1. Scale bar of large image = 20 µm. Scale bar of zoomed image = 5 µm.

d. Quantification of colocalization between Syt7, NPY-SEP and VGluT1 ($X^2(5) = 25.25$, $p < .0001$).

0.36 in Syt1KO and Syt7KO neurons, respectively). Together, this suggests that Syt1 is expressed on DCVs.

NPY-SEP colocalized only partially with Syt7 (Manders coefficient = 0.45) (Fig. 1C, D), while, conversely, Syt7 colocalized with NPY-SEP and also with the synaptic vesicle marker VGluT1 (Manders coefficient = 0.83 and 0.73, respectively). Hence, Syt7 localizes to presynaptic terminals and colocalizes with some extrasynaptic DCVs, but many DCVs may not express Syt7. Together, this suggests that DCVs express Syt1, and to a lesser extent Syt7.

Next, we expressed Syt1 or Syt7 fusion constructs with SEP fused to their N-terminus, which is expected to be incorporated at the luminal side of DCVs, as described for SVs (Perin et al., 1990). In this way, plasma membrane-targeted Syt1/7-SEP is quenched by application of acidic solution and DCV-targeted Syt1/7-SEP is dequenched by NH_4. Hence, acid and NH_4 washes probe the plasma membrane and vesicular fraction of Syt1/7-SEPs, respectively (Fig. 2A). Syt1-SEP was primarily present on acidic intracellular compartments with only ±20% on the plasma membrane (Fig. 2B, D), in line with previous reports (Liu et al., 2014; Wienisch and Klingauf, 2006). Syt7-SEP localized predominantly to the plasma membrane, and ~40% was localized to acidic intracellular compartments (Fig. 2C, D), also in line with previous reports in neurons (Dean et al., 2012; Li et al., 2016; Liu et al., 2014). These results suggest that Syt1-SEP and Syt7-SEP have different cellular distributions and that

Syt1 is primarily targeted to secretory vesicles, while Syt7 is largely targeted to the plasma membrane.

To confirm if Syt1 (and Syt7 to some extent) is indeed targeted to DCVs, we tested co-traveling of Syt1/7-mCherry fusion constructs with NPY-SEP, visualized by NH4 superfusion (Fig. 2E). In contrast to colocalization analysis (Fig 1A-D), co-traveling analysis only includes moving puncta/vesicles. To ensure these Syt1/7-mCherry fu-

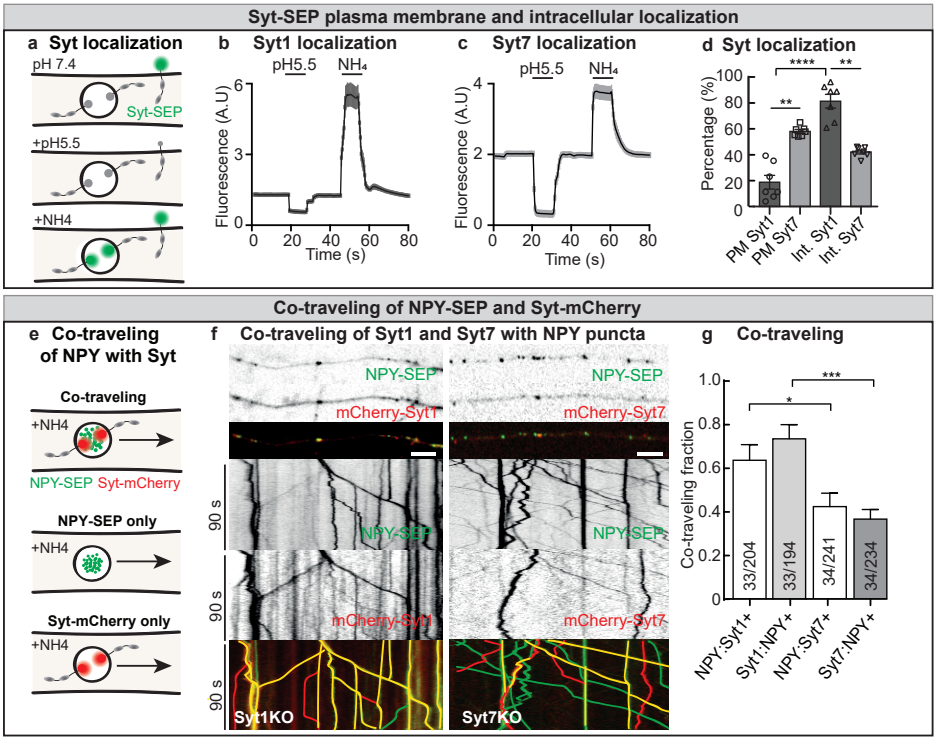

Figure 2: Syt1, and to lesser extent Syt7, localizes to intracellular acidic compartments and co-travels with DCVs.

a. Cartoon of Syt-SEP, localized at the plasma membrane or at acidic intracellular compartments, at a neutral pH (7.4), and during bath application of acidic pH (pH 5.5) or NH_4-containing imaging solution.

b, c. Average Syt1-SEP (n = 7 cells) (F) and Syt7-SEP (n = 7 cells) (G) fluorescence response during bath application of pH5.5 or 50 mM NH_4 Tyrode's solution.

d. Quantification of plasma membrane/intracellular fraction of Syt1-SEP and Syt7-SEP ($X^2(4) = 24.56$, $p < .0001$).

e. Cartoon of co-traveling of NPY-mCherry and Syt-SEP vesicles.

f. mCherry-Syt1 and mCherry-Syt7 partially co-travel with NPY-SEP vesicles. Scale bars = 5 µm.

g. Quantification of co-traveling of NPY with Syt1-SEP or Syt7-SEP, and *vice versa* ($X^2(4) = 19.47$, $p < .0002$). *$p < .05$, **$p < .01$, ***$p < .001$, ****$p < .0001$, ns $p > .05$.

sion constructs are functional in DCV fusion, we first confirmed that the mCherry-Syt constructs fully rescued DCV fusion in Syt1-KO and Syt7-KO neurons, respectively (Supplementary Fig. S2). Next, we tested the co-traveling of these rescue constructs with DCV-marker NPY-SEP (Fig. 2F, G). The DCV marker traveled together with Syt1-mCherry in 64 ± 3% of cases and to a lesser extent with Syt7 (42 ± 4%, Fig. 2F, G). These data suggest that Syt1 localizes to DCVs, and Syt7 also, but to a lesser extent.

Syt7 mediates lysosomal fusion in fibroblasts, and recent evidence suggests that Syt7 regulates lysosomal fusion in neurons as well (Martinez et al., 2000; Padamsey et al., 2017). Therefore, we next assessed whether, in addition to DCVs, Syt1 and Syt7 also co-travel with the lysosomal marker LAMP1. For this purpose, LAMP1-EGFP was expressed together with mCherry-Syt. LAMP1-EGFP puncta were abundant and highly mobile (Fig. 3A). Indeed, Syt7, and to a lesser extent Syt1, co-traveled with LAMP1 (Fig. 3B), suggesting a role of Syts in neuronal lysosomal fusion.

The high localization of LAMP1 and Syts, and of NPY and Syts, suggests that NPY and LAMP1-EGFP are (partially) expressed on the same organelles. To test this hypothesis, we expressed NPY-mCherry with LAMP1-EGFP. NPY-mCherry is a red DCV-fusion reporter that detects DCV cargo release (Gandasi et al., 2015) (in contrast to NPY-SEP, which detects fusion pore opening). Traveling LAMP1-EGFP and NPY-mCherry puncta were abundant and mobile. NPY-mCherry vesicles often co-traveled with LAMP1-EGFP (Fig. 4A). We next addressed whether fusing NPY-mCherry vesicles are LAMP1+ or LAMP1-. None of the fusing NPY-mCherry vesicles

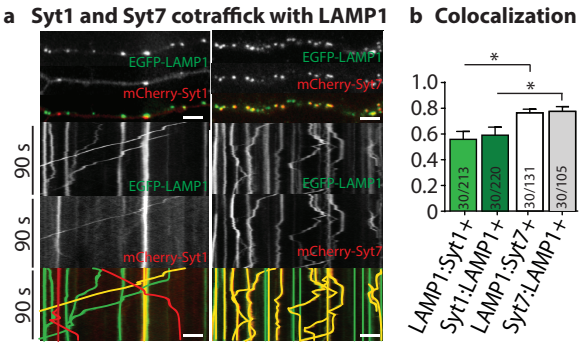

Figure 3: Syt7, and to lesser extent Syt1, co-travels with LAMP1-EGFP.

a. Representative examples of traveling EGFP-LAMP1$^+$ puncta and mCherry-Syt1$^+$ (left panel) or mCherry-Syt7$^+$ (right panel).

b. Quantification of colocalization between LAMP1 and Syt1 (green), and LAMP1 and Syt7 (white/gray) is significantly different ($X^2(4) = 11.72$, $p < .0084$). *$p < .05$.

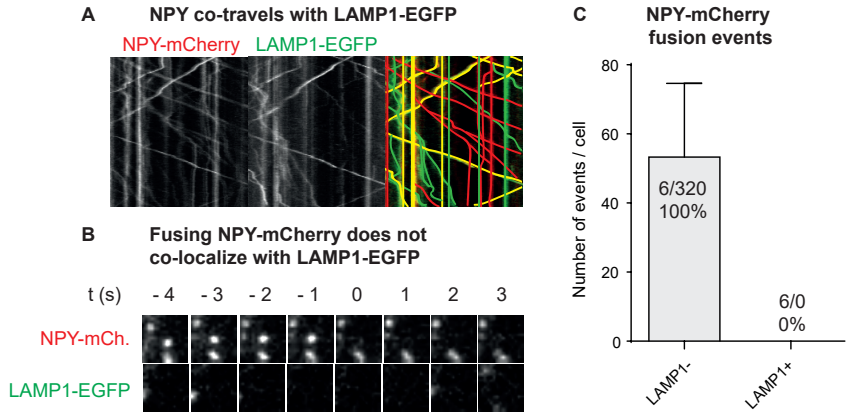

Figure 4: NPY-mCherry vesicles co-travel with LAMP1, but only LAMP- NPY+ vesicles fuse.
a. Representative kymograph of NPY-mCherry with LAMP1-EGFP.
b. Representative example of fusing LAMP-EGFP-/NPY-mCherry+ vesicle.
c. Quantification of LAMP1-EGFP presence at NPY-mCherry fusion events. Number before the dash represents the number of neurons, and after the dash presents the number of fusion events.

(n_{cells} = 6, n_{ves} = 320) co-localized with LAMP1 (Fig 4B, C). This suggests that some NPY-mCherry vesicles are LAMP1+, but that these vesicles are not fusogenic.

To test whether Syt1 and Syt7 are present on fusing DCVs, Syt1-SEP or Syt7-SEP were co-expressed with NPY-mCherry in Syt1-KO or Syt7-KO neurons respectively (Fig. 5A), together with Synapsin-ECFP as synapse marker. DCV fusion events are defined as the (sudden) disappearance of NPY-mCherry puncta, and corresponding Syt1/7-SEP dequenching in the same location was quantified.

Syt1 is an abundant component of SVs (Brose et al., 1992; Matthew et al., 1981; Takamori et al., 2006). Therefore, Syt1-SEP was co-expressed with Synapsin-ECFP to discriminate between synaptic and extrasynaptic Syt1-SEP events. Syt1-SEP fluorescence at Synapsin-ECFP labeled synapses showed a strong and gradual increase upon stimulation, most likely due to Syt1-SEP expression on fusing SVs (Supplementary Fig. S3), which was not the case at extrasynaptic sites (Supplementary Fig. S3). Therefore, only extrasynaptic NPY-mCherry fusion events were analyzed for co-occurrence of Syt1-SEP dequenching. Syt1-SEP dequenching directly preceded NPY-mCherry loss in 67% of the events (Fig. 5B-C), suggesting that the majority of fusing DCVs express Syt1-SEP.

We next tested whether Syt7 is present on fusing DCVs. In 35 ± 0.05% of the DCV fusion events, a Syt7-SEP dequenching preceded NPY-mCherry loss (Fig. 5D, E). These

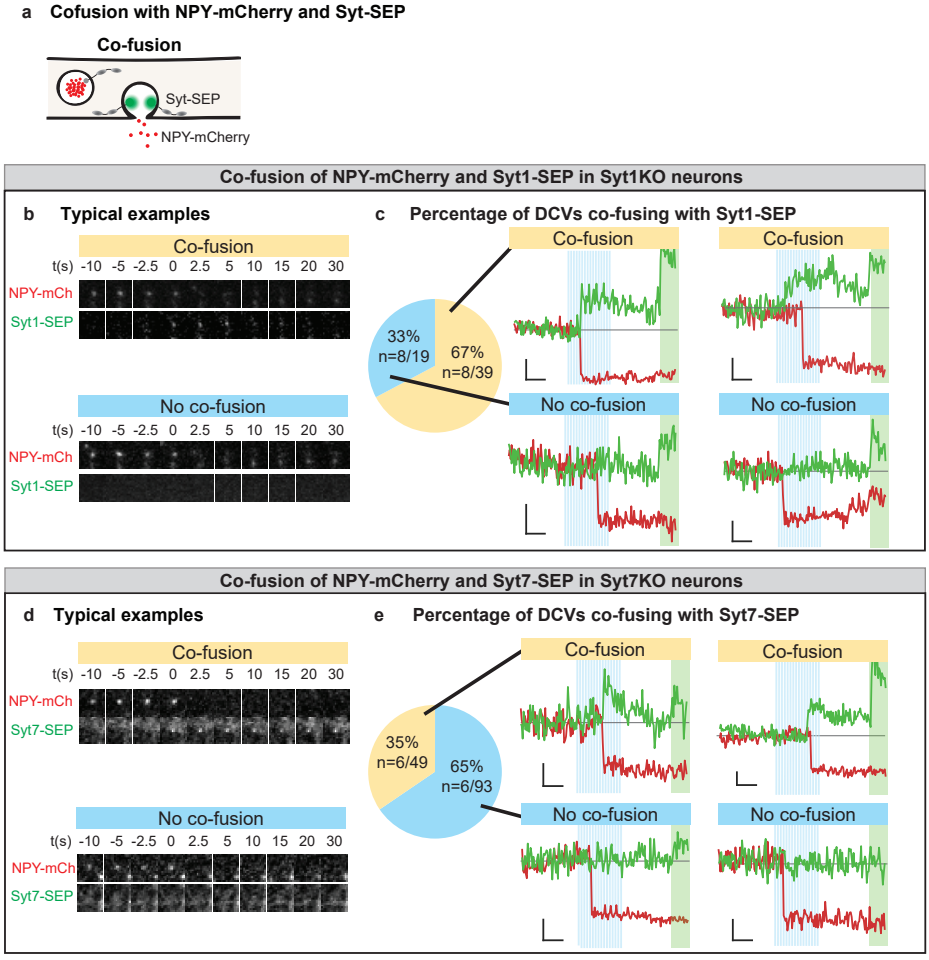

Figure 5: Fusing NPY-mCherry vesicles co-localize with Syt1-SEP and to lesser extent with Syt7-SEP events.

a. Schematic representation of NPY-mCherry events co-fusing with Syt-SEP.
b. Representative images of fusing NPY-mCherry, with and without increase of Syt1-SEP.
c. Percentage of co-localization of fusing NPY-mCherry events (red lines of typical example traces) with sudden appearance of Syt1-SEP (green lines of typical example traces). n represents the number of cells and the number of extrasynaptic NPY fusion events.
d. Representative images of fusing NPY-mCherry with and without increase of Syt7-SEP.
e. Percentage of co-localization of fusing NPY-mCherry events (red lines of typical example traces) with sudden appearance of Syt7-SEP (green lines of typical example traces). n represents the number of cells and the number of NPY fusion events.

events occurred at Synapsin-ECFP labeled synapses and outside synapses (Fig. S3). Hence, the majority of fusing DCVs does not express Syt7-SEP. Together these data suggest that Syt1 is present on traveling and fusing DCVs while Syt7 regulates DCV fusion primarily from another location, probably the plasma membrane.

DISCUSSION

In neurons, Syt1 is present on SVs and Syt7 highly localizes to the plasma membrane (Brose et al., 1992; Matthew et al., 1981; Sugita et al., 2001; Takamori et al., 2006; Taoufiq et al., 2020). Both sensors localize to secretory granules in neuroendocrine cells, but largely to different populations (Rao et al., 2014; Tawfik et al., 2020). However, whether Syt1 and Syt7 localize to neuronal DCVs remains unknown. In this study, we show that endogenous Syt1, and to a lesser extent Syt7, colocalized with the DCV reporter NPY-SEP (Fig. 1A-D). Syt1-SEP mainly localized to acidic intracellular compartments, whereas Syt7-SEP localized to the plasma membrane (Fig. 2A-D). In line with these observations, NPY-SEP co-traveled with mCherry-Syt1 through neurites, but much less so for mCherry-Syt7. Moreover, Syt1 was present on fusing DCVs, whereas Syt7 did so to a lesser extent. Syt7, on the other hand, co-traveled to a high extent with lysosomal marker LAMP1. Together these results suggest that Syt1 is present on fusing DCVs whereas Syt7 regulates DCV fusion while being located elsewhere, possibly the plasma membrane.

Our experiments with Syt1/7-mCherry and Syt1/7-SEP show that the two sensors are targeted to different cellular locations, Syt1 to DCVs (and SVs) and Syt7 mostly to the plasma membrane (Fig. 2, 5). Despite these different cellular locations, overexpression of these sensors fully compensates for each other's loss in DCV fusion (Chapter 2), producing a normal number of DCV fusion events in neurons (over-) expressing only one of the two sensors. This indicates that the subcellular location of Ca^{2+}-sensors for DCV fusion, and also their Ca^{2+}-sensitivity, is rather different between Syt1 and Syt7 (Li et al., 1995; Sugita et al., 2002), and does not have a major influence on their capacity to support DCV fusion.

Syt1 mainly localized to intracellular acidic compartments (Fig. 2B, D), as expected due to its known targeting to SVs (Brose et al., 1992; Matthew et al., 1981; Takamori et al., 2006). As many as 200-1000 SVs are present per hippocampal bouton (Harris and Sultan, 1995; Schikorski and Stevens, 1997), each carrying an estimate of 7 - 15 Synaptotagmin molecules per vesicle (Mutch et al., 2011; Takamori et al., 2006). As a result, immunostaining for Syt1 brightly stains synapses and is therefore

generally used as a synaptic marker protein. However, other weaker signals may be missed when exclusively focusing on synaptic signals. In this study, we used a higher laser power that saturates synaptic areas, to visualize weaker, extrasynaptic Syt1 signals. This visualized extrasynaptic Syt1 puncta that frequently colocalized with NPY (Fig.1A, B, Supplementary Fig. S1). NPY colocalized for ~72% with Syt1 (Fig 1B). Moreover, the majority of traveling DCVs co-traveled (64%) and co-fused (67%) with Syt1 (Fig 2G, 5C). This is in line with previous reports that detect Syt1 in DCV fractions and on isolated DCVs in neurons (Pons-Vizcarra, 2020; Walch-Solimena et al., 1993) and in neuroendocrine granules (Matthew et al., 1981). Together, this suggests that DCVs express Syt1 and that Syt1 regulates DCV fusion from this location.

In contrast, Syt7 prominently localized to the plasma membrane, in line with previous observations (Dean et al., 2012; Liu et al., 2014; Sugita et al., 2001). However, a significant portion (40%) localized to acidic intracellular compartments. Syt7 was previously not detected on SVs (Sugita et al., 2001; Takamori et al., 2006), but is detected when using more sensitive detection methods (Taoufiq et al., 2020), suggesting that low levels of Syt7 may be present on SVs. In this study, we show that NPY co-travels (42%) and co-fuses (35%) with Syt7, albeit to a significantly lower extent than with Syt1. The lower co-fusion percentages suggest that fusing DCVs do not require Syt7 on the vesicle membrane for fusion.

Possibly, overexpression results in localization artefacts (e.g. missorting to the plasma membrane or 'overflowing' to other locations) unless lentiviruses express Syts at endogenous levels in the null-mutants. Using our lentiviral vectors, expression levels increased 50% and 100% in WT neuron overexpressing Syt1 and Syt7 respectively (Chapter 2, Fig. S6C, D), and expressed Syt1 to/beyond WT levels in Syt1KO neurons (Chapter 2, Fig. S5A-C). Nevertheless, overexpression of Syt1 and Syt7 rescued DCV fusion in KO neurons (Chapter 2), suggesting that targeting was sufficient to support normal functioning of both Syts. Immunocytochemistry of endogenous Syt1 with and without permeabilization shows that ~10% of Syt1 localizes to the plasma membrane, and overexpression of Syt1-pHluorin showed ~20% surface localization (Wienisch and Klingauf, 2006), similar to our plasma membrane fraction of Syt1-pHluorin (Fig. 2B, D). This may indicate that expression of Syt1-SEP results in a slight accumulation on the plasma membrane. Similarly, expression of Syt1-SEP or Syt7-SEP may result in higher colocalization with DCVs. However, the different subcellular targeting of Syt1-SEP and Syt7-SEP was supported by immunostaining of endogenous Syt1 and Syt7 with NPY-pHluorin (Fig. 1). Genome editing, e.g. expression via CRISPR-Cas9, would allow for expression levels close to endogenous levels and would reduce the risk of overexpression artefacts.

Additionally, Syt7 co-traveled to a high extent with LAMP1 (Fig. 3). Colocalization between Syt7 and lysosomal markers has also been observed for neuroendocrine secretory granules and lysosomes in fibroblasts (Fukuda et al., 2004; Martinez et al., 2000), which is in line with Syt7 promoting lysosomal fusion in fibroblasts (Martinez et al., 2000) and possibly neurons as well (Padamsey et al., 2017). However, part of the lysosomal localization of mCherry-Syts may be a result of the resistance of mCherry/GFP-like fluorophores against lysosomal degradation (Katayama et al., 2008). Nevertheless, mCherry-Syt7 localized with LAMP1-EGFP to a significantly higher extent than mCherry-Syt1 suggesting that Syt7-mCherry is targeted to LAMP1+ organelles, rather than mCherry alone. LAMP1 is generally considered as a lysosomal marker. However, the population of $LAMP^+$ vesicles is heterogeneous. Electron microscopy shows that LAMP1 is also detected on autophagic and endolysosomal organelles lacking Cathepsin D/B, the enzymes of degradative lysosomes (Cheng et al., 2018). The acidic nature of some of these organelles may explain why ~40% of Syt7-pHluorin localize to acidic intracellular compartments, as shown by acid washes (Fig. 2C, D). Taken together, the data presented in this chapter suggest that Syt7 localizes to the plasma membrane and to intracellular acidic compartments, of which some are LAMP1+ and NPY+ vesicles.

In addition to Syt7, Syt1 colocalized considerably with LAMP1, although to a lesser extent than Syt7 (Fig 3). Syt1 co-traveling with lysosomal markers has been reported before (Vukoja et al., 2018). The $Syt1^+/NPY^+$ and $Syt1^+/LAMP1^+$ vesicles may be (partially) different populations. However, endogenous NPY is sometimes targeted to $LAMP1^+$ vesicles, likely for degradation (Nahorski et al., 2018). Likewise, we report partial colocalization between NPY and LAMP1 (Fig. 4), showing that the population of NPY^+ vesicles is heterogeneous. However, only LAMP1-/NPY-mCherry vesicles fused (Fig. 4), suggesting that fusing NPY^+ vesicles are DCVs and not lysosomes.

Together, the findings in this chapter suggest that Syt1 is present on traveling and fusing DCVs. Syt7, in contrast, localizes to DCVs to a lesser extent and may regulate fusion from another location, possibly the plasma membrane.

Acknowledgements

We thank Robbert Zalm for cloning and producing viral particles; Frank den Oudsten, Lisa Laan and Desiree Schut for producing glia feeders and primary culture assistance; Joke Wortel for animal breeding; Jurjen Broeke for technical assistance; Jurjen Broeke and Alessandro Moro for Matlab programming; Ingrid Saarloos for protein chemistry; Frank den Oudsten and Joost Hoetjes for genotyping assistance; and members of the CNCR DCV project team for fruitful discussions. This work is supported by an ERC Advanced Grant (322966) of the European Union (to M.V.).

Author contributions

R.v.W, R.F.T. and M.V. designed the experiments. R.v.W. collected and analyzed experimental data. J.P. optimized the stainings for Fig. 1C, D. R.v.W., R.F.T. and M.V. designed the figures and wrote the manuscript.

SUPPLEMENTARY MATERIAL

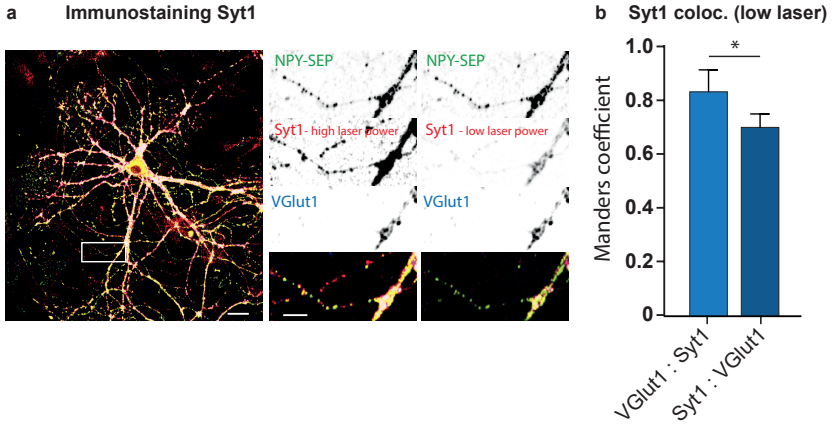

Supplementary Figure 1: Colocalization of endogenous Syt1 and endogenous VGluT1.

a. Representative image of neuron immunostained for Syt1, NPY-SEP and VGluT1 with Syt1 exposed at high (also presented in Fig. 4) and low laser power. Scale bar of the large image = 20 µm and of the zoomed image = 5 µm.

b. Quantification of colocalization between Syt1 and VGluT1 at low laser power ($U = 11.0$, $p = .02$).

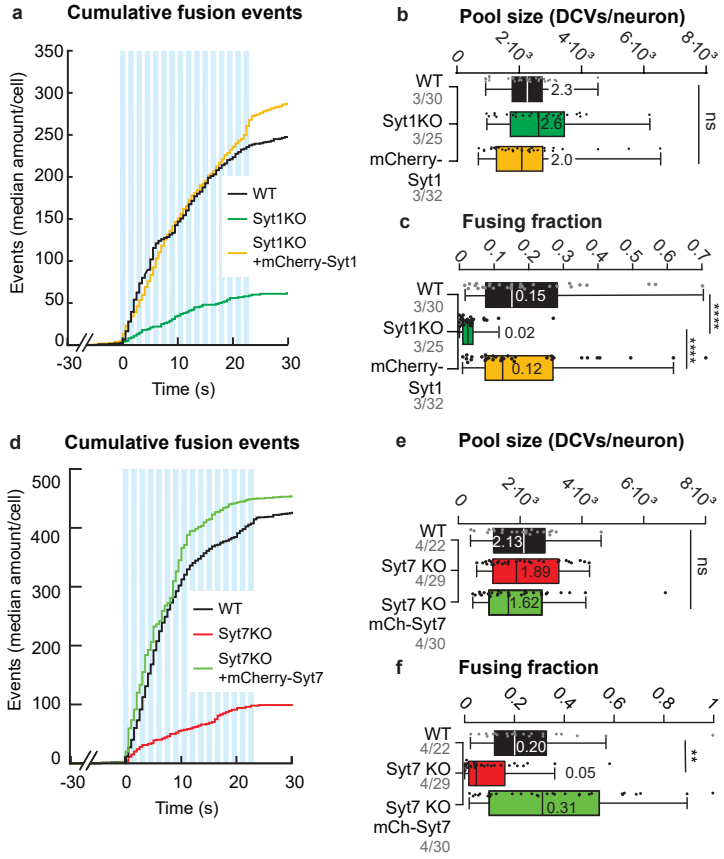

Supplementary Figure 2. mCherry-Syt1 and mCherry-Syt7 rescue DCV fusion.

a. Median number of neuropeptide vesicle fusion events in WT, and Syt1-KO neurons with and without mCherry-Syt1-OE in a cumulative plot.

b. Total number of DCVs per neuron is not significantly different between WT, Syt1-KO and Syt1-KO+mCherry-Syt1-OE ($X^2(3) = 3.02$, $p < .22$).

c. Fusing fraction is rescued by overexpressing mCherry-Syt1 in Syt1-KO neurons. ($X^2(3) = 30.21$, $p < .0001$).

d. Same as A, but with Syt7-KO neurons expressing mCherry-Syt7.

e. Total number of DCVs per neuron is not significantly different between WT, Syt7-KO and Syt7-KO+mCherry-Syt7-OE ($X^2(3) = 1.08$, $p = .58$).

f. Fusing fraction of WT, Syt7-KO and Syt7-KO neurons expression mCherry-Syt7 ($X^2(3) = 21.726$, $p < .0001$). Box plots are plotted with 25% (Q1) and 75% (Q3) interquartile range and Tukey whiskers. Number before and after dash represents number of independent experiments and number of neurons, respectively. $^{**}p < .01$, $^{****}p < .0001$, ns = p>.05

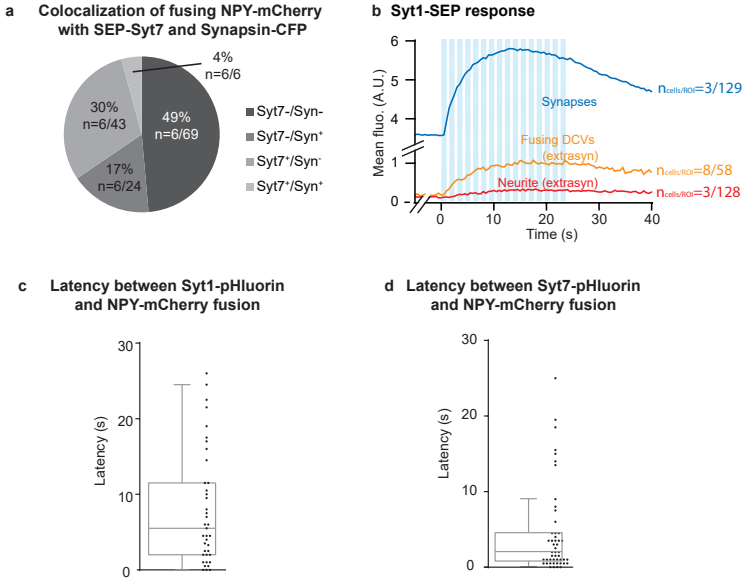

Supplementary Figure 3. Synaptic and extrasynaptic portions of fusing DCVs with Syt7-SEP and mean fluorescence intensity of synaptic and extrasynaptic SEP-Syt1 response.

a. Synaptic and extrasynaptic distributions of fusing DCVs with and without a sudden increase of Syt7-SEP of data presented in Fig. 5E. Number before and after dash represents number of neurons and number of fusing NPY-mcherry, respectively.

b. Mean Syt1-SEP fluorescence of ROIs placed in synaptic and extrasynaptic region with or without DCV fusion events. Syt1-SEP in synaptic ROIs show a strong increase in fluorescence upon stimulation (blue line). Extrasynaptic ROIs without DCV fusing events (red line) have little Syt1-SEP fluorescence increase, whereas ROIs with fusion events increase in Syt1-SEP fluorescence (orange line). Number before and after dash represents number of neurons and number of ROIs, respectively.

c. Latency between the appearance of the Syt1-SEP signal and NPY-mCherry fusion (of co-fusion events presented in Fig. 5, n = 39 events from 8 cells, median = 5.5 s).

d. Latency between the appearance of the Syt7-SEP signal and NPY-mCherry fusion (of co-fusion events presented in Fig. 5, n = 49 events from 6 cells, median = 2.0 s).

Chapter 4

Synaptotagmin-1, but not Synaptotagmin-7, regulates dense-core vesicle fusion pore duration

Rhodé van Westen[1,2], Josse Poppinga[1], Ruud F. Toonen[1*], Matthijs Verhage[1,2*]

[1] Department of Functional Genomics, Center for Neurogenomics and Cognitive Research, Neuroscience Campus Amsterdam, Vrije Universiteit (VU) Amsterdam

[2] Department of Clinical Genetics, UMC Amsterdam, The Netherlands

Parts of this chapter are accepted for publication in *Proceedings of the National Academy of Sciences of the United States of America* (PNAS) together with Chapter 2 and 3.

ABSTRACT

Calcium sensors are essential for secretory vesicle exocytosis, yet little is known regarding how calcium sensors regulate fusion pore kinetics. Here, we show that the duration of single dense-core vesicle (DCV) fusion events was reduced in Synaptotagmin-1 (Syt1)-deficient neurons, but not in Synaptotagmin-7 (Syt7)-deficient neurons. Syt7 overexpression did not rescue event duration in Syt1-deficient neurons, suggesting that Syt7 does not support fusion pore duration/stability. Additionally, Syt1 overexpression in WT neurons, but not Syt7 overexpression, increased the fusion event duration, suggesting Syt1 is sufficient to prolong fusion pores. Finally, GAP43-Syt1 did not restore fusion event duration in Syt1 deficient neurons, possibly because vesicular localization of Syt1 is required to support normal fusion pore duration. We conclude that Syt1, but not Syt7, regulates fusion pore duration. Syt1 triggers fusion and additionally promotes a prolonged open state of the fusion pore.

Keywords: Fusion pore duration, dense-core vesicles, Synaptotagmin-1, Synaptotagmin-7, hippocampal neurons

INTRODUCTION

Neuronal communication primarily relies on the Ca^{2+}-dependent secretion of chemical signals from two secretory organelles: synaptic vesicles (SVs), which release neurotransmitters, and dense-core vesicles (DCVs) secreting neuropeptides. Ca^{2+} regulates vesicle fusion pore opening as well as the fusion pore size and expansion rate (Fernández-Chacón and Alvarez de Toledo, 1995; Hartmann and Lindau, 1995; Wang et al., 2006). After DCV pore opening, the fusion pores may fully expand, merge with the plasma membrane and exocytose the neuropeptide cargo into the extracellular space (Albillos et al., 1997; Alés et al., 1999; van Kempen et al., 2011; Wit et al., 2009). Alternatively, fusion pore opening may be restricted, leading to only partial cargo release, and subsequently close and acidify, leaving the DCV intact (Alés et al., 1999; van Kempen et al., 2011; MacDonald et al., 2006). The latter mode is referred to as 'kiss-and-run'. Therefore, dilation or re-closure of fusion pores may regulate the extent of DCV cargo release.

The exocytotic fusion pore consists of a mix of membrane phospholipids and the transmembrane domains of SNAREs and Synaptotagmins (Bao et al., 2018a). In order to drive fusion, the C2 domains of the main Ca^{2+}-sensor Synaptotagmin-1 (see chapter 2) insert into acidic phospholipid membranes (for review, see McMahon et al., 2010). Via its interaction with SNAREs, Ca^{2+} and PIP2, an acidic phospholipid in the plasma membrane, Syt1 facilitates fusion pore stability and dilation (Bai et al., 2004b; Das et al., 2020; Holz et al., 2000; Micheva et al., 2001; Wu et al., 2019). In silico studies suggest that Syt1 acts as a lever that increases pore size by inserting into the plasma membrane after binding Ca^{2+} (Wu et al., 2019). Indeed, in neuroendocrine PC12 cells, a Syt1 mutant with increased membrane interaction, facilitates fusion pore expansion and cargo release (Lynch et al., 2008). In line with these findings, a Syt1 mutant incapable of binding Ca^{2+} shortens the event durations of the remaining fusion events (Lynch et al., 2008). Summarized, Syt1 requires its membrane interaction and Ca^{2+}, not only to open fusion pores, but also to support fusion pore stability, dilation and subsequent cargo release.

In neuroendocrine cells, fusion pores of secretory granules can be accurately studied by amperometry, which reports the opening and dilation of fusion pores with a pre-spike foot (PSF). The PSF is studied to gain insight in the initial fusion pore, which may last up to several seconds prior to full expansion of the pore, and is caused by release of small amounts of norepinephrine (NE) (Albillos et al., 1997; Chow, 1992; Jankowski et al., 1993). Changes in PSF kinetics or duration probably reflect changes in fusion pore expansion. Consistent with this concept, expression of a Syt1 mutant

with an increased linker length between the C2 domains in PC12 cells shortens the PSF duration, which suggests that the fusion pore stability was reduced (Bai et al., 2004a). Overexpression of Syt1 increased PSF duration, suggesting fusion pore stability increased (Wang et al., 2001). Together, Syt1 promotes duration pore stability/duration and facilitates fusion pore expansion in neuroendocrine secretion.

In PC12 cells, Syt1 mediates fusion events with a shorter event duration, whereas Syt7 fusion pores remain open for a longer amount of time (Bendahmane et al., 2018). Replacement of Syt1 C2 domains for Syt7 C2 domains slows fusion event durations, suggesting that Syt1 and Syt7 differentially regulate fusion event duration in PC12 cells (Bendahmane et al., 2018). In Syt7KO chromaffin cells, DCV cargo is released faster (Bendahmane et al., 2020) and planar lipid fusion Syt7 slows the rate of cargo release (Bendahmane et al., 2020).

To test whether Syt1 and Syt7 differentially regulate pore kinetics of neuronal DCVs, we analyzed the duration of DCV fusion events in Syt1-KO and Syt7-KO neurons, with and without Syt1 and Syt7 (cross-)expression. We show that Syt1 deficiency, but not Syt7 deficiency, strongly reduced the duration of DCV fusion events. Moreover, the number of fusion events resulting in full cargo release was reduced in Syt1KO neurons. Syt1 overexpression in WT neurons, but not Syt7 overexpression, increased the fusion event duration suggesting Syt1 is rate-limiting and sufficient to prolong fusion pore opening. Finally, GAP43-Syt1, a Syt1 mutant that lacks its TM domain and instead contains a palmitoylation site, did not restore fusion event duration in Syt1 deficient neurons. We conclude that Syt1, but not Syt7, prolongs fusion pore duration of DCVs.

RESULTS

Syt1, but not Syt7, prolongs fusion pore duration

Syt1 and Syt7 regulate fusion pore dilation and stability in PC12 and chromaffin cells (Bai et al., 2004a; Segovia et al., 2010; Wang et al., 2001, 2006; Zhang et al., 2010). To test this in neurons, the duration of single fusion events was assessed in all genotypes. The duration was defined as the time between the onset of NPY-SEP dequenching, indicating fusion pore opening, and return to baseline levels, indicating either (a) fusion pore closure followed by vesicle re-acidification ('kiss-and-run'), or (b) complete DCV cargo release ('full fusion') followed by cargo diffusion in extracellular space (Wit et al., 2009). The duration of DCV fusion events was highly variable (Fig. 1A-H, also see Chapter 2, Fig. S1A), probably due to (a1) variable fission efficiency for kiss-and-run events; (a2) variable expression of proton pumps per

DCV, (b1) variable cargo condensation limiting diffusion out of DCVs, and (b2) cargo binding to the extracellular matrix limiting diffusion after full vesicle collapse (Wit et al., 2009). These factors were considered a constant among genotypes.

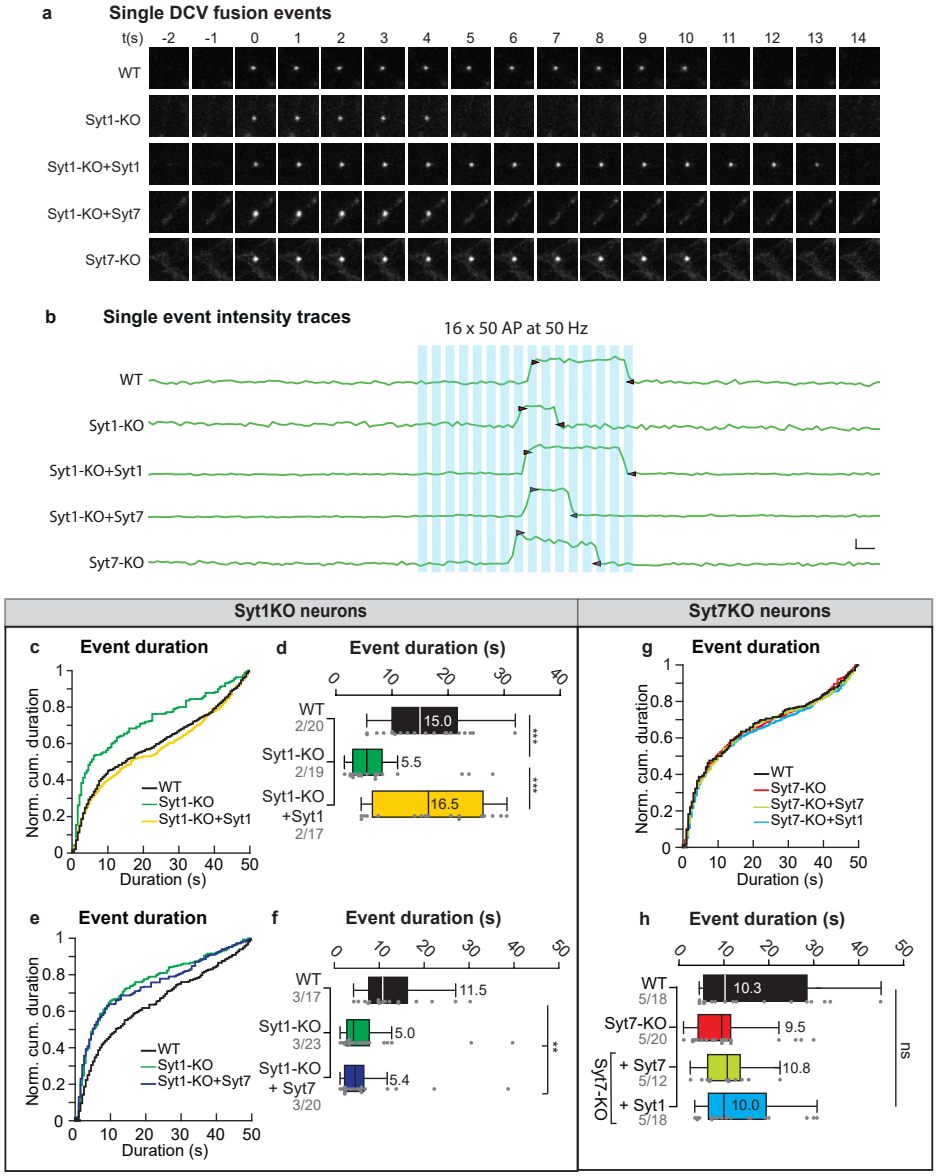

Figure 1. Caption on next page ⇢

Figure 1: Synaptotagmin-1, but not Syt7, is required for event duration.
a. Representative images of NPY-SEP events.
b. Representative fluorescence traces of NPY-SEP event regions of interest (ROIs).
c. Normalized cumulative median event duration per neuron in WT, Syt1-KO and Syt1-KO neurons with Syt1-OE. For lentiviral infection, 2 µl of lentivirus was used.
d. Event duration in Syt1-KO neurons is rescued by Syt1-OE ($X^2(3) = 13.27$, $p = .0013$).
e. Normalized cumulative median event duration per neuron in WT, Syt1-KO and Syt1-KO neurons with Syt7-OE.
f. Event duration in Syt1-KO neurons is not rescued by Syt7-OE ($X^2(3) = 13.28$, $p = .0013$).
g. Normalized cumulative median event duration per neuron in WT neurons, Syt7-KO and Syt7-KO neurons with Syt7-OE.
h. Event duration is unaltered in Syt7-KO neurons with Syt1-OE and Syt7-OE ($X^2(4) = 1.475$, $p = .67$).
Median value is presented in or next to the box plot. Number before and after dash represents number of independent experiments and number of neurons, respectively. All data presented in this figure corresponds to data presented in Chapter 2, Fig 4. $^{**}p < .01$, $^{***}p < .001$, ns p>.05.

We observed that the duration of NPY-SEP fusion events was indeed highly variable, ranging from transient events taking ≤ 0.5 s (the minimum duration within the temporal resolution of our assay), to events persisting throughout the full time of the recording (> 50 s). In WT neurons, single fusion events lasted for 10 to 15 seconds (median event duration; Fig. 1D, F, H). In Syt1-KO, relatively more transient events (< 5 s) and less persistent events were observed, reducing the median duration to 5.5 seconds (Fig. 1C-F). As expected, the event duration was rescued by overexpression of Syt1 in Syt1-KO neurons (Syt-1 OE; 16.5 s, Fig. 1C-D). However, overexpression of Syt1 in Syt7-KO neurons did not increase the event duration. In contrast, Syt7-OE did not rescue the shorter event duration in Syt1-KO neurons (5.4 s, Fig. 1E-F). Moreover, in Syt7-KO, and Syt7-KO + Syt7-OE, fusion event duration was not affected (Fig. 1G, H). Together, the data suggests that Syt1 regulates fusion event duration, which is not supported by, but requires, Syt7.

Syt1 deficiency reduces the number of full DCV fusion events

The shortened DCV fusion event duration in the absence of Syt1 may result from an increased speed of cargo release after full collapse of a vesicle with the plasma membrane or reflect an unstable fusion pore that rapidly collapses after pore opening. To test whether the remaining fusing vesicles in Syt1 deficient neurons release DCV cargo, we expressed NPY-mCherry in Syt1-KO neurons. Upon stimulation, NPY-mCherry fluorescence rapidly decreases (A), reporting cargo release upon DCV fusion. Wild-type (WT) neurons showed ~42 fusion events in response to high frequency stimulation, considerably less than the number of NPY-pHluorin events (Chapter 2). In Syt1-KO neurons, the number of full fusion events was reduced by 83% to 7 fusion events per neuron (B, D). These data show that Syt1 deficient neurons still release DCV cargo, albeit that the number of fusion events is strongly reduced, consistent with the data in chapter 2.

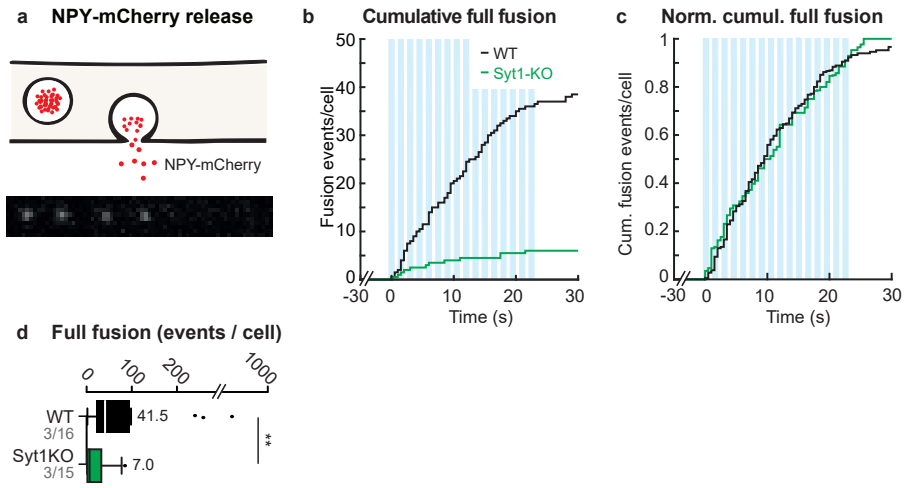

Figure 2: The number of NPY-mCherry events is reduced in Syt1-KO neurons.
a. Cartoon and representative example of NPY-mCherry fusion event.
b. Median number of neuropeptide vesicle fusion events per neuron in a cumulative plot in Syt1-KO and WT neurons.
c. Normalized median number of neuropeptide vesicle fusion events per neuron in a cumulative plot in Syt1-KO and WT neurons.
d. Deficiency of Syt1 reduces the number of fully fusing DCVs per neuron ($U = 53.0$, $p = .0069$).

Syt1 is rate-limiting for fusion pore regulation

To test whether Syt1 is also rate-limiting for fusion pore duration (as for fusion triggering, Chapter 2), we assessed if Syt1 overexpression in WT neurons increases fusion event duration. Indeed, Syt1 overexpression (Fig. 3A, B) prolonged event duration as compared to WT, whereas Syt7 overexpression did not (Fig. 3C, D). This suggests that endogenous levels of Syt1 are rate-limiting for prolonging the duration of DCV fusion events.

The transmembrane domain of Syt1 is required for fusion pore regulation

The transmembrane domain (TM) of Syt1 has been postulated to orientate Syt1 to interact with lipids and SNARE proteins (Lee et al., 2010; Stein et al., 2007). To elucidate whether the TM domain of Syt1 is required for fusion and/or for a normal fusion pore duration, the TM domain of Syt1 was replaced by a 40-amino acid GAP43-sequence containing a palmitoylation site (Fig. 4A). This replacement is reported to almost completely abolish vesicular targeting and induce retargeting to the plasma membrane (Hui et al., 2009; Yao et al., 2012a). To test whether plasma-membrane targeted Syt1 supports fusion pore opening and duration, GAP43-Syt1 was expressed in Syt1-KO neurons (Fig. 4B). Again, Syt1-KO showed a strong decrease in DCV fusion and released fraction (Fig. 4C-D), as previously observed

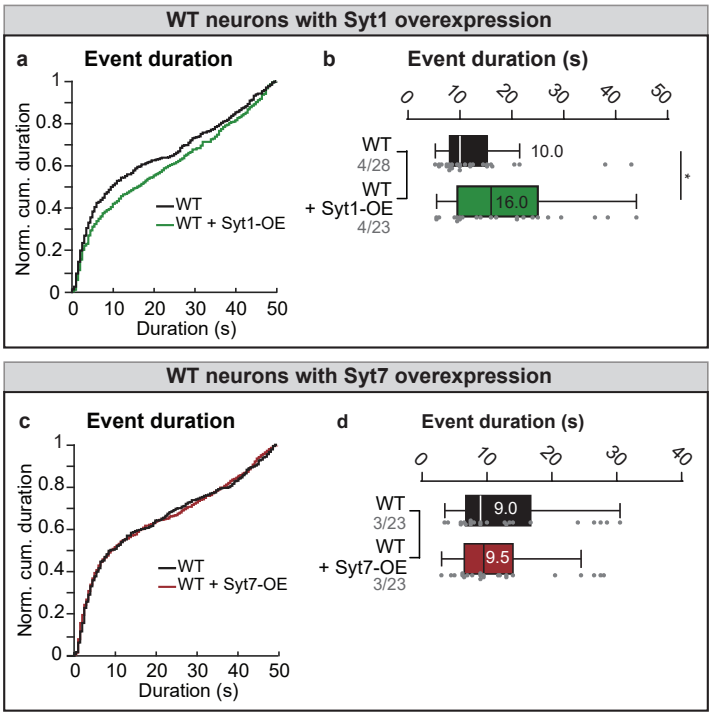

Figure 3: Syt1-OE, but not Syt7-OE, increases DCV event duration
a, b. Fusion duration is prolonged in WT neurons with Syt1-OE ($U = 218$, $p < .05$).
c, d. Fusion event duration is not affected in WT neurons with Syt7-OE ($U = 258$, $p = .89$).
Median value is presented in or next to the box plot. Number before and after dash represents number of independent experiments and number of neurons, respectively. All data presented in this figure corresponds to data presented in Chapter 2, Fig 5. *$p < .05$, ns $p > .05$.

(Chapter 2). GAP43-Syt1 expression rescued DCV fusion in Syt1-KO neurons (Fig. 4C) and released fraction (Fig. 4D) to WT levels. However, GAP43-Syt1 expression failed to prolong the event duration in Syt1KO neurons (Fig. 4E, F). In contrast, GAP43-Syt7 did not rescue DCV fusion in Syt7-KO neurons and did not alter event duration (Fig. 4G-L). These data indicate that Syt7, unlike Syt1, requires its TM domain to support DCV fusion, and that Syt1 requires its TM domain to regulate fusion pore duration (either for functional protein formation and/or correct targeting).

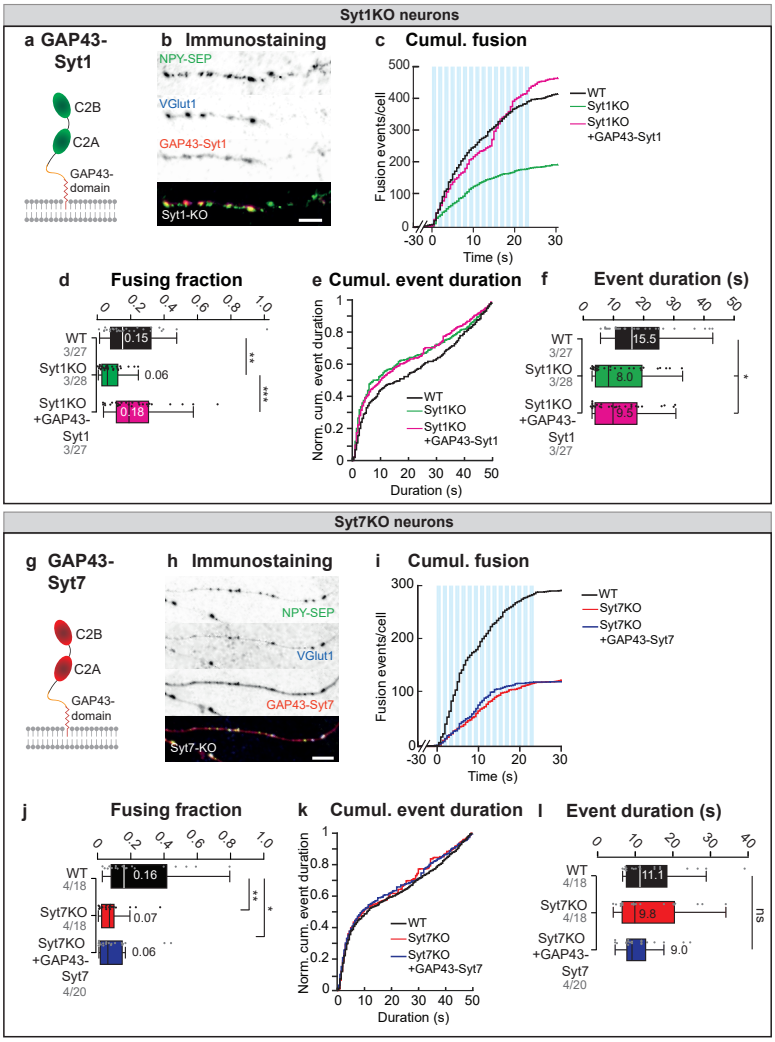

Figure 4: GAP43-Syt1 rescues DCV fusion, but not event duration.

a. Cartoon of GAP43-Syt1 fusion protein membrane-anchored by its palmitoylation site.

b. Immunocytochemistry of Syt1-KO neurons expressing GAP43-Syt1. Scale bar = 5 µm.

c. Median number of neuropeptide vesicle fusion events in WT and Syt1-KO neurons with and without GAP43-Syt1 in a cumulative plot. See Fig. 2A,B for Syt1-KO neurons rescued with Syt1.

d. Fusing fraction in Syt1-KO neurons is rescued by GAP43-Syt1 expression ($X^2(3) = 10.34$, $p = .006$).

e. Normalized cumulative median event duration per neuron in WT, Syt1-KO and Syt1-KO neurons with GAP43-Syt1 expression.

f. Event duration in Syt1-KO neurons is not rescued by GAP43-Syt1 expression ($X^2(3) = 9.27$, $p = .01$).

g. Cartoon of GAP43-Syt7 fusion protein targeted to the membrane by its palmitoylation site.

h. Immunocytochemistry of Syt7-KO neurons expressing GAP43-Syt7. Scale bar = 5 µm.

i. Median number of neuropeptide vesicle fusion events in WT and Syt7-KO neurons with and without GAP43-Syt7 in a cumulative plot. See Fig. 2E,F for Syt7-KO neurons rescued with Syt7.

j. Fusing fraction in Syt7KO neurons is not rescued by GAP43-Syt7 expression (X2(3) = 10.56, p = .005).

k. Normalized cumulative median event duration per neuron in WT, Syt7-KO and Syt7-KO neurons with GAP43-Syt7 expression.
l. Median event duration in Syt7-KO neurons is not affected by GAP43-Syt7 expression ($X2(3) = 1.305$, $p = .52$).

Box plots are plotted with 25% (Q1) and 75% (Q3) interquartile range and Tukey whiskers. Number before and after dash represents number of independent experiments and number of neurons, respectively.
* $p < .05$, ** $p < .01$, *** $p < .001$, ns $p > .05$.

DISCUSSION

DCV fusion equally depends on two Ca^{2+} sensors that compensate for each other upon overexpression (Chapter 2). However, both sensors localized to different cellular locations (Chapter 3), and it remained unclear if Syt1 and Syt7 differentially regulated vesicle fusion. In addition to its role in vesicle fusion Syt1 regulates fusion pore stability and kinetics of SVs, and secretory granules in neuroendocrine and PC12 cells (Bai et al., 2004b; Das et al., 2020; Holz et al., 2000; Lai et al., 2013; Li et al., 2016; Lynch et al., 2008; Micheva et al., 2001; Wang et al., 2001, 2003, 2006; Wu et al., 2019; Zhu et al., 2007). To explore whether Syt1 and Syt7 differentially affected fusion kinetics, we investigated the role of Syt1 and Syt7 on fusion event duration. In this study we show that Syt1 deficiency, but not Syt7 deficiency, strongly reduces DCV fusion event duration. Overexpression of Syt7 in Syt1-KO neurons did not restore a normal fusion event duration. Together, these observations suggest that Syt1, but not Syt7, regulates DCV fusion pore duration. Moreover, Syt1 overexpression in WT neurons, but not Syt7 overexpression, increased the fusion event duration indicating that Syt1 is sufficient to prolong fusion event duration. Finally, GAP43-Syt1 fully rescued DCV fusion, but not a normal fusion event duration. Together, these data suggest that the pore duration, but not the pore opening, requires the luminal/transmembrane domain of Syt1.

Syt1 deficiency, but not Syt7 deficiency, shortened the duration of DCV fusion events (Fig. 1A-H). This is consistent with previous observations of shortened event duration of single SV fusion events in Syt1-KO neurons (Li et al., 2016). A shorter event duration may reflect a narrow fusion pore that recloses after opening (kiss-and-run), or an enhanced pore dilation whereby the cargo is released more rapidly (full fusion). Alternatively, Syt1 deficiency may affect cargo aggregation and subsequently alter the time it takes for the crystalline core to dissolve. However, the main indicator of cargo processing and crystallization, the pH, was not visibly changed in neurons as Syt1 deficient vesicles were still quenched (Fig. 1A). Therefore, Syt1 may regulate fusion event duration by affecting pore stability/dilation.

Overexpression of Syt1 in WT neurons, but not of Syt7, increased the duration of fusion events (Fig. 3A-D). This indicates that Syt1 is sufficient to prolong fusion event duration. Previous observations in *in vitro* nanodisk fusion assays showed that increasing Syt1 copy numbers resulted in prolonged fusion pore duration (Wu et al., 2017b). Similar observations have been made for increasing copy numbers of v-SNAREs/VAMP2, where higher copy numbers not only increase the pore duration, but also increase the fusion pore size 2-fold and facilitate release of larger cargo (Bao et al., 2018a). Therefore, regulation of the expression levels of SNAREs and Syt1 may provide a cellular mechanism to regulate cargo release. Whereas copy numbers of VAMP2 vary considerably between SVs, the copy numbers of Syt1 displayed less variation (Mutch et al., 2011), suggesting that Syt1 expression levels are more tightly controlled. Taken together, neurons may regulate fusion DCV pore duration by regulation of Syt1 expression levels. However, overexpressing either Syt1 or Syt7 in Syt7-KO neurons did not affect DCV event duration (Fig. 1G, H), suggesting that Syt1 requires Syt7 to prolong fusion pores.

An increase in NPY-pHluorin fluorescence (dequenching) reports fusion pore opening, whereas the subsequent decrease of NPY-pHluorin either reflects full cargo release and diffusion into extracellular space, or pore re-closure followed by re-acidification (Wit et al., 2009). Therefore, NPY-pHluorin event duration cannot be directly linked to cargo release unless when combined with NPY-mCherry; a fluorescent reporter that reports cargo release (but not pore opening) (Gandasi et al., 2015). Syt1 regulates fusion pore dilation of liposomes and of secretory granules in PC12 cells (Bai et al., 2004b; Das et al., 2020; Lai et al., 2013; Lynch et al., 2008; Wang et al., 2001, 2003, 2006), and loss of Syt1 increases the rate of kiss-and-run events (Zhu et al., 2007). In neurons, full fusion and kiss-and-run events are present (Wit et al., 2009), but it is unclear whether the shortened event duration is related to changes in cargo release. Only ~40 full fusion events were detected per neuron (Fig. 2A-D), whereas ~300-400 NPY-pHluorin events are detected per neuron (Chapter 2). This suggests that the large majority of fusion events do not release a large fraction of all NPY-SEP contained in single DCVs and may therefore be classified as kiss-and-run events. Syt1 deficiency reduced the number of fusion pore openings (Chapter 2). We now show that full fusion events, detected by the sudden disappearance of NPY-mCherry, are reduced to a similar extent. This suggests that Syt1 deficiency does not selectively affect kiss-and run or full fusion. Therefore, Syt1 may affect the duration of fusion pore opening rather than the rate of full fusion/kiss-and-run.

By inserting into the plasma membrane while staying bound to the SNAREs, Syt1 has been suggested to act as a lever to dilate fusion pores (Wu et al., 2019). In

line with these observations, a Syt1 mutant with a gain-of-function for membrane insertion showed increased fusion pore expansion and cargo release in PC12 cells (Lynch et al., 2008). Indeed, Syt1 requires PIP2 to stabilize fusion pores in nanodisk planar bilayer membranes (Das et al., 2020). Together, these data suggest that Syt1 requires its membrane interaction to support fusion pore stability and dilation. The orientation of Syt1 in respect to the vesicle, SNARE complex and PM remains a topic of discussion. Lipid mixing assays show that Syt1 requires an asymmetric distribution of lipids: more negative charges on the *trans*-surface are required in order to efficiently promote fusion (Lee et al., 2010; Stein et al., 2007). Acidic charges at the vesicle membrane cause Syt1 to *cis*-interact with vesicle membrane, which causes Syt1 to lose its Ca^{2+} stimulatory function (Lee et al., 2010; Stein et al., 2007). GAP43-Syt1 is almost exclusively targeted to the plasma membrane (Yao et al., 2012a), which possibly changes the orientation of GAP43-Syt1 towards membrane lipids. This may explain why GAP43-Syt1 does not restore a normal event duration in Syt1KO neurons (Fig. 4F). DCV fusion is efficiently restored by GAP43-Syt1 in Syt1KO neurons (Fig. 4D), suggesting that the orientation does not affect pore opening in neurons. Together, these data suggest that Syt1 supports both fusion pore opening and pore stability, and that the vesicular localization is required for supporting fusion pore stability.

Syt7 deficiency or overexpression did not affect DCV fusion pore duration in our experiments (Fig. 1G, H, 3C, D), but was previously shown to have a role in pore regulation in other systems. Syt7 loss in chromaffin cells resulted in neuroendocrine granule fusion pores with a longer lifetime (up to 400 ms, instead of 200 ms for WT fusion pores) and a lower conductance, suggesting that fusion pore expansion was delayed in Syt7KO neurons (Segovia et al., 2010). Therefore, in neuroendocrine granule fusion, Syt7 may support fusion pore expansion. In line with these findings, Syt7KO chromaffin cells release less catecholamines (large molecules), but not less ATP (small molecules), suggesting that Syt7 promotes fusion pore expansion (Zhang et al., 2019). In contrast, in another study, Syt7KO chromaffin cells have faster cargo release (Bendahmane et al., 2020) and planar lipid fusion Syt7 slows the rate of cargo release (Bendahmane et al., 2020). Similarly, fusion pores of Syt7-bearing granules failed to expand or reseal, slowing the release of vesicle cargo (Rao et al., 2014). These results suggest that Syt7 regulates pore expansion and cargo release in chromaffin cells, but whether Syt7 supports or delays fusion pore expansion remains unresolved. Possibly, Syt7 requires a vesicular localization for supporting fusion pore duration. Syt7 may support fusion pore duration while being localized

to secretory granules on chromaffin cells, whereas the majority of fusing DCVs did not express Syt7 on their membrane.

The fact that Syt1, but not Syt7, regulates fusion event duration suggests that Syt1 acts downstream of Syt7 in DCV secretion. Unlike other secretory pathways, especially in synapses and chromaffin cells, the sequence of events is still poorly defined and the molecules characterized only partially. At the fusion step, multiple R-SNAREs (Hoogstraaten et al., 2020; Shimojo et al., 2015) may work with SNAP25 (Arora et al., 2017; Shimojo et al., 2015), but the Qa SNARE (syntaxin paralog) and SM-protein (Munc18 paralog) are unknown. The Rab3A/RIM/Munc13 complex is essential (Persoon et al., 2019) and may act upstream of the SNAREs. The fact that Syt1 regulates DCV fusion event duration suggests that at least one role of Syt1 is downstream of the action of all these molecules. It is quite plausible that both Syts have additional roles, as demonstrated for the synaptic vesicle and chromaffin granule pathways (Chang et al., 2018; Tawfik et al., 2020; de Wit et al., 2009). Better definitions of DCV pools and their release probabilities are required to define better working models for the DCV pathway and the molecular function(s) of Syt1 and Syt7.

Acknowledgements

We thank Robbert Zalm for cloning and producing viral particles; Frank den Oudsten, Lisa Laan and Desiree Schut for producing glia feeders and primary culture assistance; Joke Wortel for animal breeding; Jurjen Broeke for technical assistance; Jurjen Broeke and Alessandro Moro for Matlab programming; Ingrid Saarloos for protein chemistry; Frank den Oudsten and Joost Hoetjes for genotyping assistance; and members of the CNCR DCV project team for fruitful discussions. This work is supported by an ERC Advanced Grant (322966) of the European Union (to M.V.).

Author contributions

R.v.W, R.F.T. and M.V. designed the experiments. R.v.W. collected and analyzed experimental data, together with J.P., who collected data for Fig. S1C-F. R.v.W., R.F.T. and M.V. designed the figures and wrote the manuscript with input from all authors.

Chapter 5

General discussion

SUMMARY OF THE FINDINGS

The aim of this thesis was to characterize the calcium sensors involved in neuronal DCV fusion. We investigated the role of four calcium sensors, Synaptotagmin-1 (Syt1), Synaptotagmin-7 (Syt7), Doc2a and Doc2b, on DCV fusion in mouse hippocampal neurons. In **Chapter 2**, we show that DCV fusion is strongly and equally reduced in Syt1- or Syt7-deficient neurons, and combined Syt1/Syt7 deficiency did not reduce fusion further, suggesting the two sensors operate in the same pathway. Moreover, the two sensors are functionally redundant upon overexpression (they cross-rescue each other's fusion defect), showing that both sensors support fusion when expression levels are raised above endogenous levels. Overexpression of either sensor in WT neurons increased DCV fusion. Both sensors required their Ca^{2+} binding sites to support DCV fusion. These results suggest that both Ca^{2+} sensors are required, rate-limiting and redundant for DCV fusion. In **Chapter 3**, the cellular localization of Syt1 and Syt7 in hippocampal neurons is characterized. Syt1 mainly localized to acidic intracellular compartments, whereas Syt7 was largely present on the plasma membrane. Immunohistochemistry and live-cell co-traveling experiments showed that Syt1, aside from its synaptic localization, also strongly co-localized with DCVs, whereas Syt7 did so to lesser extent. Hence, Syt1 and Syt7 localized to different cellular compartments. In **Chapter 4**, the DCV fusion kinetics in Syt1- or Syt7-deficient neurons are described. We report that Syt1-, but not Syt7-deficiency strongly reduced fusion event duration, suggesting that Syt1 has a unique role in fusion pore duration/stability. Moreover, Syt1 overexpression, but not Syt7 overexpression, increased the fusion event duration, suggesting that Syt1 is rate-limiting for fusion pore duration/stability. Finally, the transmembrane domain of Syt1, which is required for vesicular targeting, is required to restore fusion pore duration in Syt1-deficient neurons. We conclude that DCV fusion requires two calcium sensors, Syt1 and Syt7, and that, despite differences in localization, these sensors can compensate for each other upon overexpression, but that only Syt1 supports fusion event duration.

SYT PARALOGS HAVE SPECIALIZED FUNCTIONS IN OTHER SYSTEMS

Seventeen Synaptotagmin paralogs are described in mammals (Craxton, 2004, 2007; Kwon et al., 1996), raising the important question: 'why so many?' (Südhof, 2002). Each sensor has a unique combination of Ca^{2+} binding properties and cellular

localization, which allow Synaptotagmins to fulfil a diversity of cellular functions. Syt1, Syt2 and Syt9 are low-affinity Ca^{2+} sensors for synchronous SV fusion (Geppert et al., 1994; Xu et al., 2007). Syt3, Syt5, Syt6 and Syt10 are medium-affinity Ca^{2+} sensors forming dimers by a S-S bond at the N-terminus (for review, see Südhof, 2002). Little is known about the roles of this group of sensors, although Syt10 is involved in fusion of IGF-1 vesicles in the olfactory bulb (Cao et al., 2011), and Syt3 regulates AMPA receptor endocytosis (Awasthi et al., 2018). Synaptotagmins that do not bind Ca^{2+} (Syt4, 8, 11-17) may negatively regulate DCV fusion (Dean et al., 2009; Zhang et al., 2011a, 2009) and are involved in endocytosis and short- and long-term plasticity (for review, see Wolfes and Dean, 2020). Finally, Syt7 is a high Ca^{2+} affinity sensor, involved in asynchronous SV fusion, vesicle replenishment, synaptic facilitation, slow secretory granule secretion and priming in chromaffin cells (Schonn et al., 2008; Südhof, 2002; Tawfik et al., 2020).

In several systems, multiple sensors regulate fusion: SV fusion and chromaffin granule (CG) fusion are both regulated by Syt1 and Syt7. But in these systems, Syt1 and Syt7 have specialized functions: Syt1 for synchronous (SV) / fast (CG) fusion, and Syt7 regulates asynchronous (SV) / slow (CG) fusion. Additionally, the two sensors appear to be targeted to different CG populations in chromaffin cells (Rao et al., 2014, Tawfik et al., 2020) and regulate CG exocytosis with different fusion kinetics: Syt1 promotes fusion pore dilation and cargo release (Bai et al., 2004b; Das et al., 2020; Holz et al., 2000; Micheva et al., 2001; Rao et al., 2014; Wu et al., 2019), whereas Syt7 slows fusion pore dilation and release cargo, and promotes fusion at lower Ca^{2+} concentrations than Syt1 (Bendahmane et al., 2020; Rao et al., 2014, 2017; Wang et al., 2005; but also see Zhang et al., 2011b, Segovia et al., 2010). Therefore, Synaptotagmins generally fulfill specialized functions in neurons and chromaffin cells, with Syt1 regulating synchronous SV fusion and Syt7 regulating slower functions. In contrast, we report that the two sensors are functionally redundant in neuronal DCV fusion, and found no obvious fast/slow specialization for either sensor, suggesting that Syt1 and Syt7 can fully compensate for each other's functions in DCV fusion (with exception for prolonging fusion pores, see Chapter 4). These data show that the mechanism of neuromodulator secretion is different from previously studied systems.

In following sections, we argue that Syt1 and Syt7 expression may function as a 'volume dial' for DCV fusion (Section 3). Next, we discuss why two functionally redundant sensors are required for DCV fusion (Section 4). Furthermore, we have not detected a fast/slow specialization in DCV fusion, in contrast to SV and CG fusion, and we discuss this in relation to Ca^{2+} sources and from an evolutionary perspective (Section 5). Additionally, the molecular mechanisms of Syt in DCV fusion are discussed (Section 6),

followed by how secretion of different neuropeptide cargo may be regulated (Section 7). We argue for a larger role for neuropeptides in disease models (Section 8) and provide a model on how two sensors regulate DCV fusion/neuropeptide secretion (9). Finally, we provide suggestions for future research (Section 10).

SYTS MAY FUNCTION AS A 'VOLUME DIAL' FOR DCV FUSION

Deletion of Syt1 or Syt7 severely reduced DCV fusion, whereas both sensors were functionally redundant upon overexpression (Chapter 2). Moreover, overexpression of Syt1 or Syt7 in wildtype neurons increased expression levels (Chapter 2, Fig. S6) and DCV fusion (Chapter 2, Fig. 5). Together, this suggests that DCVs require a minimal number of Syts to trigger vesicles fusion, that both Syts are rate-limiting for DCV fusion and that Syt expression levels regulate the number of DCV fusion events. In contrast, overexpression of Syt7 in Syt1-KO neurons did not increase SV release during train stimulation (Bacaj et al., 2013). Moreover, Syt1-OE in WT neurons did not affect evoked IPSC amplitude or spontaneous release (mIPSC) frequency (Courtney et al., 2019), suggesting that Syt expression levels are not rate-limiting for SV fusion. Hence, Syt1 and Syt7 expression levels regulate DCV, but not SV, fusion in hippocampal neurons. Syt expression levels may hereby act as a 'volume dial', whereby increasing Syt expression levels provides neurons a powerful tool to increase the number of fusing DCVs. As Syt expression levels are developmentally regulated (Sugita et al., 2001), these mechanisms may affect neuropeptide secretion during development.

SV fusion requires a minimal number of two SNARE complexes (Sinha et al., 2011), and fast neuroendocrine fusion requires three SNARE complexes (Hua and Scheller, 2001; Mohrman et al., 2010), possibly because a larger vesicle radius (and subsequently lower membrane tension) relates to a higher energy barrier for fusion (Lee and Schick, 2008; Shillcock and Lipowsky, 2005). Only a few SNAREs are required for fusion pore opening, but higher SNARE numbers are required to dilate fusion pores and increase pore conductance (Bao et al., 2018b; Wu et al., 2017b). Syt1 also supports fusion pore dilation and cargo release (Bai et al., 2004b; Das et al., 2020; Holz et al., 2000; Micheva et al., 2001; Rao et al., 2014; Wu et al., 2019). We report that DCV fusion in Syt1-KO neurons is rescued by lower volumes of Syt1-expressing virus than fusion pore duration (Chapter 2, Fig. S5). Taken together, this suggests that higher Syt1 expression levels increase pore conductance/neuropeptide release. Regulation of Syt expression levels may therefore regulate the number of DCV fusion events and the amount of neuropeptide release (also see section below).

WHY ARE TWO REDUNDANT SENSORS REQUIRED FOR DCV FUSION?

Two very different Syt paralogs are functionally redundant

Cross-expression of Syt1 and Syt7 fully rescued DCV fusion in Syt7-KO and Syt1-KO neurons, respectively (Chapter 2, Fig. 4), suggesting that the two sensors are functionally redundant in supporting DCV fusion. This redundancy was rather surprising, as Syt1 differs from Syt7 in several aspects. First, Syt1 localizes to SVs and DCVs (Brose et al., 1992; Matthew et al., 1981; Takamori et al., 2006) (Chapter 3), whereas Syt7 is mainly present on the PM and not/to a low extent on SVs and DCVs (Sugita et al., 2001; Taoufiq et al., 2020)(Chapter 3). Second, Syt7 has a high affinity for Ca^{2+} (Kd ~1.5-2.5 uM in liposome fusion assays), whereas the intrinsic Ca^{2+} affinity of the C2 domains of Syt1 is 10-fold lower (Kd ~10-20 uM) (Sugita et al., 2002). Additionally, Syt7 has slow phospholipid binding and unbinding kinetics, in contrast to Syt1 (Hui et al., 2005). Moreover, Syt1 and Syt7 require different C2 domains to trigger fusion. Syt7 mediates fusion through its first C2 domain, the C2A domain (Bacaj et al., 2013). The C2B domain of Syt7 is dispensable for SV fusion (Bacaj et al., 2013). In contrast, Syt1 requires its C2B domain, whereas its C2A domain appears to be modulatory (Mackler et al., 2002; Nishiki and Augustine, 2004; Robinson et al., 2002; Shin et al., 2009). Finally, as discussed in previous paragraphs, functionally, Syt7 is generally linked to slower processes that occur at residual Ca^{2+} concentrations, such as asynchronous/slow release, synaptic facilitation, SV/neuroendocrine vesicle replenishment and neuroendocrine granule priming (Bacaj et al., 2013; Jackman et al., 2016; Liu et al., 2014; Schonn et al., 2008; Tawfik et al., 2020; Wen et al., 2010), whereas Syt1 regulates synchronous SV release and fast neuroendocrine granule fusion (Geppert et al., 1994; Voets et al., 2001). Taken together, Syt1 and Syt7 differ in their localization, Ca^{2+} affinities, binding kinetics, and C2 domain requirements and have specialized (fast/slow) functions in SV and neuroendocrine fusion. Despite all of these differences, these two Syt paralogs can fully cross-rescue DCV fusion, showing that specific Syt1/Syt7 kinetics, Ca^{2+} affinity or localization are not essential for DCV fusion. Instead, the number of C2 domains/Syt molecules (also see previous section), rather than the isoform, regulates DCV fusion. It remains an open question what properties make Syt1/Syt7 the preferred Ca^{2+} sensors over Doc2a/b and other Syt paralogs. Probably multiple factors contribute, such as the restricted expression in the brain (Syt2, 6, 9, 10), the complete absence of Ca^{2+} binding (Syt4, 8, 11-17), or the absence of the TM domain (Doc2a/b). However, despite the redundancy in DCV fusion, Syt1 and Syt7 may still have important unique functions, as will be discussed in the following sections.

Two sensors may differentially regulate cargo release

Both Syts trigger fusion of neuroendocrine granules in chromaffin cells (albeit with different fast/slow kinetics), showing that both Syts could act as standalone sensors for vesicle fusion (Schonn et al., 2008; Tawfik et al., 2020; Voets et al., 2001). In neuronal DCV fusion, Syt1 and Syt7 cross-rescued Syt7-KO and Syt1-KO neurons, respectively, showing that both Syts trigger DCV fusion pore opening as well (Chapter 2, Fig. 4). This raises the question: why are two different, but redundant sensors required for fusion? Syt1, but not Syt7, affected DCV fusion event duration (Chapter 4). Also, higher expression levels of Syt1 increased DCV event duration, suggesting that Syt1 expression levels regulate fusion pore stability (Chapter 4, Fig. 3). As discussed in Chapter 4, Syt1 increases fusion pore size and supports the formation of large, stable fusion pores in chromaffin and PC12 cells (Das et al., 2020; Lynch et al., 2008; Wang et al., 2006; Wu et al., 2019; Zhu et al., 2007). Similar to neuroendocrine secretion, Syt1 may stabilize fusion pores and increase fusion pore dilation to support cargo release from fusing DCVs. Syt7 did not affect DCV event duration (Chapter 4), in contrast to previous findings in neuroendocrine cells, where Syt7 regulates fusion pore dilation and supports release of large, but not small cargo (Bendahmane et al., 2020; Rao et al., 2014; Segovia et al., 2010; Zhang et al., 2019) (for discussion, see Chapter 4). The different roles for Syt1 and Syt7 in DCV pore duration of fusing DCVs suggest that Syt1-mediated fusion supports the release of different DCV cargo than Syt7-mediated DCV fusion events by modulation of fusion pores. However, there is currently no data that support this hypothesis for DCV fusion in neurons.

Two sensors may regulate fusion with different Ca^{2+} kinetics

Additionally, the two sensors may regulate vesicle fusion at different Ca^{2+} levels. In neuroendocrine secretion, Syt1 and Syt7 trigger fusion with different release kinetics/timing, with Syt7 promoting release at lower stimulation frequency and at lower Ca^{2+} levels than Syt1 (Rao et al., 2014, 2017; Wang et al., 2005). The Ca^{2+} affinity is an intrinsic property of the Syt gene and similar mechanisms may therefore apply to DCV fusion, but may have been missed by our robust stimulation paradigm (16 x 50 AP at 50 Hz). However, milder stimulation/lower Ca^{2+} levels may activate Syt7 but not Syt1 (due to their respective high and low Ca^{2+} affinity). As both sensors are required for fusion in hippocampal neurons (Chapter 2, Fig. 3), activation of one sensor at low Ca^{2+} concentrations will not trigger fusion of many DCVs. However, the cross-rescue (Chapter 2, Fig. 4) suggests that high expression levels of one sensor can compensate for the other. Therefore, at high expression levels Syt7 may efficiently trigger fusion, and possibly at lower Ca^{2+} concentrations. This may especially be relevant for

specific groups of neurons that express high levels of one Syt, such as certain nuclei in the inferior olive (Turecek and Regehr, 2019), or during developmental regulation of Syt1/7 expression levels (Sugita et al., 2001).

Other reasons why two sensors are required

Large vesicles may require more Syt molecules (and SNARE complexes) for fusion, because large vesicles have less surface tension and therefore a larger barrier for fusion (Nir et al., 1982; Ohki, 1984). Using the same sensors for DCV fusion as for SV fusion may be energetically favorable, as strict separation of Synaptotagmin paralogs between two secretory systems (SV and DCV) requires an (energetically demanding) level of sorting. Additionally, Syt1 and Syt7 may have functional specializations that were not assessed in this study, such as (1) regulating secretion from synaptic (or extrasynaptic) locations, as shown for Munc13-1/2 (Bospoort et al., 2012); and (2) sensing Ca^{2+} from different sources (also see discussion at section 5). Taken together, two sensors support DCV fusion, but possibly with different cargo release, Ca^{2+} kinetics or fusion locations.

SYT1 AND SYT7 MAY HAVE NO FAST/SLOW SPECIALIZATION IN DCV FUSION

Fast DCV fusion may not be detected in our imaging assay

In comparison to SV fusion, DCV fusion is a slow process that requires strong stimulation (Fig 1). In contrast the electrophysiological measurements of SV and neuroendocrine fusion, neuronal DCV fusion is studied with slower imaging approaches using fluorescently labelled DCV-cargo. Hence, fast and slow phases of DCV fusion are discriminated at a different, slower, temporal resolution. We did not detect any changes in DCV fusion timing (the delay between the start of stimulation to the dequenching of the vesicle). However, we currently do not know on what timescale to expect fast (or slow) DCV fusion. For SV and CG fusion, Syt1-mediated synchronous/fast fusion occurs within 20 and 60 ms after stimulation, respectively (Geppert et al., 1994; Voets et al., 2001) and asynchronous/slow fusion occurs within 200 ms and 600 ms, and is regulated by Syt7 (Bacaj et al., 2013; Chen et al., 2017; Luo and Südhof, 2017; Luo et al., 2015; Schonn et al., 2008; Tawfik et al., 2020; Turecek and Regehr, 2018, 2019; Turecek et al., 2017; Wen et al., 2010). Imaging frames are recorded at 2 Hz, and even 500 ms may be too slow to discriminate fast or slow fusion. Additionally, DCV fusion requires intense repetitive stimulation (16 x 50 AP

at 50 Hz), and it is unclear whether DCVs that fuse later in the stimulation paradigm could still be considered 'fast' fusion events as these events may quickly follow an AP. Because of these two issues, our stimulation paradigm/imaging method does not allow for discrimination between fast and slow fusion as defined with electrophysiological measurements. We could define the fraction of fusion events that occur after the last action potential (so after the 16 x 50 AP) as asynchronous/slow DCV fusion. This component of DCV fusion may be comparable to delayed release in SV fusion, which is the component of asynchronous SV fusion that occurs after prolonged stimulation, and is also regulated by Syt7 (Luo et al., 2015; Maximov et al., 2008). In contrast, in Syt1-KO and Syt7-KO neurons the fraction of DCV fusion events occurring after the stimulation was not significantly affected (Chapter 2, Fig. S4). These results suggest that Syts do not specifically affect fast or slow DCV fusion in neurons. DCV fusion may be inherently slow, e.g. due to their localization, as will be discussed in the following section. However, imaging methods with higher temporal resolution are required to draw stronger conclusions on the role of Syt1/Syt7 in fast/slow DCV fusion.

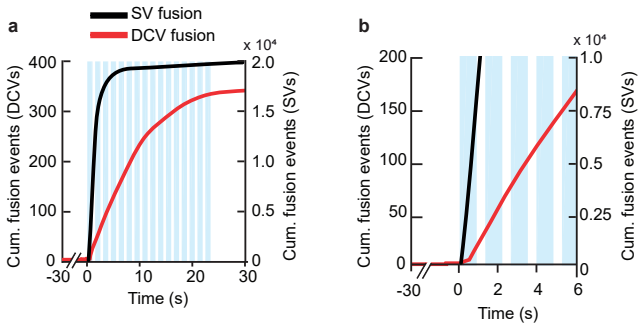

Figure 1: comparison of SV and DCV fusion speed in a cumulative plot (a) and a zoom of the cumulative plot (b). Hundreds to thousands of SVs are estimated to fuse before a very limited number of DCVs fuse. Graphs presents estimated SV data and smoothed DCV fusion data presented in Chapter 2, Fig. 5A.

DCV localization and Ca^{2+} sources may contribute to slow DCV fusion

Since Syt1 is among the Ca^{2+} sensors with the lowest Ca^{2+} sensitivity (Sugita et al., 2002), Ca^{2+} must rise to high micromolar level to activate this sensor, in contrast to Syt7, which has a high Ca^{2+} affinity (Sugita et al., 2002). During mild stimulation, calcium influx is specifically high in microdomains near Ca^{2+} channels, and quickly buffered outside these regions (reviewed by Schwaller, 2010). The strong stimulation paradigm for DCV fusion (16 x 50 AP at 50 Hz) may increase Ca^{2+} levels far outside

the microdomains, and extend to the location of the DCVs, which typically reside outside the active zone (Persoon et al., 2018; Verhage et al., 1991), and partially outside synapses. Also, DCV fusion is triggered by partially different (slower) sources for fusion than SVs: DCV fusion relies on L-type channels (which have slow activation kinetics (for review, see Lipscombe et al., 2004)), and to a lesser extent the faster P/Q-type and N-type Ca^{2+} channels (Leenders et al., 1999; Matsuda et al., 2009; Xia et al., 2009), whereas SV fusion requires P/Q-type and N-type Ca^{2+} channels (for review, see Catterall, 2000; Olivera et al., 1994). Moreover, Ca^{2+} release through ryanodine receptors (RyR) from intracellular stores supports BDNF release (Balkowiec and Katz, 2002; Kolarow et al., 2007). Therefore, it may take time before these slow Ca^{2+} sources increase Ca^{2+} to concentrations that can activate Syt1. Additionally, DCVs localized in synapses were generally not pre-docked to the plasma membrane (Persoon et al., 2018, but also see Bospoort et al., 2012), and may therefore not be located closely to Ca^{2+} channels. Previous studies indicate a considerable delay between the peak of (bulk) Ca^{2+} increase in axons and the onset of DCV fusion (Persoon et al., 2018). Hence, additional factors probably contribute to the slow DCV release onset. For instance, DCVs are transported through neurites on molecular motor complexes (kinesins, dyneins (Hoogenraad and Akhmanova, 2016; Lo et al., 2011)) and may need time to dissociate from these motors and translocate to a fusion site (Bharat et al., 2017; Stucchi et al., 2018). Taken together, there may not be a 'fast/synchronous' phase of DCV fusion, as observed for SV and neuroendocrine granule fusion, due to the distal localization of DCVs to their fusion sites and Ca^{2+} sources.

Lack of evolutionary pressure may cause lack of fast/slow secretion

The lack of fast/slow specialization of Syt1 and Syt7 in DCV fusion stands in contrast to SV and secretory granule secretion in chromaffin cells, where both sensors have clear specialized functions in fast/slow secretion (see section 2). This difference between SV and DCV fusion may be explained by evolutionary adaptations, optimizing CG and SV exocytosis for fast and ultrafast kinetics, respectively. In contrast, there may not be a further evolutionary advantage for optimizing neuromodulator signalling. Syt1 and Syt7 most likely emerged by gene duplication of an ancestral Syt. Our data suggest that this duplication happened first, making secretory pathways more efficient and stimulus-dependent, and that Syt1 and Syt7 subsequently became more specialized to drive different phases of fast or ultrafast vesicle fusion in highly specialized secretory pathways, but not in the DCV pathway.

MOLECULAR MECHANISMS OF SYT IN DCV FUSION

Both sensors are capable to trigger DCV fusion (Chapter 2, Fig. 3 and 4). Additionally, Syt1-KO shortened event duration, and overexpression increased DCV event duration, suggesting that Syt1 regulates fusion pore stability and dilation (Chapter 4). Taken together, Syt1 probably regulates fusion pore opening and stability of DCVs in neurons. However, the exact molecular mechanism of Syt7 remains a topic of considerable debate. In addition to its role in asynchronous/slow vesicle fusion (Geppert et al., 1994; Voets et al., 2001), Syt7 supports synaptic facilitation (Jackman et al., 2016) and (independent of Ca^{2+}) slows SV endocytosis (Li et al., 2016). Moreover, Syt7 supports the Syt1-mediated fast phase of neuroendocrine secretion through priming of secretory granules (Schonn et al., 2008; Tawfik et al., 2020). This supporting role on the RRP is enhanced when chromaffin cells are pre-stimulated by Ca^{2+} uncaging of 0.8 µM Ca^{2+}, which increased the size of the fast burst, suggesting that Syt7 regulates vesicle priming in neuroendocrine secretion (Tawfik et al., 2020). In neurons, Syt1 and Syt7 both (redundantly) maintain the RRP of SVs (Bacaj et al., 2015), and Syt7 enhances SV docking after stimulation (Vevea et al., 2021). Similarly, Syt7 supports SV replenishment during prolonged stimulation and may support vesicle recruitment (Liu et al., 2014), suggesting that Syt7 recruits or primes vesicles to the RRP. Therefore, Syt7 supports SV, neuroendocrine and neuronal DCV fusion in absence of Syt1, but may also regulate priming/docking and/or endocytosis of vesicles in the presence of Syt1. However, its role in DCV priming is difficult to assess, because in contrast to SVs or CGs, there is currently no clear definition of the RRP for neuronal DCVs (no protocol/stimulus to define the release-ready DCV pool like hyperosmotic sucrose for SVs or uncaging caged Ca^{2+} for CGs). Therefore, the 'primed' state/pool is not yet defined for DCVs. For these reasons, we cannot discriminate between effects on fusion competence or the number of fusion-competent DCVs. The low temporal resolution of our imaging assay may not be able to discriminate fast vesicle fusion (by fusion of primed/release-ready DCVs) from slow DCVs (see section 5). However, there are indications that DCV priming occurs on a slow timescale, missed by our imaging assay. When applying two stimulations 8 x 50 AP at 50 Hz separated by an interval of ~80 s, DCV fusion seems to 'synchronize' in the second stimulation (having relatively more fusion events in the first 50 AP of the second burst), and this acceleration of fusion may be affected in Syt7KO neurons (*R. Hoogstraaten, unpublished data*). The acceleration in the second burst may result from an increased number of release-ready DCVs (e.g. through newly docked/primed vesicles), triggered by Syt7 and the residual Ca^{2+} levels after the first stimulation. As the acceleration requires a time interval between

the two stimulations, our experimental set-up (16 x 50 AP) is not optimal to address the role of Syt7 in DCV priming. Taken together, Syt7 supports DCV fusion pore opening, which is supported by our data, and may additionally fulfil an upstream role, such as priming/pool replenishment, which is not detected with the current stimulation paradigm. However, if Syt7 fulfills such roles, they are not unique to Syt7, as Syt1 overexpression fully compensates for the loss of Syt7 in DCV fusion.

REGULATION OF DIFFERENT NEUROPEPTIDE CARGO

Single cell expression analysis of eighteen neuropeptide genes in cortical neurons shows that most neurons express more than one neuropeptide gene, frequently between two and seven, but also up to ten per neuron (Smith et al., 2019). Given the very different functions of neuropeptide molecules (see Chapter 1), neuropeptide cargo may be differentially released. It is currently unknown to what extent these neuropeptides are targeted to the same DCVs or whether and how they are sorted into different DCV populations, and possibly released by different mechanisms. Some neuropeptide cargo, such as IGF-1 and ANF, are targeted to different DCVs (Cao et al., 2013). However, co-storage of neuropeptides into the same vesicle does occur, as shown for BDNF, CGRP and substance P (Salio et al., 2007), and BDNF and substance P can be differentially released upon stimulation (Lever et al., 2001). In mouse olfactory bulb neurons, Syt10 may specifically regulate a pool of DCVs that secrete IGF-1, but not ANF vesicles (Cao et al., 2013). Therefore, Syt paralogs may differentially regulate DCVs with specific cargo (see section 4). However, the lack of additive effect in hippocampal neurons (Chapter 2, Fig. 3) suggests that Syt1 and Syt7 act in the same pathway and argues against DCV pools that are differentially regulated by these sensors. Therefore, other mechanisms may regulate differential secretion of DCV pools/neuropeptide cargo. One example of regulation may be by localization of vesicles to axons vs. dendrites. Differential release between cellular compartments is reported for oxytocin, where stimulation with α-MSH triggers release from dendrites, but not axons (Sabatier et al., 2003). Similarly, hypertonic saline triggers axonal vasopressin release, whereas dendritic vasopressin is released hours later (Ludwig et al., 1994). Indeed, different neuropeptide cargo can be differentially distributed over axons and dendrites (Fisher et al., 1988; Landry et al., 2003). Therefore, differential localization to axons/dendrites may regulate release of different neuropeptide cargo. However, given the large variety in neuropeptides per neuron (Smith et al., 2019), multiple mechanisms may be involved to specifically regulate neuropeptide cargo.

ROLE OF NEUROPEPTIDES IN DISEASE PHENOTYPES

Neuropeptides provide many interesting therapeutic targets, and clinical trials are ongoing to treat a variety of diseases (see Chapter 1). In the past five years, FDA approved two neuropeptide-drugs: Afamelanotide and Bremelanotide, two α-MSH analogs to treat skin damage and hypoactive sexual desire, respectively (de la Torre and Albericio, 2020). Despite the effort from researchers and pharmaceutical companies, the number of neuropeptide-related drugs on the market remains low. The majority of trails fail due to lack of efficacy, e.g. due to low accessibility of the brain or low *in vivo* stability, but also because of unforeseen side effects or safety issues. That these side effects can have severe consequences is, among other things, reflected by the clinical trial for Rimonabant, an endocannabinoid receptor inverse agonist to treat obesity, which was discontinued after reports of severe depression and suicide of multiple clinical trial patients (Topol et al., 2010).

Despite receiving considerable attention in clinical trials, few studies address neuropeptide release mechanisms. Some Syt1 missense mutations result in a dominant-negative effect on neurotransmission and lead to a severe, but heterogeneous neurodevelopmental disorder (Baker et al., 2018; Bradberry et al., 2020). K^+ channel antagonists restore neurotransmission in neurons expressing mutant Syt1 (Bradberry et al., 2020), but the effects of dominant-negative Syt1 mutations (and antagonists) on neuropeptide secretion are currently unknown, but may contribute to the disease phenotype. In case of Syt7, deficiency is linked to bipolar-like and manic-like behaviour in mice and humans, together with reduced anxiety in the light phase of the day, a disorganized circadian rhythm, and a distorted energy metabolism in mice (Shen et al., 2020; Wang et al., 2020). This is proposed to be caused by attenuated NMDAR activity (Shen et al., 2020; Wang et al., 2020). However, given the role of Syt7 in neuropeptide signalling (Chapter 2), and the influence of neuropeptides on circadian rhythm (for reviews, see Freeman and Herzog, 2011; He et al., 2017), energy metabolism (for review, see Nguyen et al., 2011) and anxiety (for review, see Kormos and Gaszner, 2013), it is likely that (Syt7 mediated) neuropeptide release contributes to bipolar phenotype. In general, knowledge on how neuropeptide transport and release is affected, may provide useful assays for efficacy testing of novel therapeutic compounds. Moreover, understanding of neuropeptide signalling pathways is essential to select for the most promising drug targets and to predict and prevent severe safety issues.

MODEL

Localization: from which location do Syts support DCV fusion?

This thesis addressed the cellular localization of Syts, and reports that Syt1, and to lesser extent Syt7, localizes to DCVs (Chapter 3). This suggests that Syt1 regulates fusion while located on vesicles, as previously reported for SVs and CGs (Brose et al., 1992; Matthew et al., 1981; Takamori et al., 2006). In contrast, Syt7 localized mostly to the plasma membrane and may regulate fusion from this location (Fig. 2). However, GAP43-Syt7 did not support DCV fusion (Chapter 4, Fig. S1). Syt7 may require its TM domain, possibly because the cleavage- and palmitoylation site close to the TM domain is essential for Syt7 functioning (Vevea et al. (2021). Syt7 may support DCV fusion from the plasma membrane, although upstream functions cannot be excluded (also see section 6). However, these functions have to be in the same pathway as Syt1 as they can be by-passed by Syt1 overexpression (Chapter 2, Fig. 4). Therefore, we favour a model where both Syts act together at the same step in the secretory pathway, the fusion step, each participating from its specific location: Syt1 at the vesicle and Syt7 at the plasma membrane.

Additionally, Syt7, and to a lesser extent Syt1, co-localized with trafficking LAMP1^{+} vesicles (Chapter 3). NPY-mCherry also colocalized with trafficking LAMP1+ vesicles (for discussion, see Chapter 3). Fusing DCVs, however, never colocalized with LAMP1 (Chapter 3), suggesting that DCVs are fusogenic but lysosomes may not fuse/release cargo in response to our stimulation paradigm.

A single action potential does not trigger DCV fusion

When a single action potential arrives, Ca^{2+} increases up to 100 µM in the microdomains around Ca^{2+} channels (Chapter 1). This triggers SV fusion mediated by Syt1 (Fig. 2, panel 2), which has a low Ca^{2+} affinity (Sugita et al., 2002). A single action potential triggers little asynchronous SV fusion despite Syt7s high Ca^{2+} affinity, probably due to the slow Ca^{2+} binding kinetics of Syt7 (Hui et al., 2005) combined with rapid Ca^{2+} cellular buffering (Chapter 1). The lack of Syt7 activation may partially explain why DCVs do not fuse in response one AP, together with differences in localization of DCVs and Ca^{2+} sources required for DCV fusion (see section 5). Also, Syt1's low Ca^{2+} affinity combined with the localization on DCVs, which are possibly not pre-docked and located further away from Ca^{2+} channels (see section 5), may also explain why multiple action potentials are required for DCV fusion. These properties of Syt1 and Syt7 probably prevent substantial DCV fusion during mild stimulation.

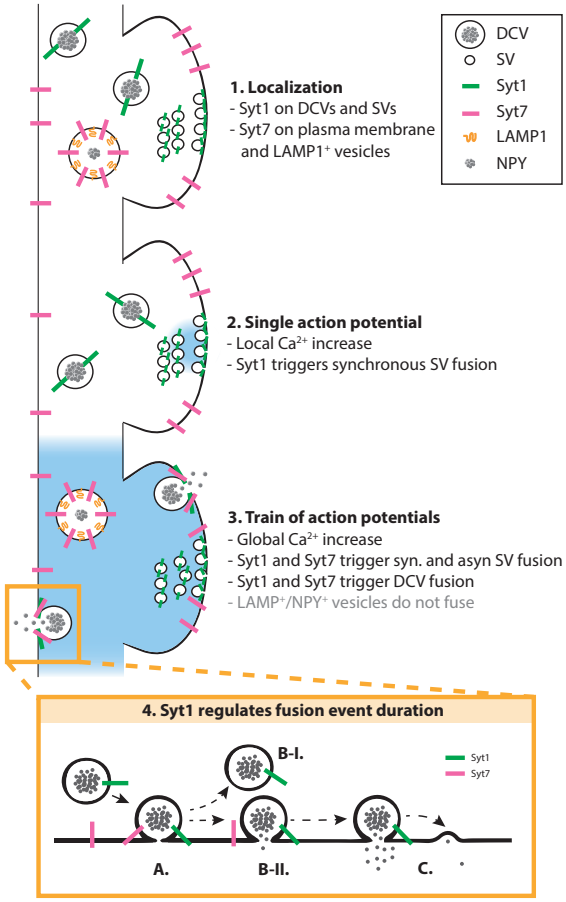

Figure 2: Cartoon of an axon with three synaptic boutons: one in rest (upper), one upon arrival of a single action potential (middle) and one upon train stimulation (bottom). 1. Syts partially localize to different cellular compartments. 2. A single action potential triggers Syt1-mediated synchronous SV fusion, but not DCV fusion. 3. Train stimulation increases Ca^{2+} globally, activates both Syt1 and Syt7 and triggers DCV and SV fusion. 4. Syt1, but not Syt7, prolongs DCV fusion event duration. For detailed discussion, see text.

Train of action potentials

When neurons are stimulated repeatedly, Ca^{2+} increases far outside microdomains (Fig. 2, panel 3) (for reviews, see Neher and Sakaba, 2008; Regehr, 2012). This triggers synchronous SV fusion, dependent on Syt1 (Fernández-Chacón et al., 2001), but also asynchronous fusion, regulated by Syt7 (Bacaj et al., 2013). The strong stimulation additionally triggers the fusion of DCVs, at synaptic and extrasynaptic locations, and requires both Syt1 and Syt7, which trigger fusion pore opening and possibly

regulate other upstream processes, such as priming (see section 6). Syt expression levels probably regulate DCV fusion efficiency (section 3). The amount of Syt1/Syt7 involved in DCV fusion may influence the Ca^{2+} requirements for fusion (section 4) and regulate the rate of neuropeptide cargo release through regulation of the fusion pore (section 4).

Syt1, but not Syt7, regulates fusion pore duration

As discussed above, both Syts are required for DCV fusion and probably act at the fusion site to trigger fusion pore opening (Fig. 2, panel 4A). After pore opening, a DCV can either (1) reseal ('kiss-and-run' or cavicapture), without cargo release and sparing the DCV (Fig. 2, panel 4B-I), or dilate its fusion pore and merge with the plasma membrane (Fig. 2, panel 4 BII-C). Syt1 prolongs DCV event duration, and may support dilation of fusion pores and cargo release (see section 4). DCV fusion events had a variable event duration and Syt1-pHluorin was present on the majority, but not on all fusing DCVs (Chapter 4). Therefore, Syt levels may be variable between individual DCVs. As Syt1 prolongs fusion pores (Chapter 4), fusion events that lack Syt1 may be the portion of fusion events with shorter duration.

Syt7 did not affect DCV fusion event duration, in contrast to previous findings for secretory granules in neuroendocrine cells (Segovia et al., 2010). Possibly, the localization of Syts affects whether or not a Syt can support fusion pore stability. Syt1 requires lipid interactions to dilate fusion pores in neuroendocrine cells (Bai et al., 2004b; Das et al., 2020; Holz et al., 2000; Micheva et al., 2001; Wu et al., 2019). Possibly, the orientation of plasma membrane Syt with respect to the SNARE complex/plasma membrane are incompatible with fusion pore stabilization. This could explain why GAP43-Syt1, which previously showed to relocate to the plasma membrane (Hui et al., 2009; Yao et al., 2012a), does not rescue DCV event duration (Chapter 4). By extension, it may also explain why Syt7, which highly localizes to the plasma membrane, does not rescue fusion event duration in Syt1-KO neurons (Chapter 4, Fig. S1), even though it triggers fusion pore opening. Therefore, the localization of Syts, rather than the paralog, may determine fusion pore duration and possibly cargo release from fusing DCVs. However, other factors, such as Ca^{2+} affinity or lipid-interaction preferences, may also contribute to the different effects of Syt1 and Syt7 on pore stabilization.

FUTURE DIRECTIONS

Syt7 as a docking/priming protein

As discussed in section 6, the roles of Syt7 are still under considerable debate. Syt7 supports the placement of CGs and SVs to the plasma membrane, which may reflect priming/docking of vesicles (Tawfik et al., 2020; Vevea et al., 2021). This occurs after electrical stimulation or is triggered by pre-stimulation with Ca^{2+} (Tawfik et al., 2020; Vevea et al., 2021). As discussed in section 6, DCV fusion synchronizes in the second stimulation when application two stimulations of 8 x 50 AP at 50 Hz, separated by ~80 s. This stimulation paradigm may be used in WT and Syt7KO neurons to test whether Syt7 regulates the synchronization of DCV fusion. Additionally, bath application of N-ethylmaleimide (NEM), a substance used to inhibit de-priming of vesicles (He et al., 2017a), rescues the priming defect in Syt7KO chromaffin cells (Tawfik et al., 2020), suggesting that Syt7 promotes priming by inhibiting de-priming. NEM may be used to assess whether Syt7 inhibits de-priming of DCVs. These experiments would provide further insight on the molecular mechanisms of Syt7 in DCV fusion.

Relation between fusion event duration and cargo release

As discussed previously (section 4, and Chapter 4), Syt1 and Syt7 may differentially regulate neuropeptide cargo release. Syt1 prolonged DCV event duration (Chapter 4), but pore size or conductance has not been assessed in this thesis. In chromaffin cells, pore kinetics and catecholamine secretion can be assessed with patch-amperometry. Secreted NPY is not detected by amperometry (unless when tagged, see Whim, 2006), which complicates studying pore kinetics of fusing DCVs in neurons. However, fusion pore size can be tested by bath application of labelled dextrans with different sizes (Lynch et al., 2008). Additionally, cargo release is reflected by release of NPY-mCherry (Gandasi et al., 2015), which can be combined with NPY-pHluorin to simultaneously assess DCV pore opening and cargo release. With these methods, future experiments can focus on the relation between fusion pore dynamics and cargo release of fusing DCVs, and test whether Syt1 and Syt7 indeed differentially regulate neuropeptide secretion from fusing DCVs.

Role of Syt localization on fusion pore stability

Syt1 and Syt7 can cross-rescue DCV fusion but not fusion event duration (Chapter 2, 4). GAP43-Syt1 rescued DCV fusion but not event duration, suggesting that plasma membrane targeted Syt1 does not support pore stability. It is currently unknown to what

extent Syt localization contributes to Syt functioning. As discussed in Chapter 4, the vesicular localization of Syt1 and Syt7 may be required to stabilize fusion pores. Vesicular localization of Syt1 depends on a N-glycosylation site, which is required and sufficient to target Syt1, but also Syt7, to vesicles (Han et al., 2004). A Syt7-mutant with the N-glycosylation site may be targeted to DCVs (and SVs) instead of the plasma membrane, and may allow to Syt7 promote fusion pore stability of DCVs and expand the repertoire of functional redundancy between the two Syts. This construct can be used to specify what factors contribute to the unique functions of Syt1 and Syt7 in vesicle fusion.

Roles of Syt in other brain regions

Syt7 is abundantly expressed in the brain (Mittelsteadt et al., 2009) and important for both neurotransmitter and neuropeptide vesicle fusion. Nevertheless, Syt7-KO mice are viable and fertile (Maximov et al., 2008). In contrast, mice deficient for BDNF die early postnatally due to breathing deficits, which can be prevented by sufficient BDNF levels in the brainstem (Erickson et al., 1996; Fox et al., 2013). This suggests that BDNF secretion in brainstem does not require Syt7 or that Syt7 is redundant with other sensors, such as Syt2, which is highly expressed in this region (Pang et al., 2006). Therefore, the role of Syt paralogs in neuropeptide fusion in other brain areas remains a topic for future investigation.

Candidates for a third sensor

Approximately 20% of DCV remained in Syt1/Syt7 double-deficient neurons (Chapter 2, Fig. 3). As DCV fusion strictly depend on Ca^{2+} (Balkowiec and Katz, 2002; Hartmann et al., 2001; de Wit et al., 2009), there may be a third sensor that regulates secretion. Both Syt3 and Syt5[1] are universally expressed in most brain areas (Mittelsteadt et al., 2009; Zeisel et al., 2015) and mediate Ca^{2+}-dependent liposome fusion (Bhalla et al., 2008) and bind SNARE proteins (Vrljic et al., 2010). Very few studies address potential roles of Syt3 and Syt5. Both sensors do not mediate synchronous release or LTP (Wu et al., 2017a; Xu et al., 2007), but Syt3 mediates AMPA-receptor internalization and LTD (Awasthi et al., 2018). No functions are reported for Syt5. Given the universal expression in brain, the SNARE, Ca^{2+} and lipid binding capacity, Syt3 and Syt5 are good candidates for DCV fusion in neurons.

1 Syt5 refers to the Syt isoform with medium Ca2+ affinity (GenBank acc.# U20108). In literature, Syt9, an isoform with high Ca2+ affinity, mediating fast synchronous fusion in some cell types (GenBank acc.# NM_019350), is also referred to as Syt5.

6

MATERIALS AND METHODS

Animals

Primary hippocampal cultures were prepared from Doc2ab-DKO and DHz littermates, or Syt1-KO, Syt7-KO C57BL/6J mice with WT littermates, of both sexes. Doc2a/b-DKO animals were previously described (Groffen et al., 2010). Syt1-KO (Geppert et al., 1994) and Syt7-KO animals (Maximov et al., 2008) were a kind gift from T. C. Südhof. Syt heterozygous animals were cross-bred to generate wild-type (WT) and knock-out (KO) littermate pups for culturing. Animals were genotyped at E18 (Syt1) or P0 (Syt7 and Doc2a/b), prior to culturing. All animals were bred and housed in line with institutional and Dutch governmental guidelines and all procedures were approved by the ethical committee of the Vrije Universiteit, Amsterdam, The Netherlands (DEC-FGA 11-03 and AVD112002017824).

Primary neuronal cultures

Glia microdot islands were prepared on UV-sterilized, etched, agarose coated glass coverslips stamped with 0.1 mg ml^{-1} poly-D-lysine and 0.2 mg ml^{-1} rat tail collagen and 10 mM acetic acid. Hippocampal cultures were prepared from E18 Syt1-KO or P0 Syt7-KO animals. As DCV fusion is variable between different litters/culturing sessions, WT littermates were included as controls. For Chapter 2, Fig. 3, Syt1 knock-down was used, because of a higher probability for WT littermates in double-Hz breedings (Xu et al., 2012). Animals were quickly decapitated and the brains transferred to HBSS buffered with 1 mM HEPES for hippocampal dissection. Hippocampi were digested with 0.25% trypsin for 20 min at 37°C in HBSS, washed 3 times with HBSS, triturated in Glutamax-containing DMEM supplemented with 10% heat-inactivated FCS, 1% NEAA solution, and 1% Pen/strep to inactivate trypsin, and centrifuged for 5 min. The pellet was gently resuspended in pre-warmed enriched

Neurobasal supplemented with 2% B-27, 1.8% HEPES, 0.25% Glutamax, and 0.1% penicillin–streptomycin, and counted in a Fuchs-Rosenthal chamber. Cells were plated at 2K in pre-warmed, enriched Neurobasal-filled 12 wells Cellstar plates. For Western Blot analysis, cortices were isolated and counted as described above, and plated on 0.01% poly-L-ornithine and 2.5 µg/ml laminin diluted in Dulbecco's phosphate-buffered saline coated 6-wells Cellstar plates (Greiner Bio-One) at 300K/well.

Constructs and infections

hNPY-SEP and hNPY-mCherry were made by replacement of NPY-Venus (Nagai et al., 2002) with superecliptic pHluorin (SEP) or mCherry. NPY-SEP is used for all experiments with exception of those presented in Chapter 3, Fig. 3, 4, 5 and Fig. S3. NPY-SEP is targeted to DCVs and quenched by the acidic intraluminal pH. Upon DCV fusion pore opening, SEP is rapidly visualized by the pH of the extracellular solution (pH 7.4). From this point onwards, a DCV may follow one of two scenarios (Wit et al., 2009): (a) fusion pore closing without (full) cargo release, followed by re-acidification or (b) diffusion of cargo out of the vesicle ('full fusion'), which rapidly diffuses in the extracellular solution. In both cases, the NPY-SEP signal de-quenches to baseline levels, which typically takes several seconds. NPY-SEP is an excellent reporter for the duration of a DCV fusion event, but does not discriminate between the two scenarios. The duration of NPY-SEP events ranges from 500 ms (the shortest measurable duration) to the end of the recording (50 s). If cargo diffusion is fast, NPY-SEP fluorescence increase might be too transient to detect reliably, due to the sampling rate (250 ms exposure time at 2 Hz). In Chapter 3, Fig. 5 and Supplementary Fig. S3, Syt1-SEP and Syt7-SEP were used to test if Syt1/7 is on fusing vesicles. Here, the disappearance of NPY-mCherry reports full DCV cargo release, and Syt-SEP report coinciding deacidification of the fusing vesicle.

Syt1 open reading frame and Syt1-shRNA were a kind gift from T. C. Südhof (Xu et al., 2012). Mouse cDNA was prepared from the short (403aa, ENSEMBL Syt7-201) splice variant of Syt7 and sequenced. Syt1 and Syt7 were cloned into a lentivirus backbone, additionally encoding a nuclear targeted mCherry signal. To generate Ca^{2+} binding mutant Syts (Syt1-DA and Syt7-DA), Ca^{2+} binding aspartates where substituted for alanines as described previously (Bacaj et al., 2013). Fluorescent-Syt fusion constructs were made by cloning a fluorescent protein (mCherry or SEP) to the N-terminus of Syt1 and Syt7, preceded by a preprotachykinin signal peptide to ensure ER targeting (kind gift from J. B. Sørensen (Weber et al., 2014)). GAP43-Syt1, encoding GAP43 1-41 aa fused to the N-terminus of Syt1 96-422 aa, was a kind gift from E. R.

Chapman (Hui et al., 2009; Yao et al., 2012a). GAP43-Syt7 was generated by fusing the coding sequence of GAP43 1-41 aa to Syt7 41-403 aa. All constructs were driven by a Synapsin promoter, sequence verified and cloned into a pLenti vector and produced as described (Naldini et al., 1996). Syt1-KD and Syt-rescue constructs were applied to neuronal cultures at DIV2. All other infections were performed at DIV10.

Live-cell imaging

Live-cell imaging (LCI) was performed at DIV15-20 using a custom-built inverted imaging microscope (IX81; Olympus) with an MT20 light source (Olympus), the appropriate filter sets (Semrock, Rochester, NY), a 40× oil objective (NA 1.3) and an EM charge-coupled device camera (C9100-02; Hamamatsu Photonics, Japan). Recordings were made using Xcellence RT imaging software (Olympus). Sampling occurred at 2 Hz with an exposure time of 250 ms. Master 8 (AMPI, Germany) and a stimulus generator (A385RC, World Precision Instruments, Germany) were used to drive two parallel platinum field stimulation electrodes, to deliver 16 trains of 50 action potentials at 50 Hz with 500 ms intervals. No stimulation was used for Syt-localization and co-traveling experiments (Chapter 3, Fig. 2, 3, 4). Cultures were kept at room temperature (RT; 21–24°C), perfused with Tyrode's solution (2 mM $CaCl_2$, 2.5 mM KCl, 119 mM NaCl, 2 mM $MgCl_2$, 30 mM glucose and 25 mM HEPES, pH 7.4). A 10 sec exposure to Tyrode's-NH4 (50 mM NH_4Cl, 2 mM $CaCl_2$, 2.5 mM KCl, 69 mM NaCl, 2 mM $MgCl_2$, 30 mM glucose and 25 mM HEPES, pH 7.4) was used to dequench SEP at the end of each stimulation. For visualization purposes, brightness, and contrast of representative examples was adjusted in a linear and equal fashion between groups.

Immunocytochemistry

Neuronal cultures were fixed with pre-warmed (37°C) 3.7% PFA for 20 min, and washed with phosphate buffered saline (PBS, pH 7.4). Cells were washed with PBS and permeabilized for 5 min with 0.5% Triton X-100 in PBS, and blocked with 5% bovine serum albumin and 0.1% Triton X-100 in PBS for 30 min. Primary and secondary antibodies were incubated overnight at 4°C and at RT for 1 hour, respectively. Primary antibodies were: anti-Syt1 (SySy, 105 001 and 105 008, anti-Syt7 (Neuromab, Q9R0N7), anti-VGlut1 (Millipore, AB5905), and anti-GFP (Bio-Connect, GTX20290 and AVES, 1020). Secondary antibodies were: Fisher Emergo 10286672, Life Technologies A-11010 and A-21450; Fisher Emergo 10739374, Life Technologies A-11008 and A-11074; Life Technologies A-11010 and A-21450; Life Technologies A-11040, A-11001, A-21450. Coverslips were mounted in Mowiol 4-88 (Sigma, 81381) and imaged within 2 weeks on a Nikon confocal laser-scanning microscope with a 40x objective (NA 1.3), controlled by NIS Elements 4.30 software. Semrock filter sets for green (500-550 nm)

and red (580-650 nm or, when combined with far-red, 590-620 nm) and far-red (long pass 650 nm) were used, together with a quad band 405/488/561/635 beam splitter. No bleed through was observed for SEP/Alexa 488, Alexa 546 and Alexa 647 in each other's channels. Laser settings were kept constant within experimental conditions. For visualization purposes, brightness and contrast of representative examples were adjusted in a linear and equal fashion between groups.

Imaging analysis

In ImageJ, ROIs of 3x3 pixels (equals 0.6x0.6 µm) were placed manually on SEP-fusion events, somatic events not included. Movement of de-quenched vesicles out of the ROIs in X/Y direction is very rare, but was detected by an expert observer during validation of the ROI placements in the image stack (movie) and lead to re-positioning or cancellation of the ROI. ROI intensity measures were exported to Matlab for semi-automated detection of fusion events and duration. Intensity traces were plotted as $\Delta F/F_0$, with the average fluorescence of the first 10 frames used to determine F_0. Events were defined as a sudden increase of 2 SD above F_0. Pool estimation was performed using SynD software (Schmitz et al., 2011) in Matlab. For this, a neurite mask (soma not included) was drawn in SynD to estimate the number of puncta/DCVs. Detection parameters were optimized to detect vesicle puncta and kept constant during all datasets. For each neuron, the intensity of an individual DCV was estimated by taking the fluorescence intensity mode per cell in the first two quantiles. Pool size was estimated by correcting the puncta intensities on the individual DCV intensity. Manders overlap coefficient (M1/M2) was determined on neurites exclusively, including above-threshold fluorescence as determined in ImageJ using the JACoP plugin (Bolte and Cordelières, 2006). The Mander's coefficient can be defined as the fraction of total signal in one channel that overlaps/co-occurs with (above threshold) signal of the other channel: 0 representing no overlap, and 1 indicating complete overlap.

Statistics

Data that violated normality (D'Agostino-Pearson) and homogeneity (Fligner-Killeen) was tested with two-sided Mann-Whitney *U* test or Kruskal-Wallis (generating a *U*-statistic and X^2-statistic, respectively) and Dunn's multiple comparison with Benjamini-Hochberg correction. For cumulative plots, the cumulative median number of events were taken for each time point, for each neuron. Box plots were plotted with 25% and 75% interquartile range and Tukey whiskers, presenting the median value in or next to the box plot. Number before and after dash represents

number of independent experiments and number of neurons, respectively. When assumptions of homogeneity and normality were met, data were tested with student's *t*-test or 1-way ANOVA and Holm-Sidak correction and plotted as mean ± SEM. N represents the number of litters, n represents the number of individual neurons, unless stated otherwise.

Westen Blotting

To confirm efficiency of Syt1-KD, cells were scraped in loading sample buffer (2%SDS, 10% glycerol, 0.26 M B-mercaptoethanol, 60 mM Tris pH 6.8) and loaded on a 10% SDS-polyacrylamide gel and transferred on a PVDF membrane. Blots were blocked using 2% milk, 0.5% BSA in PBS containing 0.1% Tween-20 for 1h at 4°C, and incubated overnight at 4°C with monoclonal mouse-anti-Syt1 (BD Biosciences, #610434 and #S39520) and polyclonal rabbit-anti-GAPDH (Abcam, #ab9485) in PBS containing 0.1% Tween-20. Blots were imaged using AttoPhos (Promega, S1001) and a Fuji Film FLA 5000 scanner.

7

SUMMARY

The human brain contains billions of brain cells (**neurons**), which process visual and auditory information, regulate muscle movement and execute cognitive functions. Neurons communicate with each other through the release of signaling molecules. Of these molecules, **neurotransmitters** are best-known. Neurotransmitter release is very fast, as the communication between two neurons takes on 1/50th of a second. Aside from this fast communication, neurons also release slow signaling molecules: **neuropeptides**. Neuropeptides regulate numerous processes in the brain. They are the 'cuddling hormones' of the brain, dampen hyperactivity during an epileptic seizure, let neurons grow in response to physical activity, and can be released in the blood stream to regulate blood pressure, or trigger start the birth of a child. Understandably, neuropeptides are very important for health function of the human brain and body. Multiple clinical trials investigate whether neuropeptides provide an effective treatment for diabetes, post-traumatic stress disorder (PTSD), autism, alcohol addiction, migraine, depression, and others.

Release of neuropeptides is accurately regulated by neurons. Neuropeptides are not free-floating in the brain cell, but are packaged in vesicles, surrounded by a lipid membrane. The vesicles contain many neuropeptide molecules, which gives the vesicle a dark core under the microscope. Therefore, neuropeptide vesicles are called '**dense-core vesicles**' (**DCVs**). Neurons release neuropeptides when the calcium concentration in the cell is high. This happens when the neuron is activated: channels in the cell membrane open, resulting in calcium influx. Calcium triggers the fusion of vesicles with the outer membrane of the neuron, the **plasma membrane** (Fig. 1). Ca^{2+} triggers fusion via the activation of Ca^{2+} binding proteins, the Ca^{2+} sensors. Upon Ca^{2+} binding, Ca^{2+} sensors can fuse the membrane of dense-core vesicles with the plasma membrane of the neuron. Now, neuropeptides can diffuse out of the vesicle and fulfill their signaling function.

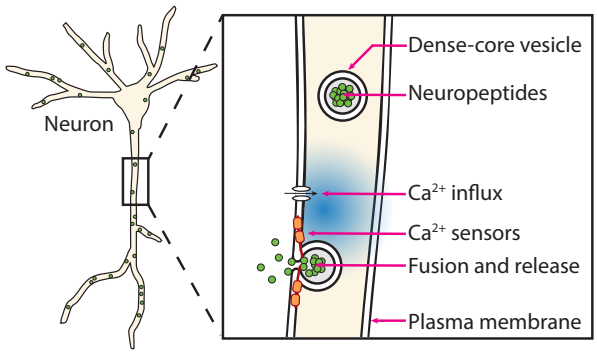

Figure 1: cartoon of a neuron with a zoom-in of two dense-core vesicles: one filled neuropeptides (left), and one dense-core vesicle fusing with the plasma membrane (right), which results in neuropeptide release.

Aim and main findings of this thesis

Neurons express many different calcium sensors, which are all slightly different from each other. This thesis describes which calcium sensors regulate the fusion of dense-core vesicles with the plasma membrane, which allows for the release of neuropeptides.

Chapter 1 provides a general introduction on the topic. I describe the functions of neuropeptides, the production of DCVs, how neurons regulate intracellular Ca^{2+} and which proteins (specifically Ca^{2+} sensors) regulate vesicle fusion.

Chapter 2, describes that two calcium sensors, Synaptotagmin-1 (Syt1) and Synaptotamin-7 (Syt7), are required for the fusion of dense-core vesicles, whereas two other sensors (Doc2a/b) have no effect on DCV fusion. Both Syt1 and Syt7 are required for fusion, because DCV fusion is strongly reduced in absence of these sensors. Additionally, the absence of two sensors does not have an additive effect, suggesting that both sensors operate in the same pathway. Although both sensors are required, they are functionally redundant upon overexpression. Moreover, overexpression of Syt1 and Syt7 increases DCV fusion, suggesting that both sensors are rate-limiting for fusion. As expected, a Ca^{2+} binding mutant that lacks Ca^{2+} binding does not restore DCV fusion in Syt1-KO or Syt7-KO neurons. Finally, Syt1 and Syt7 do not specifically regulate 'fast' or 'slow' DCV fusion in neurons, in contrast to other systems, such as SV and neuroendocrine granule fusion. Taken together, both sensors are required for DCV fusion in the same pathway, in a functionally redundant and dose-dependent manner.

Chapter 3 shows that both calcium sensors are located on different locations in the neuron. Synaptotagmin-1 was present on both on fusing and trafficking DCVs. Synaptotagmin-7 localized to DCVs to lesser extent, but highly localized to the plasma membrane. Syt7 additionally localized to lysosomes. Therefore, Syt1 and Syt7 are present on different cellular compartments, and probably support DCV fusion from different locations.

Chapter 4 describes the kinetics of fusing dense-core vesicles into greater detail and reports that Syt1 and Syt7 differentially regulate the duration of DCV fusion events. Syt1 supports fusion event duration: in absence of Syt1, fusion event duration is shortened, whereas Syt1 overexpression prolongs fusion event duration. This suggests that Syt1 supports pore stability of fusing DCVs. Syt7, in contrast, did not affect fusion event duration.

In **Chapter 5**, I summarize and discuss the findings, and provide suggestions on how Syt1 and Syt7 regulate DCV fusion. This dissertation provides new insights on how Ca^{2+} regulates neuropeptide release, and identifies two sensor sensors, Syt1 and Syt7, that are required for DCV fusion. Moreover, I show that DCV fusion differs from neurotransmitter and neuroendocrine fusion in certain aspects. Hereby, this thesis contributes to our understanding of fundamental molecular mechanisms of neuropeptide signaling in the brain.

8

SAMENVATTING

De menselijke hersenen bevatten miljarden hersencellen (**neuronen**) die sensorische informatie verwerken, spieren aansturen en cognitieve functies uitvoeren. Neuronen communiceren met elkaar door de afgifte van signaalstofjes. Van deze signaalstoffen zijn **neurotransmitters** de bekendste. Neurotransmitterafgifte werkt heel snel, de communicatie tussen twee neuronen duurt slechts 1/50^{e} van een seconde. Naast deze snelle communicatie geven neuronen ook langzame signaalstofjes af: **neuropeptiden**. Neuropeptiden regelen tal van processen in de hersenen. Ze zijn het 'knuffelhormoon' van de hersenen, dempen overactiviteit bij een epileptische aanval, laten neuronen groeien na het sporten, kunnen in de bloedbaan afgegeven worden en bloeddruk regelen of de geboorte van een kind in gang zetten. Begrijpelijkerwijs zijn neuropeptiden erg belangrijk om gezond te functioneren. Er lopen klinische trials die onderzoeken of neuropeptiden ingezet kunnen worden voor goede behandelingen bij diabetes, posttraumatisch stresssyndroom (PTSS), autisme, alcoholverslaving, migraine, depressie en andere aandoeningen.

De afgifte van neuropeptiden wordt nauwkeurig gereguleerd door neuronen. Neuropeptiden zweven niet los door de hersencel, maar zijn verpakt in blaasjes (**vesicles**), omgeven met een vetmembraan. De vesicles bevatten erg veel neuropeptidemoleculen, waardoor de vesicles onder de microscoop een donkere kern hebben. Daarom heten ze **dense-core vesicles** (**DCVs**). Neuronen geven neuropeptiden af wanneer er veel calcium in de cel is. Dit gebeurt wanneer het neuron actief is: kanaaltjes in het celmembraan schieten open en calcium vloeit de cel binnen. Calcium triggert de fusie van vesicles met de buitenkant van de hersencel, het **plasma membraan** (Fig. 1). Calcium doet dit niet op zichzelf, maar door te binden aan Ca^{2+}-sensoren. Wanneer Ca^{2+}-sensoren Ca^{2+} binden, kunnen ze het plasmamembraan fuseren met het vesicle-membraan. Hierdoor worden de neuropeptiden afgegeven en kan het zijn signaalfunctie vervullen.

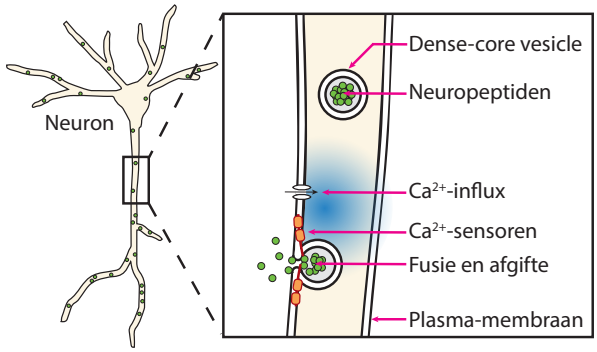

Figuur 1: cartoon van een neuron met een zoom-in van twee dense-core vesicles: één gevuld met neuropeptiden (boven), en één dense-core vesicle die fuseert met de plasma membraan (onder), waardoor neuropeptiden worden afgegeven.

Doel en hoofdbevindingen van deze thesis

Er zijn veel verschillende calcium sensoren, die allemaal net een beetje anders zijn. Deze thesis beschrijft welke calcium-sensoren er voor zorgen dat DCVs met het celmembraan fuseren, waardoor neuropeptiden afgegeven kunnen worden.

Hoofdstuk 1 geeft een algemene introductie van het onderwerp. Ik beschrijf de functies van neuropeptiden, de productie van DCVs, hoe neuronen Ca^{2+} reguleren en welke eiwitten (in het bijzonder Ca^{2+}-sensoren) de fusie van vesicles regelen.

In **hoofdstuk 2** beschrijf ik dat twee calcium sensoren, Synaptotagmin-1 (Syt1) en Synaptotamin-7 (Syt7), nodig zijn voor de fusie van DCVs, maar dat twee andere sensoren (Doc2a/b) geen invloed hebben op DCV-fusie. Zowel Syt1 en Syt7 zijn nodig voor fusie, want als één van de twee wegvalt, fuseren er bijna geen DCVs meer. Bovendien zorgt de afwezigheid van beide sensoren niet voor een sterkere reductie in fusie dan wanneer één van de twee sensoren aanwezig is. Dit duidt er op dat Syt1 en Syt7 fusie regelen van dezelfde DCVs, in dezelfde 'pathway'. Hoewel beide sensoren nodig zijn, kunnen ze tóch elkaars functie overnemen, zolang er maar veel van één soort aanwezig is. Daarnaast laat ik zien dat overexpressie van beide Synaptotagmins zorgt voor méér DCV-fusie, wat er op wijst dat het aantal Syt-moleculen beperkend (rate-limiting) is voor DCV-fusie. Zoals verwacht kunnen sensoren waarvan de Ca^{2+}-bindende domeinen gemuteerd zijn (ze kunnen dus geen Ca^{2+} meer binden) geen vesiclefusie triggeren. Als laatste laat ik zien dat Syt1 en Syt7 niet specifiek 'snelle' of 'langzame' DCV-fusie regelen, in tegenstelling tot wat tot nu toe bekend is over deze sensoren. Dit alles wijst erop dat beide Ca^{2+}-sensoren

DCV fusie regelen in dezelfde pathway, en dat het aantal Syt-moleculen bepalend is voor de efficiëntie daarvan.

In **hoofdstuk 3** laat ik zien dat beide calciumsensoren op verschillende plekken in de hersencel aanwezig zijn. Synaptotagmin-1 zit op DCVs, zowel op fuserende als op bewegende, niet-fuserende DCVs. Synaptotagmin-7 zit veel minder op DCVs, maar is daarentegen meer aanwezig op de plasmamembraan van de hersencel. Daarnaast is Syt7 veel aanwezig op lysosomen, de afvalverwerkers van de cel. Syt1 en Syt7 zijn dus aanwezig in verschillende compartimenten, en ondersteunen/regelen DCV-fusie waarschijnlijk vanaf verschillende locaties in het neuron.

Hoofdstuk 4 gaat dieper in op de eigenschappen van fuserende dense-core vesicles en rapporteert dat Syt1 and Syt7 een verschillende invloed hebben op de duur van fuserende DCVs (**fusie events**). Synaptotagmin-1 zorgt ervoor dat fusie-events lang aan de membraan blijven zitten: wanneer Syt1 niet aanwezig is, duurt een fusie-event korter, en een fusie-event duurt juist langer wanneer Syt1 tot overexpressie wordt gebracht. Dit betekent waarschijnlijk dat Synaptotagmin-1 voor stabiliteit zorgt (van de 'fusie pore') van het fuserende vesicle aan de plasma membraan. Synaptotagmin-7 daarentegen had geen invloed op de duur van fusie-events.

In **hoofdstuk 5** worden de bevindingen samengevat en bediscussieerd en doe ik verschillende suggesties over de werkingsmechanismen van Syts in DCV-fusie. Dit proefschrift geeft nieuwe inzichten in hoe Ca^{2+} de afgifte van neuropeptiden reguleert en identificeert twee Ca^{2+}-sensoren, Syt1 en Syt7, die nodig zijn voor de fusie van DCVs. Daarnaast laat ik zien dat DCV-fusie in bepaalde aspecten verschilt van de afgifte van neurotransmitters en neuro-endocriene signaalstoffen. Al met al draagt deze thesis bij aan het begrip van fundamentele moleculaire mechanismen van neuropeptide-gemedieerde signaaloverdacht in het brein.

9

ACKNOWLEDGEMENTS / DANKWOORD

Finally, the thesis (iterating through several 'final' versions) has been completed! Adhering to the rules of scientific writing, the text in this thesis has been meticulously stripped from all emotional load. You will therefore not read sentences like 'manual detection of DCV fusion events (a.k.a. 'clicking') was a near-RSI experience, but was kept in the doable range thanks to the continuous supply of podcasts, TED-talks, and documentaries', but instead find it formulated as '3 x 3 pixel ROIs were manually placed using ImageJ'. This way of formulation supports readability and objectivity, although most scientists will acknowledge that research is a continuous oscillation between success and failure. To the researcher the task to come up with new experiments to flip the balance to the first. One of many things I learned during a PhD, is that the prerequisite for finishing a PhD lies in successful mood management. This thesis would not have been possible without the support of others. Therefore, I would like to thank everyone who has been on my side and contributed to the success of this intense and wonderful life experience.

First, I would like to express my sincere gratitude towards **Matthijs**. Matthijs, your incredible scientific knowledge and insight gave me the foundation to shape the project and to stay focused on the right research question. Thanks to your writing skills, this thesis and especially the manuscript improved immensely. You have shown patience and gave me a great deal of freedom when I needed it most, but also knew when to increase pressure to improve and perform. Overall, you helped me grow as a researcher, and I am sure that I can benefit a life-time from it. Thank you very much for your supervision and support in the past years.

Ruud, thank you for your endless supply of enthusiasm and the ability to motivate me in almost every meeting we've had. Without a doubt, many of my presentations were brought to a higher level thanks to your – always very clear – feedback. Thanks for all the discussions and for your scientific input, which helped to shape the experiments and often provided me input for new interesting research questions. Your positivity and support along the way has been of great value.

I would like to thank the **doctorate committee** for reading this thesis and for discussing it during the defense.

As all my experiments revolved around microscopes and analysis software, the one person that deserves an enormous amounts of 'thanks', are you, **Jurjen**. You were always prepared to patiently resolve any issue that came across, and provided me many, many technical solutions – sometimes being as short as 'RTFM'. It was a pleasure to share an office with you, and to share many fun moments, in-or outside the 16-o'clock sessions.

Josse, it was a pleasure to have you as a student. You were not only motivated and incredibly well-organized, but also very productive. A supervisor can only dream of the amount of results you obtained in just a couple of months. I highly appreciated the positivity you brought to the lab and find it great to see that you decided to spend another couple of (PhD) years at FGA.

Els and **Sjaak**, thanks both of you for being so helpful and for the smooth organization of the department.

Thanks to all the **technicians**, the backbone of FGA. Your help was indispensable. Thanks **Robbie** for your help with the plenty of constructs and the production of numerous batches of viruses. I lost count on the number of lentiviral constructs I requested, of which some were not easy to clone. Thanks for thinking along while designing them, for producing all of them, and for your kindness along the way. Thanks **Desiree** and **Lisa**, for your continuous supply of glia plates and trouble-shooting to increase culturing quality. Moreover, thanks for all your efforts to maintain the lab clean, well-organized and stocked, which is not your sole responsibility, but many times came down on your shoulders nevertheless. Thanks **Joke**, for managing my mouse lines, and your efforts and help to scale up to the maximum of our capacity when time was running out. **Joost**, thanks for all those tails you genotyped! **Ingrid**,

thanks for your help with western blotting and cloning. All other technicians, thanks for all your help and support in making everything work.

Thanks to all the members of the **DCV team** for the discussions and support along the way. In particular thanks to **Alessandro** for your help on coding, which saved me an incredible amount of time. **Rein**, thanks for being on my side – literally in this case, as office-member, to discuss Syt7 every now and then. **Daniël**, thanks for all the talks and data discussions we had, and for smooth TIM1 agenda alignments.

Rein, Annemiek, Nikki, Miriam, Lola, Jurjen, Roberta, Enqi, Ana Rita, Sverrir, Fatima: what a great collection of office-mates I have! Thanks for all the discussions, the good laughs and for the talks when needed, the coffees, horoscopes, room outings, fixed cow brains, and weird foods you brought. Thanks for making A445 such a great office.

To **all other (former) collegues** from FGA, thanks for your scientific input, and for making the workplace a much more enjoyable place to be.

Ioannis, thanks for introducing me into the CNCR institute, first being my internship supervisor, but soon as a dear friend. With this thesis defense, may the Advalvas not be required for the occasion, our VU era comes to an end. The breaks at the lush green back of the VU stay with me as one of the most precious memories from my time at the VU. Thanks for your support and trust in my research capabilities, even before I started my PhD. Your open view of the world that still manages to surprise me every now and then, as it did recently with your swift career switch to carpentry, and I am grateful to have you as a friend. Now, let's quickly check that final box from the VU-do-to list, and celebrate with a fine whisky on Weesps sunniest and greenest corner.

Julia, we only shared a very little part of our CNCR career, me as a fresh master's student at INF and you as a senior PhD student. However, you significantly contributed to a very warming welcome at the CNCR, even letting me stay in your Real Estate at the Zuidas for a while, to save traveling time. Looking forward to many more dinners together and if you ever need to plant another water lily, I'm at your service!

In het bijzonder dank aan **pap en mam**, en natuurlijk mijn **broer** en **zussen,** voor jullie niet-aflatende interesse, advies, steun, warmte en gezelligheid.

Dank aan mijn lieve **vrienden**, waaronder mijn paranymf **Hannah**, die altijd naast mij hebben gestaan.

Maarten, mijn allergrootste liefde. Zoveel grote woorden strijden om voorrang bij het schrijven van dit stukje. Onze jaren samen beschouw ik als de kostbaarste jaren van mijn leven, en ik kan niet wachten op de toekomst met jou. Zonder jou was dit niet gelukt.

10

REFERENCES

Ahras, M., Otto, G.P., and Tooze, S.A. (2006). Synaptotagmin IV is necessary for the maturation of secretory granules in PC12 cells. J. Cell Biol. *173*, 241–251.

Albillos, A., Dernick, G., Horstmann, H., Almers, W., de Toledo, G.A., and Lindau, M. (1997). The exocytotic event in chromaffin cells revealed by patch amperometry. Nature *389*, 509–512.

Alés, E., Tabares, L., Poyato, J.M., Valero, V., Lindau, M., and Toledo, G.A. de (1999). High calcium concentrations shift the mode of exocytosis to the kiss-and-run mechanism. Nature Cell Biology *1*, 40.

Araç, D., Chen, X., Khant, H.A., Ubach, J., Ludtke, S.J., Kikkawa, M., Johnson, A.E., Chiu, W., Südhof, T.C., and Rizo, J. (2006). Close membrane-membrane proximity induced by Ca 2+ -dependent multivalent binding of synaptotagmin-1 to phospholipids. Nat Struct Mol Biol *13*, 209–217.

Arora, S., Saarloos, I., Kooistra, R., Bospoort, R. van de, Verhage, M., and Toonen, R.F. (2017). SNAP-25 gene family members differentially support secretory vesicle fusion. J Cell Sci *130*, 1877–1889.

Awasthi, A., Ramachandran, B., Ahmed, S., Benito, E., Shinoda, Y., Nitzan, N., Heukamp, A., Rannio, S., Martens, H., Barth, J., et al. (2018). Synaptotagmin-3 drives AMPA receptor endocytosis, depression of synapse strength, and forgetting. Science eaav1483.

Bacaj, T., Wu, D., Yang, X., Morishita, W., Zhou, P., Xu, W., Malenka, R.C., and Südhof, T.C. (2013a). Synaptotagmin-1 and Synaptotagmin-7 Trigger Synchronous and Asynchronous Phases of Neurotransmitter Release. Neuron *80*, 947–959.

Bacaj, T., Wu, D., Yang, X., Morishita, W., Zhou, P., Xu, W., Malenka, R.C., and Südhof, T.C. (2013b). Synaptotagmin-1 and Synaptotagmin-7 Trigger Synchronous and Asynchronous Phases of Neurotransmitter Release. Neuron *80*, 947–959.

Bacaj, T., Wu, D., Burré, J., Malenka, R.C., Liu, X., and Südhof, T.C. (2015). Synaptotagmin-1 and -7 Are Redundantly Essential for Maintaining the Capacity of the Readily-Releasable Pool of Synaptic Vesicles. PLOS Biol *13*, e1002267.

Bai, J., Wang, C.-T., Richards, D.A., Jackson, M.B., and Chapman, E.R. (2004a). Fusion Pore Dynamics Are Regulated by Synaptotagmin•t-SNARE Interactions. Neuron *41*, 929–942.

Bai, J., Tucker, W.C., and Chapman, E.R. (2004b). PIP 2 increases the speed of response of synaptotagmin and steers its membrane-penetration activity toward the plasma membrane. Nat Struct Mol Biol *11*, 36–44.

Baker, K., Gordon, S.L., Melland, H., Bumbak, F., Scott, D.J., Jiang, T.J., Owen, D., Turner, B.J., Boyd, S.G., Rossi, M., et al. (2018). SYT1-associated neurodevelopmental disorder: a case series. Brain.

Balkowiec, A., and Katz, D.M. (2000). Activity-Dependent Release of Endogenous Brain-Derived Neurotrophic Factor from Primary Sensory Neurons Detected by ELISAIn Situ. J. Neurosci. *20*, 7417–7423.

Balkowiec, A., and Katz, D.M. (2002). Cellular Mechanisms Regulating Activity-Dependent Release of Native Brain-Derived Neurotrophic Factor from Hippocampal Neurons. J. Neurosci. *22*, 10399–10407.

Banerjee, A., Lee, J., Nemcova, P., Liu, C., and Kaeser, P.S. (2020). Synaptotagmin-1 is the Ca2+ sensor for fast striatal dopamine release. ELife *9*, e58359.

Bao, H., Goldschen-Ohm, M., Jeggle, P., Chanda, B., Edwardson, J.M., and Chapman, E.R. (2016). Exocytotic fusion pores are composed of both lipids and proteins. Nat Struct Mol Biol *23*, 67–73.

Bao, H., Das, D., Courtney, N.A., Jiang, Y., Briguglio, J.S., Lou, X., Roston, D., Cui, Q., Chanda, B., and Chapman, E.R. (2018a). Trans-SNARE complex dynamics and number determine nascent fusion pore properties. Nature *554*, 260–263.

Bao, H., Das, D., Courtney, N.A., Jiang, Y., Briguglio, J.S., Lou, X., Roston, D., Cui, Q., Chanda, B., and Chapman, E.R. (2018b). Dynamics and number of *trans*-SNARE complexes determine nascent fusion pore properties. Nature *554*, 260–263.

Baraban, S.C., Hollopeter, G., Erickson, J.C., Schwartzkroin, P.A., and Palmiter, R.D. (1997). Knock-Out Mice Reveal a Critical Antiepileptic Role for Neuropeptide Y. J. Neurosci. *17*, 8927–8936.

Bartfai, T., Iverfeldt, K., Fisone, G., and Serfözö, P. (1988). Regulation of the release of coexisting neurotransmitters. Annu. Rev. Pharmacol. Toxicol. *28*, 285–310.

Bendahmane, M., Bohannon, K.P., Bradberry, M.M., Rao, T.C., Schmidtke, M.W., Abbineni, P.S., Chon, N.L., Tran, S., Lin, H., Chapman, E.R., et al. (2018). The synaptotagmin C2B domain calcium-binding loops modulate the rate of fusion pore expansion. MBoC *29*, 834–845.

Bendahmane, M., Morales, A., Kreutzberger, A.J.B., Schenk, N.A., Mohan, R., Bakshi, S., Philippe, J.M., Zhang, S., Kiessling, V., Tamm, L.K., et al. (2020). Synaptotagmin-7 enhances calcium-sensing of chromaffin cell granules and slows discharge of granule cargos. J Neurochem *154*, 598–617.

Bhalla, A., Chicka, M.C., and Chapman, E.R. (2008). Analysis of the Synaptotagmin Family during Reconstituted Membrane Fusion. J Biol Chem *283*, 21799–21807.

Bharat, V., Siebrecht, M., Burk, K., Ahmed, S., Reissner, C., Kohansal-Nodehi, M., Steubler, V., Zweckstetter, M., Ting, J.T., and Dean, C. (2017). Capture of Dense Core Vesicles at Synapses by JNK-Dependent Phosphorylation of Synaptotagmin-4. Cell Rep *21*, 2118–2133.

Bolte, S., and Cordelières, F.P. (2006). A guided tour into subcellular colocalization analysis in light microscopy. J Microsc *224*, 213–232.

Bospoort, R. van de, Farina, M., Schmitz, S.K., Jong, A. de, Wit, H. de, Verhage, M., and Toonen, R.F. (2012). Munc13 controls the location and efficiency of dense-core vesicle release in neurons. J Cell Biol *199*, 883–891.

Boucrot, E., Saffarian, S., Zhang, R., and Kirchhausen, T. (2010). Roles of AP-2 in clathrin-mediated endocytosis. PLoS ONE *5*, e10597.

Bradberry, M.M., Courtney, N.A., Dominguez, M.J., Lofquist, S.M., Knox, A.T., Sutton, R.B., and Chapman, E.R. (2020). Molecular Basis for Synaptotagmin-1-Associated Neurodevelopmental Disorder. Neuron *107*, 52-64.e7.

Brandt, D.S., Coffman, M.D., Falke, J.J., and Knight, J.D. (2012). Hydrophobic Contributions to the Membrane Docking of Synaptotagmin 7 C2A Domain: Mechanistic Contrast between Isoforms 1 and 7. Biochemistry *51*, 7654–7664.

Brose, N., Petrenko, A.G., Südhof, T.C., and Jahn, R. (1992). Synaptotagmin: A Calcium Sensor on the Synaptic Vesicle Surface. Science, New Series *256*, 1021–1025.

Brose, N., Hofmann, K., Hata, Y., and Südhof, T.C. (1995). Mammalian homologues of Caenorhabditis elegans unc-13 gene define novel family of C2-domain proteins. J Biol Chem *270*, 25273–25280.

Brownstein, M.J., Russell, J.T., and Gainer, H. (1980). Synthesis, transport, and release of posterior pituitary hormones. Science *207*, 373–378.

Burbach, J.P.H. (2011). What Are Neuropeptides? In Neuropeptides, (Humana Press), pp. 1–36.

Cao, P., Maximov, A., and Südhof, T.C. (2011). Activity-Dependent IGF-1 Exocytosis is Controlled by the Ca2+-Sensor Synaptotagmin-10. Cell *145*, 300–311.

Cao, P., Yang, X., and Südhof, T.C. (2013). Complexin Activates Exocytosis of Distinct Secretory Vesicles Controlled by Different Synaptotagmins. J. Neurosci. *33*, 1714–1727.

Catterall, W.A. (2000). Structure and regulation of voltage-gated Ca2+ channels. Annu Rev Cell Dev Biol *16*, 521–555.

Chakrabarti, S., Kobayashi, K.S., Flavell, R.A., Marks, C.B., Miyake, K., Liston, D.R., Fowler, K.T., Gorelick, F.S., and Andrews, N.W. (2003). Impaired membrane resealing and autoimmune myositis in synaptotagmin VII–deficient mice. J Cell Biol *162*, 543–549.

Chang, S., Trimbuch, T., and Rosenmund, C. (2018). Synaptotagmin-1 drives synchronous Ca2+-triggered fusion by C2B-domain-mediated synaptic-vesicle-membrane attachment. Nat. Neurosci. *21*, 33–40.

Chen, C., Satterfield, R., Young, S.M., and Jonas, P. (2017). Triple Function of Synaptotagmin 7 Ensures Efficiency of High-Frequency Transmission at Central GABAergic Synapses. Cell Reports *21*, 2082–2089.

Cheng, X.-T., Xie, Y.-X., Zhou, B., Huang, N., Farfel-Becker, T., and Sheng, Z.-H. (2018). Characterization of LAMP1-labeled nondegradative lysosomal and endocytic compartments in neurons. J Cell Biol *217*, 3127–3139.

Chini, B., Verhage, M., and Grinevich, V. (2017). The Action Radius of Oxytocin Release in the Mammalian CNS: From Single Vesicles to Behavior. Trends in Pharmacological Sciences *38*, 982–991.

Chow, R.H. (1992). Delay in vesicle fusion revealed by electrochemical monitoring of single secretory events in adrenal chromaffin cells. *356*, 4.

Courtney, N.A., Briguglio, J.S., Bradberry, M.M., Greer, C., and Chapman, E.R. (2018). Excitatory and Inhibitory Neurons Utilize Different Ca2+ Sensors and Sources to Regulate Spontaneous Release. Neuron *98*, 977-991.e5.

Courtney, N.A., Bao, H., Briguglio, J.S., and Chapman, E.R. (2019). Synaptotagmin 1 clamps synaptic vesicle fusion in mammalian neurons independent of complexin. Nat Commun *10*, 1–14.

Craxton, M. (2004). Synaptotagmin gene content of the sequenced genomes. BMC Genomics *5*, 43.

Craxton, M. (2007). Evolutionary genomics of plant genes encoding N-terminal-TM-C2 domain proteins and the similar FAM62 genes and synaptotagmin genes of metazoans. BMC Genomics *8*, 259.

Craxton, M. (2010). A manual collection of Syt, Esyt, Rph3a, Rph3al, Doc2, and Dblc2 genes from 46 metazoan genomes - an open access resource for neuroscience and evolutionary biology. BMC Genomics *11*, 37.

Craxton, M., and Goedert, M. (1999). Alternative splicing of synaptotagmins involving transmembrane exon skipping. FEBS Lett *460*, 417–422.

Das, D., Bao, H., Courtney, K.C., Wu, L., and Chapman, E.R. (2020). Resolving kinetic intermediates during the regulated assembly and disassembly of fusion pores. Nat Commun *11*, 1–12.

Dean, C., Liu, H., Mark Dunning, F., Chang, P.Y., Jackson, M.B., and Chapman, E.R. (2009). Synaptotagmin-IV modulates synaptic function and long-term potentiation by regulating BDNF release. Nat Neurosci *12*, 767–776.

Dean, C., Dunning, F.M., Liu, H., Bomba-Warczak, E., Martens, H., Bharat, V., Ahmed, S., and Chapman, E.R. (2012). Axonal and dendritic synaptotagmin isoforms revealed by a pHluorin-syt functional screen. Mol Biol Cell *23*, 1715–1727.

DeLaney, K., Buchberger, A.R., Atkinson, L., Gründer, S., Mousley, A., and Li, L. (2018). New techniques, applications and perspectives in neuropeptide research. J Exp Biol *221*, jeb151167.

Díez-Arazola, R., Meijer, M., Bourgeois-Jaarsma, Q., Cornelisse, L.N., Verhage, M., and Groffen, A.J. (2020). Doc2 Proteins Are Not Required for the Increased Spontaneous Release Rate in Synaptotagmin-1-Deficient Neurons. J. Neurosci. *40*, 2606–2617.

Dubé, C. (2007). Neuropeptide Y: potential role in recurrent developmental seizures. Peptides *28*, 441–446.

Dulubova, I., Sugita, S., Hill, S., Hosaka, M., Fernandez, I., Südhof, T.C., and Rizo, J. (1999). A conformational switch in syntaxin during exocytosis: role of munc18. EMBO J. *18*, 4372–4382.

Duncan, R.R., Betz, A., Shipston, M.J., Brose, N., and Chow, R.H. (1999). Transient, Phorbol Ester-induced DOC2-Munc13 Interactions in Vivo. J. Biol. Chem. *274*, 27347–27350.

Dutton, A., and Dyball, R.E. (1979). Phasic firing enhances vasopressin release from the rat neurohypophysis. J. Physiol. (Lond.) *290*, 433–440.

Eggermann, E., Bucurenciu, I., Goswami, S.P., and Jonas, P. (2011). Nanodomain coupling between Ca2+ channels and sensors of exocytosis at fast mammalian synapses. Nat Rev Neurosci *13*, 7–21.

Emperador-Melero, J., Huson, V., Weering, J. van, Bollmann, C., Mollard, G.F. von, Toonen, R.F., and Verhage, M. (2018). Vti1a/b regulate synaptic vesicle and dense core vesicle secretion via protein sorting at the Golgi. Nature Communications *9*, 3421.

Erickson, J.T., Conover, J.C., Borday, V., Champagnat, J., Barbacid, M., Yancopoulos, G., and Katz, D.M. (1996). Mice lacking brain-derived neurotrophic factor exhibit visceral sensory neuron losses distinct from mice lacking NT4 and display a severe developmental deficit in control of breathing. Journal of Neuroscience *16*, 5361–5371.

Fernandez, I., Araç, D., Ubach, J., Gerber, S.H., Shin, O., Gao, Y., Anderson, R.G.W., Südhof, T.C., and Rizo, J. (2001). Three-Dimensional Structure of the Synaptotagmin 1 C2B-Domain: Synaptotagmin 1 as a Phospholipid Binding Machine. Neuron *32*, 1057–1069.

Fernández-Chacón, R., and Alvarez de Toledo, G. (1995). Cytosolic calcium facilitates release of secretory products after exocytotic vesicle fusion. FEBS Lett. *363*, 221–225.

Fernández-Chacón, R., Königstorfer, A., Gerber, S.H., García, J., Matos, M.F., Stevens, C.F., Brose, N., Rizo, J., Rosenmund, C., and Südhof, T.C. (2001). Synaptotagmin I functions as a calcium regulator of release probability. Nature *410*, 41–49.

Fisher, J.M., Sossin, W., Newcomb, R., and Scheller, R.H. (1988). Multiple neuropeptides derived from a common precursor are differentially packaged and transported. Cell *54*, 813–822.

Fox, E.A., Biddinger, J.E., Jones, K.R., McAdams, J., and Worman, A. (2013). Mechanism of Hyperphagia Contributing to Obesity in Brain-Derived Neurotrophic Factor Knockout Mice. Neuroscience *229*, 176–199.

Freeman, G.M., and Herzog, E.D. (2011). Neuropeptides go the distance for circadian synchrony. PNAS *108*, 13883–13884.

Friedrich, R., Groffen, A.J., Connell, E., van Weering, J.R.T., Gutman, O., Henis, Y.I., Davletov, B., and Ashery, U. (2008). DOC2B Acts as a Calcium Switch and Enhances Vesicle Fusion. J Neurosci *28*, 6794–6806.

Fukuda, M., and Mikoshiba, K. (2000). Doc2gamma, a third isoform of double C2 protein, lacking calcium-dependent phospholipid binding activity. Biochem. Biophys. Res. Commun. *276*, 626–632.

Fukuda, M., Kanno, E., and Mikoshiba, K. (1999). Conserved N-terminal Cysteine Motif Is Essential for Homo- and Heterodimer Formation of Synaptotagmins III, V, VI, and X. J. Biol. Chem. *274*, 31421–31427.

Fukuda, M., Saegusa, C., Kanno, E., and Mikoshiba, K. (2001). The C2A domain of double C2 protein gamma contains a functional nuclear localization signal. J. Biol. Chem. *276*, 24441–24444.

Fukuda, M., Kowalchyk, J.A., Zhang, X., Martin, T.F.J., and Mikoshiba, K. (2002). Synaptotagmin IX Regulates Ca2+-dependent Secretion in PC12 Cells. J. Biol. Chem. *277*, 4601–4604.

Fukuda, M., Kanno, E., Satoh, M., Saegusa, C., and Yamamoto, A. (2004). Synaptotagmin VII Is Targeted to Dense-core Vesicles and Regulates Their Ca2+-dependent Exocytosis in PC12 Cells. J. Biol. Chem. *279*, 52677–52684.

Gainer, H., Wolfe, S.A., Obaid, A.L., and Salzberg, B.M. (1986). Action potentials and frequency-dependent secretion in the mouse neurohypophysis. Neuroendocrinology *43*, 557–563.

Gandasi, N.R., Vestö, K., Helou, M., Yin, P., Saras, J., and Barg, S. (2015). Survey of Red Fluorescence Proteins as Markers for Secretory Granule Exocytosis. PLoS One *10*.

Gao, Y., Zorman, S., Gundersen, G., Xi, Z., Ma, L., Sirinakis, G., Rothman, J.E., and Zhang, Y. (2012). Single Reconstituted Neuronal SNARE Complexes Zipper in Three Distinct Stages. Science *337*, 1340–1343.

Gao, Z., Reavey-Cantwell, J., Young, R.A., Jegier, P., and Wolf, B.A. (2000). Synaptotagmin III/VII isoforms mediate Ca2+-induced insulin secretion in pancreatic islet beta -cells. J. Biol. Chem. *275*, 36079–36085.

García-Junco-Clemente, P., Cantero, G., Gómez-Sánchez, L., Linares-Clemente, P., Martínez-López, J.A., Luján, R., and Fernández-Chacón, R. (2010). Cysteine String Protein-α Prevents Activity-Dependent Degeneration in GABAergic Synapses. J Neurosci *30*, 7377–7391.

Gauthier, B.R., Duhamel, D.L., Iezzi, M., Theander, S., Saltel, F., Fukuda, M., Wehrle-Haller, B., and Wollheim, C.B. (2007). Synaptotagmin VII splice variants α, β, and δ are expressed in pancreatic β-cells and regulate insulin exocytosis. The FASEB Journal *22*, 194–206.

Geppert, M., Goda, Y., Hammer, R.E., Li, C., Rosahl, T.W., Stevens, C.F., and Südhof, T.C. (1994). Synaptotagmin I: A major Ca2+ sensor for transmitter release at a central synapse. Cell *79*, 717–727.

Grimmelikhuijzen, C.J., Leviev, I., and Carstensen, K. (1996). Peptides in the nervous systems of cnidarians: structure, function, and biosynthesis. Int. Rev. Cytol. *167*, 37–89.

Grimmelikhuijzen, C.J., Hauser, F., Eriksen, K.K., and Williamson, M. (1999). Invertebrate neurohormones and their receptors. Results Probl Cell Differ *26*, 339–362.

Groffen, A.J., Martens, S., Díez Arazola, R., Cornelisse, L.N., Lozovaya, N., de Jong, A.P.H., Goriounova, N.A., Habets, R.L.P., Takai, Y., Borst, J.G., et al. (2010). Doc2b is a high-affinity Ca2+ sensor for spontaneous neurotransmitter release. Science *327*, 1614–1618.

Groffen, A.J.A., Brian, E.C., Dudok, J.J., Kampmeijer, J., Toonen, R.F., and Verhage, M. (2004). Ca2+-induced Recruitment of the Secretory Vesicle Protein DOC2B to the Target Membrane. J. Biol. Chem. *279*, 23740–23747.

Groffen, A.J.A., Friedrich, R., Brian, E.C., Ashery, U., and Verhage, M. (2006). DOC2A and DOC2B are sensors for neuronal activity with unique calcium-dependent and kinetic properties. Journal of Neurochemistry *97*, 818–833.

Gustavsson, N., Lao, Y., Maximov, A., Chuang, J.-C., Kostromina, E., Repa, J.J., Li, C., Radda, G.K., Südhof, T.C., and Han, W. (2008). Impaired insulin secretion and glucose intolerance in synaptotagmin-7 null mutant mice. Proc. Natl. Acad. Sci. U.S.A. *105*, 3992–3997.

Gustavsson, N., Wei, S.-H., Hoang, D.N., Lao, Y., Zhang, Q., Radda, G.K., Rorsman, P., Südhof, T.C., and Han, W. (2009). Synaptotagmin-7 is a principal Ca2+ sensor for Ca2+-induced glucagon exocytosis in pancreas. The Journal of Physiology *587*, 1169–1178.

Han, W., Rhee, J.-S., Maximov, A., Lao, Y., Mashimo, T., Rosenmund, C., and Südhof, T.C. (2004). N-Glycosylation Is Essential for Vesicular Targeting of Synaptotagmin 1. Neuron *41*, 85–99.

Hanyaloglu, A.C., and von Zastrow, M. (2008). Regulation of GPCRs by endocytic membrane trafficking and its potential implications. Annu. Rev. Pharmacol. Toxicol. *48*, 537–568.

Harris, K.M., and Sultan, P. (1995). Variation in the number, location and size of synaptic vesicles provides an anatomical basis for the nonuniform probability of release at hippocampal CA1 synapses. Neuropharmacology *34*, 1387–1395.

Hartmann, J., and Lindau, M. (1995). A novel Ca(2+)-dependent step in exocytosis subsequent to vesicle fusion. FEBS Lett. *363*, 217–220.

Hartmann, M., Heumann, R., and Lessmann, V. (2001). Synaptic secretion of BDNF after high-frequency stimulation of glutamatergic synapses. EMBO J *20*, 5887–5897.

He, E., Wierda, K., van Westen, R., Broeke, J.H., Toonen, R.F., Cornelisse, L.N., and Verhage, M. (2017a). Munc13-1 and Munc18-1 together prevent NSF-dependent de-priming of synaptic vesicles. Nature Communications *8*, 15915.

He, Q., Wu, B., Price, J.L., and Zhao, Z. (2017b). Circadian Rhythm Neuropeptides in Drosophila: Signals for Normal Circadian Function and Circadian Neurodegenerative Disease. Int J Mol Sci *18*.

Hefft, S., and Jonas, P. (2005). Asynchronous GABA release generates long-lasting inhibition at a hippocampal interneuron–principal neuron synapse. Nature Neuroscience *8*, 1319.

Helmchen, F., Borst, J.G., and Sakmann, B. (1997). Calcium dynamics associated with a single action potential in a CNS presynaptic terminal. Biophys J *72*, 1458–1471.

Helwig, M., Vivoli, M., Fricker, L.D., and Lindberg, I. (2011). Regulation of Neuropeptide Processing Enzymes by Catecholamines in Endocrine Cells. Mol Pharmacol *80*, 304–313.

Hewes, R.S., and Taghert, P.H. (2001). Neuropeptides and neuropeptide receptors in the Drosophila melanogaster genome. Genome Res. *11*, 1126–1142.

Holliday, N.D., Michel, M.C., and Cox, H.M. (2004). NPY Receptor Subtypes and Their Signal Transduction. In Neuropeptide Y and Related Peptides, M.C. Michel, ed. (Berlin, Heidelberg: Springer), pp. 45–73.

Holz, R.W., Hlubek, M.D., Sorensen, S.D., Fisher, S.K., Balla, T., Ozaki, S., Prestwich, G.D., Stuenkel, E.L., and Bittner, M.A. (2000). A Pleckstrin Homology Domain Specific for Phosphatidylinositol 4,5-Bisphosphate (PtdIns-4,5-P2) and Fused to Green Fluorescent Protein Identifies Plasma Membrane PtdIns-4,5-P2 as Being Important in Exocytosis. J. Biol. Chem. *275*, 17878–17885.

Hoogenraad, C.C., and Akhmanova, A. (2016). Bicaudal D Family of Motor Adaptors: Linking Dynein Motility to Cargo Binding. Trends in Cell Biology *26*, 327–340.

Hoogstraaten, R.I., van Keimpema, L., Toonen, R.F., and Verhage, M. (2020a). Tetanus insensitive VAMP2 differentially restores synaptic and dense core vesicle fusion in tetanus neurotoxin treated neurons. Sci Rep *10*.

Hoogstraaten, R.I., van Keimpema, L., Toonen, R.F., and Verhage, M. (2020b). (in press). Tetanus insensitive VAMP2 differentially restores synaptic and dense core vesicle fusion. Scientific Reports.

Houy, S., Groffen, A.J., Ziomkiewicz, I., Verhage, M., Pinheiro, P.S., and Sørensen, J.B. (2017). Doc2B acts as a calcium sensor for vesicle priming requiring synaptotagmin-1, Munc13-2 and SNAREs. ELife Sciences *6*, e27000.

Hua, Y., and Scheller, R.H. (2001). Three SNARE complexes cooperate to mediate membrane fusion. PNAS *98*, 8065–8070.

Hui, E., Bai, J., Wang, P., Sugimori, M., Llinas, R.R., and Chapman, E.R. (2005a). Three distinct kinetic groupings of the synaptotagmin family: Candidate sensors for rapid and delayed exocytosis. Proc Natl Acad Sci U S A *102*, 5210–5214.

Hui, E., Bai, J., Wang, P., Sugimori, M., Llinas, R.R., and Chapman, E.R. (2005b). Three distinct kinetic groupings of the synaptotagmin family: Candidate sensors for rapid and delayed exocytosis. Proc Natl Acad Sci U S A *102*, 5210–5214.

Hui, E., Johnson, C.P., Yao, J., Dunning, F.M., and Chapman, E.R. (2009). Synaptotagmin-mediated bending of the target membrane is a critical step in Ca2+-regulated fusion. Cell *138*, 709–721.

Iezzi, M., Kouri, G., Fukuda, M., and Wollheim, C.B. (2004). Synaptotagmin V and IX isoforms control Ca2+-dependent insulin exocytosis. Journal of Cell Science *117*, 3119–3127.

Imig, C., Min, S.-W., Krinner, S., Arancillo, M., Rosenmund, C., Südhof, T.C., Rhee, J., Brose, N., and Cooper, B.H. (2014). The Morphological and Molecular Nature of Synaptic Vesicle Priming at Presynaptic Active Zones. Neuron *84*, 416–431.

Jackman, S.L., and Regehr, W.G. (2017). The Mechanisms and Functions of Synaptic Facilitation. Neuron *94*, 447–464.

Jackman, S.L., Turecek, J., Belinsky, J.E., and Regehr, W.G. (2016a). The calcium sensor synaptotagmin 7 is required for synaptic facilitation. Nature *529*, 88–91.

Jackman, S.L., Turecek, J., Belinsky, J.E., and Regehr, W.G. (2016b). The calcium sensor synaptotagmin 7 is required for synaptic facilitation. Nature *529*, 88–91.

Jahn, R., and Fasshauer, D. (2012). Molecular machines governing exocytosis of synaptic vesicles. Nature *490*, 201.

Jaiswal, J.K., Chakrabarti, S., Andrews, N.W., and Simon, S.M. (2004). Synaptotagmin VII Restricts Fusion Pore Expansion during Lysosomal Exocytosis. PLoS Biol *2*.

Jankowski, J.A., Schroeder, T.J., Ciolkowski, E.L., and Wightman, R.M. (1993). Temporal characteristics of quantal secretion of catecholamines from adrenal medullary cells. Journal of Biological Chemistry *268*, 14694–14700.

Jékely, G. (2013). Global view of the evolution and diversity of metazoan neuropeptide signaling. Proc Natl Acad Sci U S A *110*, 8702–8707.

Kaeser, P.S., and Regehr, W.G. (2014). Molecular Mechanisms for Synchronous, Asynchronous, and Spontaneous Neurotransmitter Release. Annu Rev Physiol *76*, 333–363.

Katayama, H., Yamamoto, A., Mizushima, N., Yoshimori, T., and Miyawaki, A. (2008). GFP-like Proteins Stably Accumulate in Lysosomes. Cell Structure and Function *33*, 1–12.

Ke, B., Oh, E., and Thurmond, D.C. (2007). Doc2beta is a novel Munc18c-interacting partner and positive effector of syntaxin 4-mediated exocytosis. J. Biol. Chem. *282*, 21786–21797.

van Kempen, G.Th.H., vanderLeest, H.T., van den Berg, R.J., Eilers, P., and Westerink, R.H.S. (2011). Three Distinct Modes of Exocytosis Revealed by Amperometry in Neuroendocrine Cells. Biophys J *100*, 968–977.

Kim, T., Gondré-Lewis, M.C., Arnaoutova, I., and Loh, Y.P. (2006). Dense-Core Secretory Granule Biogenesis. Physiology *21*, 124–133.

Knabbe, J., Nassal, J.P., Verhage, M., and Kuner, T. (2018). Secretory vesicle trafficking in awake and anaesthetized mice: differential speeds in axons versus synapses. J Physiol *596*, 3759–3773.

Kolarow, R., Brigadski, T., and Lessmann, V. (2007). Postsynaptic secretion of BDNF and NT-3 from hippocampal neurons depends on calcium calmodulin kinase II signaling and proceeds via delayed fusion pore opening. J. Neurosci. *27*, 10350–10364.

Koob, G.F., and Volkow, N.D. (2010). Neurocircuitry of Addiction. Neuropsychopharmacol *35*, 217–238.

Kormos, V., and Gaszner, B. (2013). Role of neuropeptides in anxiety, stress, and depression: from animals to humans. Neuropeptides *47*, 401–419.

Korteweg, N., Denekamp, F.A., Verhage, M., and Burbach, J.P. (2000). Different spatiotemporal expression of DOC2 genes in the developing rat brain argues for an additional, nonsynaptic role of DOC2B in early development. Eur. J. Neurosci. *12*, 165–171.

Kovac, S., and Walker, M.C. (2013). Neuropeptides in epilepsy. Neuropeptides *47*, 467–475.

Kwon, O.J., Gainer, H., Wray, S., and Chin, H. (1996). Identification of a novel protein containing two C2 domains selectively expressed in the rat brain and kidney. FEBS Lett *378*, 135–139.

Lai, Y., Diao, J., Liu, Y., Ishitsuka, Y., Su, Z., Schulten, K., Ha, T., and Shin, Y.-K. (2013). Fusion pore formation and expansion induced by Ca2+ and synaptotagmin 1. Proc Natl Acad Sci U S A *110*, 1333–1338.

Lai, Y., Choi, U.B., Leitz, J., Rhee, H.J., Lee, C., Altas, B., Zhao, M., Pfuetzner, R.A., Wang, A.L., Brose, N., et al. (2017). Molecular mechanisms of synaptic vesicle priming by Munc13 and Munc18. Neuron *95*, 591-607.e10.

Landry, M., Vila-Porcile, E., Hökfelt, T., and Calas, A. (2003). Differential routing of coexisting neuropeptides in vasopressin neurons. European Journal of Neuroscience *17*, 579–589.

Lee, J., and Littleton, J.T. (2015). Transmembrane tethering of synaptotagmin to synaptic vesicles controls multiple modes of neurotransmitter release. Proc Natl Acad Sci U S A *112*, 3793–3798.

Lee, J.Y., and Schick, M. (2008). Calculation of Free Energy Barriers to the Fusion of Small Vesicles. Biophysical Journal *94*, 1699–1706.

Lee, H.-K., Yang, Y., Su, Z., Hyeon, C., Lee, T.-S., Lee, H.-W., Kweon, D.-H., Shin, Y.-K., and Yoon, T.-Y. (2010). Dynamic Ca2+-dependent stimulation of vesicle fusion by membrane-anchored synaptotagmin 1. Science *328*, 760–763.

Leenders, A.G., Scholten, G., Wiegant, V.M., Da Silva, F.H., and Ghijsen, W.E. (1999). Activity-dependent neurotransmitter release kinetics: correlation with changes in morphological distributions of small and large vesicles in central nerve terminals. Eur. J. Neurosci. *11*, 4269–4277.

Lever, I.J., Bradbury, E.J., Cunningham, J.R., Adelson, D.W., Jones, M.G., McMahon, S.B., Marvizón, J.C.G., and Malcangio, M. (2001). Brain-Derived Neurotrophic Factor Is Released in the Dorsal Horn by Distinctive Patterns of Afferent Fiber Stimulation. J Neurosci *21*, 4469–4477.

Li, C., Ullrich, B., Zhang, J.Z., Anderson, R.G.W., Brose, N., and Südhof, T.C. (1995). Ca 2+ -dependent and -independent activities of neural and non-neural synaptotagmins. Nature *375*, 594–599.

Li, Y.C., Chanaday, N.L., Xu, W., and Kavalali, E.T. (2016). Synaptotagmin-1- and Synaptotagmin-7-Dependent Fusion Mechanisms Target Synaptic Vesicles to Kinetically Distinct Endocytic Pathways. Neuron.

Lingueglia, E., Champigny, G., Lazdunski, M., and Barbry, P. (1995). Cloning of the amiloride-sensitive FMRFamide peptide-gated sodium channel. Nature *378*, 730–733.

Lipscombe, D., Helton, T.D., and Xu, W. (2004). L-type calcium channels: the low down. J Neurophysiol *92*, 2633–2641.

Liu, H., Bai, H., Hui, E., Yang, L., Evans, C.S., Wang, Z., Kwon, S.E., and Chapman, E.R. (2014). Synaptotagmin 7 functions as a Ca2+-sensor for synaptic vesicle replenishment. ELife *3*.

Liu, X., Seven, A.B., Camacho, M., Esser, V., Xu, J., Trimbuch, T., Quade, B., Su, L., Ma, C., Rosenmund, C., et al. (2020). Functional synergy between the Munc13 C-terminal C1 and C2 domains. ELife *5*.

Llinás, R., Sugimori, M., and Silver, R.B. (1992). Microdomains of High Calcium Concentration in a Presynaptic Terminal. Science *256*, 677–679.

Lo, K.Y., Kuzmin, A., Unger, S.M., Petersen, J.D., and Silverman, M.A. (2011). KIF1A is the primary anterograde motor protein required for the axonal transport of dense-core vesicles in cultured hippocampal neurons. Neurosci. Lett. *491*, 168–173.

Ludwig, M., Callahan, M.F., Neumann, I., Landgraf, R., and Morris, M. (1994). Systemic osmotic stimulation increases vasopressin and oxytocin release within the supraoptic nucleus. J Neuroendocrinol *6*, 369–373.

Luo, F., and Südhof, T.C. (2017). Synaptotagmin-7-Mediated Asynchronous Release Boosts High-Fidelity Synchronous Transmission at a Central Synapse. Neuron *94*, 826-839.e3.

Luo, F., Bacaj, T., and Südhof, T.C. (2015). Synaptotagmin-7 Is Essential for Ca2+-Triggered Delayed Asynchronous Release But Not for Ca2+-Dependent Vesicle Priming in Retinal Ribbon Synapses. J. Neurosci. *35*, 11024–11033.

Lynch, K.L., and Martin, T.F.J. (2007). Synaptotagmins I and IX function redundantly in regulated exocytosis but not endocytosis in PC12 cells. J Cell Sci *120*, 617–627.

Lynch, K.L., Gerona, R.R.L., Kielar, D.M., Martens, S., McMahon, H.T., and Martin, T.F.J. (2008). Synaptotagmin-1 Utilizes Membrane Bending and SNARE Binding to Drive Fusion Pore Expansion. Mol. Biol. Cell *19*, 5093–5103.

Ma, C., Su, L., Seven, A.B., Xu, Y., and Rizo, J. (2013). Reconstitution of the vital functions of Munc18 and Munc13 in neurotransmitter release. Science *339*, 421–425.

MacDonald, P.E., Braun, M., Galvanovskis, J., and Rorsman, P. (2006). Release of small transmitters through kiss-and-run fusion pores in rat pancreatic β cells. Cell Metabolism *4*, 283–290.

Mackler, J.M., Drummond, J.A., Loewen, C.A., Robinson, I.M., and Reist, N.E. (2002). The C_2B Ca^{2+}-binding motif of synaptotagmin is required for synaptic transmission *in vivo*. Nature *418*, nature00846.

Maravall, M., Mainen, Z.F., Sabatini, B.L., and Svoboda, K. (2000). Estimating intracellular calcium concentrations and buffering without wavelength ratioing. Biophys J *78*, 2655–2667.

Marder, E. (2012). Neuromodulation of neuronal circuits: back to the future. Neuron *76*, 1–11.

Marquhze, B., Boudier, J.A., Mizuta, M., Inagaki, N., Seine, S., Seagar', M., and de Medecine-Nord, F. Cellular Localization of Synaptotagmin I, II, and Ill mRNAs in the Central Nervous System and Pituitary and Adrenal Glands of the Rat. 12.

Marshall, J., Zhou, X.-Z., Chen, G., Yang, S.-Q., Li, Y., Wang, Y., Zhang, Z.-Q., Jiang, Q., Birnbaumer, L., and Cao, C. (2018). Antidepression action of BDNF requires and is mimicked by Gαi1/3 expression in the hippocampus. Proc. Natl. Acad. Sci. U.S.A. *115*, E3549–E3558.

Martin, T.F.J. (2015). PI(4,5)P2-binding effector proteins for vesicle exocytosis. Biochim Biophys Acta *1851*, 785–793.

Martinez, I., Chakrabarti, S., Hellevik, T., Morehead, J., Fowler, K., and Andrews, N.W. (2000). Synaptotagmin VII Regulates Ca2+-Dependent Exocytosis of Lysosomes in Fibroblasts. The Journal of Cell Biology *148*, 1141–1150.

Matsuda, N., Lu, H., Fukata, Y., Noritake, J., Gao, H., Mukherjee, S., Nemoto, T., Fukata, M., and Poo, M. (2009). Differential Activity-Dependent Secretion of Brain-Derived Neurotrophic Factor from Axon and Dendrite. J Neurosci *29*, 14185–14198.

Matthew, W.D., Tsavaler, L., and Reichardt, L.F. (1981). Identification of a synaptic vesicle-specific membrane protein with a wide distribution in neuronal and neurosecretory tissue. J. Cell Biol. *91*, 257–269.

Maximov, A., and Südhof, T.C. (2005). Autonomous Function of Synaptotagmin 1 in Triggering Synchronous Release Independent of Asynchronous Release. Neuron *48*, 547–554.

Maximov, A., Lao, Y., Li, H., Chen, X., Rizo, J., Sørensen, J.B., and Südhof, T.C. (2008). Genetic analysis of synaptotagmin-7 function in synaptic vesicle exocytosis. PNAS *105*, 3986–3991.

McAdam, R.L., Varga, K.T., Jiang, Z., Young, F.B., Blandford, V., McPherson, P.S., Gong, L.-W., and Sossin, W.S. (2015). The juxtamembrane region of synaptotagmin 1 interacts with dynamin 1 and regulates vesicle fission during compensatory endocytosis in endocrine cells. J. Cell. Sci. *128*, 2229–2235.

McMahon, H.T., Kozlov, M.M., and Martens, S. (2010). Membrane Curvature in Synaptic Vesicle Fusion and Beyond. Cell *140*, 601–605.

Merighi, A. (2018). Costorage of High Molecular Weight Neurotransmitters in Large Dense Core Vesicles of Mammalian Neurons. Front. Cell. Neurosci. *12*.

Meyer-Lindenberg, A., Domes, G., Kirsch, P., and Heinrichs, M. (2011). Oxytocin and vasopressin in the human brain: social neuropeptides for translational medicine. Nat Rev Neurosci *12*, 524–538.

Micheva, K.D., Holz, R.W., and Smith, S.J. (2001). Regulation of presynaptic phosphatidylinositol 4,5-biphosphate by neuronal activity. J Cell Biol *154*, 355–368.

Min, D., Kim, K., Hyeon, C., Hoon Cho, Y., Shin, Y.-K., and Yoon, T.-Y. (2013). Mechanical unzipping and rezipping of a single SNARE complex reveals hysteresis as a force-generating mechanism. Nat Commun *4*, 1705.

Miranda, M., Morici, J.F., Zanoni, M.B., and Bekinschtein, P. (2019). Brain-Derived Neurotrophic Factor: A Key Molecule for Memory in the Healthy and the Pathological Brain. Front. Cell. Neurosci. *13*.

Mittelsteadt, T., Seifert, G., Alvárez-Barón, E., Steinhäuser, C., Becker, A.J., and Schoch, S. (2009). Differential mRNA expression patterns of the synaptotagmin gene family in the rodent brain. J. Comp. Neurol. *512*, 514–528.

Mohrman, R., Wit, H. de, Verhage, M., Neher, E., and Sørensen, J.B. (2010). Fast Vesicle Fusion in Living Cells Requires at Least Three SNARE Complexes. Science *330*, 502–505.

Monterrat, C., Boal, F., Grise, F., Hémar, A., and Lang, J. (2006). Synaptotagmin 8 is expressed both as a calcium-insensitive soluble and membrane protein in neurons, neuroendocrine and endocrine cells. Biochimica et Biophysica Acta (BBA) - Molecular Cell Research *1763*, 73–81.

Monterrat, C., Grise, F., Benassy, M.N., Hémar, A., and Lang, J. (2007). The calcium-sensing protein synaptotagmin 7 is expressed on different endosomal compartments in endocrine, neuroendocrine cells or neurons but not on large dense core vesicles. Histochem Cell Biol *127*, 625–632.

Moughamian, A.J., and Holzbaur, E.L.F. (2012). Synaptic Vesicle Distribution by Conveyor Belt. Cell *148*, 849–851.

Mutch, S., Kensel-Hammes, P., Gadd, J., Fujimoto, B., Allen, Schiro, P., Lorenz, R., Kuyper, C., Kuo, J., Bajjalieh, S., et al. (2011). Protein quantification at the single vesicle level reveals that a subset of synaptic vesicle proteins are trafficked with high precision. J Neurosci *31*, 1461–1470.

Nagai, T., Ibata, K., Park, E.S., Kubota, M., Mikoshiba, K., and Miyawaki, A. (2002). A variant of yellow fluorescent protein with fast and efficient maturation for cell-biological applications. Nat. Biotechnol. *20*, 87–90.

Nahorski, M.S., Borner, G.H.H., Shaikh, S.S., Davies, A.K., Al-Gazali, L., Antrobus, R., and Woods, C.G. (2018). Clathrin heavy chain 22 contributes to the control of neuropeptide degradation and secretion during neuronal development. Scientific Reports *8*, 2340.

Naldini, L., Blömer, U., Gage, F.H., Trono, D., and Verma, I.M. (1996). Efficient transfer, integration, and sustained long-term expression of the transgene in adult rat brains injected with a lentiviral vector. PNAS *93*, 11382–11388.

Neher, E., and Sakaba, T. (2008). Multiple Roles of Calcium Ions in the Regulation of Neurotransmitter Release. Neuron *59*, 861–872.

Neumann, I., Douglas, A.J., Pittman, Q.J., Russell, J.A., and Landgraf, R. (1996). Oxytocin released within the supraoptic nucleus of the rat brain by positive feedback action is involved in parturition-related events. J. Neuroendocrinol. *8*, 227–233.

Nguyen, A.D., Herzog, H., and Sainsbury, A. (2011). Neuropeptide Y and peptide YY: important regulators of energy metabolism. Curr Opin Endocrinol Diabetes Obes *18*, 56–60.

Nibuya, M., Morinobu, S., and Duman, R.S. (1995). Regulation of BDNF and trkB mRNA in rat brain by chronic electroconvulsive seizure and antidepressant drug treatments. J. Neurosci. *15*, 7539–7547.

Nir, S., Wilschut, J., and Bentz, J. (1982). The rate of fusion of phospholipid vesicles and the role of bilayer curvature. Biochimica et Biophysica Acta (BBA) - Biomembranes *688*, 275–278.

Nishiki, T., and Augustine, G.J. (2004). Dual Roles of the C2B Domain of Synaptotagmin I in Synchronizing Ca2+-Dependent Neurotransmitter Release. J. Neurosci. *24*, 8542–8550.

Ogren, S.O., Kuteeva, E., Elvander-Tottie, E., and Hökfelt, T. (2010). Neuropeptides in learning and memory processes with focus on galanin. Eur. J. Pharmacol. *626*, 9–17.

Ohki, S. (1984). Effects of divalent cations, temperature, osmotic pressure gradient, and vesicle curvature on phosphatidylserine vesicle fusion. J Membr Biol *77*, 265–275.

Olivera, B.M., Miljanich, G.P., Ramachandran, J., and Adams, M.E. (1994). Calcium channel diversity and neurotransmitter release: the omega-conotoxins and omega-agatoxins. Annu Rev Biochem *63*, 823–867.

Padamsey, Z., McGuinness, L., Bardo, S.J., Reinhart, M., Tong, R., Hedegaard, A., Hart, M.L., and Emptage, N.J. (2017). Activity-Dependent Exocytosis of Lysosomes Regulates the Structural Plasticity of Dendritic Spines. Neuron *93*, 132–146.

Pang, Z.P., Melicoff, E., Padgett, D., Liu, Y., Teich, A.F., Dickey, B.F., Lin, W., Adachi, R., and Südhof, T.C. (2006). Synaptotagmin-2 Is Essential for Survival and Contributes to Ca2+ Triggering of Neurotransmitter Release in Central and Neuromuscular Synapses. J. Neurosci. *26*, 13493–13504.

Pang, Z.P., Bacaj, T., Yang, X., Zhou, P., Xu, W., and Südhof, T.C. (2011). Doc2 supports spontaneous synaptic transmission by a Ca(2+)-independent mechanism. Neuron *70*, 244–251.

Perin, M.S., Fried, V.A., Mignery, G.A., Jahn, R., and Südhof, T.C. (1990). Phospholipid binding by a synaptic vesicle protein homologous to the regulatory region of protein kinase C. Nature *345*, 260–263.

Perin, M.S., Brose, N., Jahn, R., and Südhof, T.C. (1991). Domain structure of synaptotagmin (p65). J. Biol. Chem. *266*, 623–629.

Persoon, C.M., Moro, A., Nassal, J.P., Farina, M., Broeke, J.H., Arora, S., Dominguez, N., Weering, J.R. van, Toonen, R.F., and Verhage, M. (2018). Pool size estimations for dense-core vesicles in mammalian CNS neurons. The EMBO Journal e99672.

Persoon, C.M., Hoogstraaten, R.I., Nassal, J.P., van Weering, J.R.T., Kaeser, P.S., Toonen, R.F., and Verhage, M. (2019). The RAB3-RIM Pathway Is Essential for the Release of Neuromodulators. Neuron *104*, 1065-1080.e12.

van den Pol, A.N. (2012). Neuropeptide transmission in brain circuits. Neuron *76*, 98–115.

Pons-Vizcarra, M. (2020). Resolving the molecular architecture of secretory vesicles and their fusion sites.

Poo, M. (2001). Neurotrophins as synaptic modulators. Nature Reviews Neuroscience *2*, 24.

Poser, C. von, Ichtchenko, K., Shao, X., Rizo, J., and Südhof, T.C. (1997). The Evolutionary Pressure to Inactivate A SUBCLASS OF SYNAPTOTAGMINS WITH AN AMINO ACID SUBSTITUTION THAT ABOLISHES Ca2+ BINDING. J. Biol. Chem. *272*, 14314–14319.

Poskanzer, K.E., Marek, K.W., Sweeney, S.T., and Davis, G.W. (2003). Synaptotagmin I is necessary for compensatory synaptic vesicle endocytosis in vivo. Nature *426*, 559–563.

Purohit, Y., and Grosman, C. (2006). Estimating Binding Affinities of the Nicotinic Receptor for Low-efficacy Ligands Using Mixtures of Agonists and Two-dimensional Concentration–Response Relationships. J Gen Physiol *127*, 719–735.

Rao, T.C., Passmore, D.R., Peleman, A.R., Das, M., Chapman, E.R., and Anantharam, A. (2014a). Distinct fusion properties of synaptotagmin-1 and synaptotagmin-7 bearing dense core granules. Mol Biol Cell *25*, 2416–2427.

Rao, T.C., Passmore, D.R., Peleman, A.R., Das, M., Chapman, E.R., and Anantharam, A. (2014b). Distinct fusion properties of synaptotagmin-1 and synaptotagmin-7 bearing dense core granules. Mol Biol Cell *25*, 2416–2427.

Rao, T.C., Passmore, D.R., Peleman, A.R., Das, M., Chapman, E.R., and Anantharam, A. (2014c). Distinct fusion properties of synaptotagmin-1 and synaptotagmin-7 bearing dense core granules. Mol Biol Cell *25*, 2416–2427.

Rao, T.C., Santana Rodriguez, Z., Bradberry, M.M., Ranski, A.H., Dahl, P.J., Schmidtke, M.W., Jenkins, P.M., Axelrod, D., Chapman, E.R., Giovannucci, D.R., et al. (2017). Synaptotagmin isoforms confer distinct activation kinetics and dynamics to chromaffin cell granules. J Gen Physiol *149*, 763–780.

Reddy, A., Caler, E.V., and Andrews, N.W. (2001). Plasma Membrane Repair Is Mediated by Ca2+-Regulated Exocytosis of Lysosomes. Cell *106*, 157–169.

Regehr, W.G. (2012). Short-Term Presynaptic Plasticity. Cold Spring Harb Perspect Biol *4*.

Reim, K., Mansour, M., Varoqueaux, F., McMahon, H.T., Südhof, T.C., Brose, N., and Rosenmund, C. (2001). Complexins Regulate a Late Step in Ca2+-Dependent Neurotransmitter Release. Cell *104*, 71–81.

Rescher, U., and Gerke, V. (2004). Annexins – unique membrane binding proteins with diverse functions. Journal of Cell Science *117*, 2631–2639.

Richmond, J.E., Weimer, R.M., and Jorgensen, E.M. (2001). An open form of syntaxin bypasses the requirement for UNC-13 in vesicle priming. Nature *412*, 338–341.

Robinson, I.M., Ranjan, R., and Schwarz, T.L. (2002). Synaptotagmins I and IV promote transmitter release independently of Ca(2+) binding in the C(2)A domain. Nature *418*, 336–340.

Roper, L.K., Briguglio, J.S., Evans, C.S., Jackson, M.B., and Chapman, E.R. (2015). Sex-specific regulation of follicle-stimulating hormone secretion by synaptotagmin 9. Nat Commun *6*, 1–10.

Rose, J.B., Crews, L., Rockenstein, E., Adame, A., Mante, M., Hersh, L.B., Gage, F.H., Spencer, B., Potkar, R., Marr, R.A., et al. (2009). Neuropeptide Y fragments derived from neprilysin processing are neuroprotective in a transgenic model of Alzheimer's disease. J. Neurosci. *29*, 1115–1125.

Sabatier, N., Caquineau, C., Dayanithi, G., Bull, P., Douglas, A.J., Guan, X.M.M., Jiang, M., Van der Ploeg, L., and Leng, G. (2003). Alpha-melanocyte-stimulating hormone stimulates oxytocin release from the dendrites of hypothalamic neurons while inhibiting oxytocin release from their terminals in the neurohypophysis. J Neurosci *23*, 10351–10358.

Sabatini, B.L., and Regehr, W.G. (1996). Timing of neurotransmission at fast synapses in the mammalian brain. Nature *384*, 170–172.

Salio, C., Averill, S., Priestley, J.V., and Merighi, A. (2007). Costorage of BDNF and neuropeptides within individual dense-core vesicles in central and peripheral neurons. Dev Neurobiol *67*, 326–338.

Saw, N.M.N., Kang, S.-Y.A., Parsaud, L., Han, G.A., Jiang, T., Grzegorczyk, K., Surkont, M., Sun-Wada, G.-H., Wada, Y., Li, L., et al. (2011). Vacuolar H+-ATPase subunits Voa1 and Voa2 cooperatively regulate secretory vesicle acidification, transmitter uptake, and storage. Mol Biol Cell *22*, 3394–3409.

Schikorski, T., and Stevens, C.F. (1997). Quantitative Ultrastructural Analysis of Hippocampal Excitatory Synapses. J Neurosci *17*, 5858–5867.

Schmitz, S.K., Hjorth, J.J.J., Joemai, R.M.S., Wijntjes, R., Eijgenraam, S., de Bruijn, P., Georgiou, C., de Jong, A.P.H., van Ooyen, A., Verhage, M., et al. (2011). Automated analysis of neuronal morphology, synapse number and synaptic recruitment. J. Neurosci. Methods *195*, 185–193.

Schonn, J.-S., Maximov, A., Lao, Y., Südhof, T.C., and Sørensen, J.B. (2008). Synaptotagmin-1 and -7 are functionally overlapping Ca2+ sensors for exocytosis in adrenal chromaffin cells. PNAS *105*, 3998–4003.

Schwaller, B. (2010). Cytosolic Ca2+ buffers. Cold Spring Harb Perspect Biol *2*, a004051.

Schwartz, M.W., Woods, S.C., Porte, D., Seeley, R.J., and Baskin, D.G. (2000). Central nervous system control of food intake. Nature *404*, 661–671.

Segovia, M., Alés, E., Montes, M.A., Bonifas, I., Jemal, I., Lindau, M., Maximov, A., Südhof, T.C., and Toledo, G.A. de (2010). Push-and-pull regulation of the fusion pore by synaptotagmin-7. PNAS *107*, 19032–19037.

Shao, X., Li, C., Fernandez, I., Zhang, X., Südhof, T.C., and Rizo, J. (1997). Synaptotagmin–Syntaxin Interaction: The C2 Domain as a Ca2+-Dependent Electrostatic Switch. Neuron *18*, 133–142.

Shen, W., Wang, Q.-W., Liu, Y.-N., Marchetto, M.C., Linker, S., Lu, S.-Y., Chen, Y., Liu, C., Guo, C., Xing, Z., et al. (2020). Synaptotagmin-7 is a key factor for bipolar-like behavioral abnormalities in mice. PNAS.

Shillcock, J.C., and Lipowsky, R. (2005). Tension-induced fusion of bilayer membranes and vesicles. Nature Materials *4*, 225–228.

Shimojo, M., Courchet, J., Pieraut, S., Torabi-Rander, N., Sando, R., Polleux, F., and Maximov, A. (2015). SNAREs Controlling Vesicular Release of BDNF and Development of Callosal Axons. Cell Rep *11*, 1054–1066.

Shin, O.-H., Xu, J., Rizo, J., and Südhof, T.C. (2009). Differential but convergent functions of Ca2+ binding to synaptotagmin-1 C2 domains mediate neurotransmitter release. Proc. Natl. Acad. Sci. U.S.A. *106*, 16469–16474.

Sinha, R., Ahmed, S., Jahn, R., and Klingauf, J. (2011). Two synaptobrevin molecules are sufficient for vesicle fusion in central nervous system synapses. Proc Natl Acad Sci U S A *108*, 14318–14323.

Smith, S.J., Sümbül, U., Graybuck, L., Collman, F., Seshamani, S., Gala, R., Gliko, O., Elabbady, L., Miller, J.A., Bakken, T., et al. (2019). Single-Cell Transcriptomic Evidence for Dense Intracortical Neuropeptide Networks. BioRxiv 519694.

Sørensen, J.B., Wiederhold, K., Müller, E.M., Milosevic, I., Nagy, G., de Groot, B.L., Grubmüller, H., and Fasshauer, D. (2006). Sequential N- to C-terminal SNARE complex assembly drives priming and fusion of secretory vesicles. EMBO J *25*, 955–966.

Stein, A., Radhakrishnan, A., Riedel, D., Fasshauer, D., and Jahn, R. (2007). Synaptotagmin activates membrane fusion through a Ca 2+ -dependent trans interaction with phospholipids. Nat Struct Mol Biol *14*, 904–911.

Stucchi, R., Plucińska, G., Hummel, J.J.A., Zahavi, E.E., Guerra San Juan, I., Klykov, O., Scheltema, R.A., Altelaar, A.F.M., and Hoogenraad, C.C. (2018). Regulation of KIF1A-Driven Dense Core Vesicle Transport: Ca2+/CaM Controls DCV Binding and Liprin-α/TANC2 Recruits DCVs to Postsynaptic Sites. Cell Reports *24*, 685–700.

Südhof, T.C. (2002). Synaptotagmins: Why So Many? J. Biol. Chem. *277*, 7629–7632.

Südhof, T.C., and Rothman, J.E. (2009). Membrane Fusion: Grappling with SNARE and SM Proteins. Science *323*, 474–477.

Sugita, S., Han, W., Butz, S., Liu, X., Fernández-Chacón, R., Lao, Y., and Südhof, T.C. (2001). Synaptotagmin VII as a Plasma Membrane Ca2+ Sensor in Exocytosis. Neuron *30*, 459–473.

Sugita, S., Shin, O.-H., Han, W., Lao, Y., and Südhof, T.C. (2002). Synaptotagmins form a hierarchy of exocytotic Ca2+ sensors with distinct Ca2+ affinities. EMBO J *21*, 270–280.

Sutton, R.B., Davletov, B.A., Berghuis, A.M., Sudhof, T.C., and Sprang, S.R. (1995). Structure of the first C2 domain of synaptotagmin I: A novel Ca2+/phospholipid-binding fold. Cell *80*, 929–938.

Takamori, S., Holt, M., Stenius, K., Lemke, E.A., Grønborg, M., Riedel, D., Urlaub, H., Schenck, S., Brügger, B., Ringler, P., et al. (2006). Molecular Anatomy of a Trafficking Organelle. Cell *127*, 831–846.

Tang, J., Maximov, A., Shin, O.-H., Dai, H., Rizo, J., and Südhof, T.C. (2006). A Complexin/Synaptotagmin 1 Switch Controls Fast Synaptic Vesicle Exocytosis. Cell *126*, 1175–1187.

Taoufiq, Z., Ninov, M., Villar-Briones, A., Wang, H.-Y., Sasaki, T., Roy, M.C., Beauchain, F., Mori, Y., Yoshida, T., Takamori, S., et al. (2020). Hidden proteome of synaptic vesicles in the mammalian brain. Proc Natl Acad Sci USA *117*, 33586–33596.

Tasan, R.O., Verma, D., Wood, J., Lach, G., Hörmer, B., de Lima, T.C.M., Herzog, H., and Sperk, G. (2016). The role of Neuropeptide Y in fear conditioning and extinction. Neuropeptides *55*, 111–126.

Tawfik, B., Martins, J.S., Houy, S., Imig, C., Pinheiro, P.S., Wojcik, S.M., Brose, N., Cooper, B.H., and Sørensen, J.B. (2020). Synaptotagmin-7 places dense-core vesicles at the cell membrane to promote Munc13-2- and Ca2+-dependent priming. BioRxiv 2020.11.02.365478.

Tooze, S.A., Flatmark, T., Tooze, J., and Huttner, W.B. (1991). Characterization of the immature secretory granule, an intermediate in granule biogenesis. J Cell Biol *115*, 1491–1503.

Topalidou, I., Cattin-Ortolá, J., Pappas, A.L., Cooper, K., Merrihew, G.E., MacCoss, M.J., and Ailion, M. (2016). The EARP Complex and Its Interactor EIPR-1 Are Required for Cargo Sorting to Dense-Core Vesicles. PLOS Genetics *12*, e1006074.

Topol, E.J., Bousser, M.-G., Fox, K.A., Creager, M.A., Despres, J.-P., Easton, J.D., Hamm, C.W., Montalescot, G., Steg, P.G., Pearson, T.A., et al. (2010). Rimonabant for prevention of cardiovascular events (CRESCENDO): a randomised, multicentre, placebo-controlled trial. The Lancet *376*, 517–523.

de la Torre, B.G., and Albericio, F. (2020). Peptide Therapeutics 2.0. Molecules *25*, 2293.

Trimbuch, T., Xu, J., Flaherty, D., Tomchick, D.R., Rizo, J., and Rosenmund, C. (2014). Re-examining how complexin inhibits neurotransmitter release. ELife *3*.

Turecek, J., and Regehr, W.G. (2018). Synaptotagmin 7 Mediates Both Facilitation and Asynchronous Release at Granule Cell Synapses. J. Neurosci. *38*, 3240–3251.

Turecek, J., and Regehr, W.G. (2019). Neuronal Regulation of Fast Synaptotagmin Isoforms Controls the Relative Contributions of Synchronous and Asynchronous Release. Neuron.

Turecek, J., Jackman, S.L., and Regehr, W.G. (2017). Synaptotagmin 7 confers frequency invariance onto specialized depressing synapses. Nature *551*, 503.

Ubach, J., Zhang, X., Shao, X., Südhof, T.C., and Rizo, J. (1998). Ca2+ binding to synaptotagmin: how many Ca2+ ions bind to the tip of a C2-domain? EMBO J *17*, 3921–3930.

Verhage, M., McMahon, H.T., Ghijsen, W.E.J.M., Boomsma, Frans., Scholten, G., Wiegant, V.M., and Nicholls, D.G. (1991). Differential release of amino acids, neuropeptides, and catecholamines from isolated nerve terminals. Neuron *6*, 517–524.

Verhage, M., Vries, K.J. de, Røshol, H., Burbach, J.P.H., Gispen, W.H., and Südhof, T.C. (1997). DOC2 Proteins in Rat Brain: Complementary Distribution and Proposed Function as Vesicular Adapter Proteins in Early Stages of Secretion. Neuron *18*, 453–461.

Vevea, J.D., Kusick, G.F., Chen, E., Courtney, K.C., and Watanabe, S. (2021). Synaptotagmin 7 is enriched at the plasma membrane through γ-secretase processing to promote vesicle docking and control synaptic plasticity in mouse hippocampal neurons. 52.

Vicario-Abejón, C., Owens, D., McKay, R., and Segal, M. (2002). Role of neurotrophins in central synapse formation and stabilization. Nat Rev Neurosci *3*, 965–974.

Virmani, T., Han, W., Liu, X., Südhof, T.C., and Kavalali, E.T. (2003). Synaptotagmin 7 splice variants differentially regulate synaptic vesicle recycling. EMBO J *22*, 5347–5357.

Voets, T., Moser, T., Lund, P.-E., Chow, R.H., Geppert, M., Südhof, T.C., and Neher, E. (2001). Intracellular calcium dependence of large dense-core vesicle exocytosis in the absence of synaptotagmin I. Proc Natl Acad Sci U S A *98*, 11680–11685.

Vrljic, M., Strop, P., Ernst, J.A., Sutton, R.B., Chu, S., and Brunger, A.T. (2010). Molecular mechanism of the synaptotagmin-SNARE interaction in Ca2+-triggered vesicle fusion. Nat. Struct. Mol. Biol. *17*, 325–331.

Vukoja, A., Rey, U., Petzoldt, A.G., Ott, C., Vollweiter, D., Quentin, C., Puchkov, D., Reynolds, E., Lehmann, M., Hohensee, S., et al. (2018). Presynaptic Biogenesis Requires Axonal Transport of Lysosome-Related Vesicles. Neuron.

Walch-Solimena, C., Takei, K., Marek, K.L., Midyett, K., Sudhof, T.C., Camilli, P.D., and Jahn, R. (1993). Synaptotagmin: a membrane constituent of neuropeptide-containing large dense-core vesicles. J. Neurosci. *13*, 3895–3903.

Walter, A.M., Groffen, A.J., Sørensen, J.B., and Verhage, M. (2011). Multiple Ca2+ sensors in secretion: teammates, competitors or autocrats? Trends in Neurosciences *34*, 487–497.

Wang, C.-T., Grishanin, R., Earles, C.A., Chang, P.Y., Martin, T.F.J., Chapman, E.R., and Jackson, M.B. (2001). Synaptotagmin Modulation of Fusion Pore Kinetics in Regulated Exocytosis of Dense-Core Vesicles. Science *294*, 1111–1115.

Wang, C.-T., Lu, J.-C., Bai, J., Chang, P.Y., Martin, T.F.J., Chapman, E.R., and Jackson, M.B. (2003). Different domains of synaptotagmin control the choice between kiss-and-run and full fusion. Nature *424*, 943.

Wang, C.-T., Bai, J., Chang, P.Y., Chapman, E.R., and Jackson, M.B. (2006). Synaptotagmin–Ca2+ triggers two sequential steps in regulated exocytosis in rat PC12 cells: fusion pore opening and fusion pore dilation. J Physiol *570*, 295–307.

Wang, P., Chicka, M.C., Bhalla, A., Richards, D.A., and Chapman, E.R. (2005). Synaptotagmin VII Is Targeted to Secretory Organelles in PC12 Cells, Where It Functions as a High-Affinity Calcium Sensor. Mol Cell Biol *25*, 8693–8702.

Wang, Q.-W., Lu, S.-Y., Liu, Y.-N., Chen, Y., Wei, H., Shen, W., Chen, Y.-F., Fu, C.-L., Wang, Y.-H., Dai, A., et al. (2020). Synaptotagmin-7 deficiency induces mania-like behavioral abnormalities through attenuating GluN2B activity. PNAS *117*, 31438–31447.

Wang, Z., Liu, H., Gu, Y., and Chapman, E.R. (2011). Reconstituted synaptotagmin I mediates vesicle docking, priming, and fusion. J Cell Biol *195*, 1159–1170.

Weber, J.P., Toft-Bertelsen, T.L., Mohrmann, R., Delgado-Martinez, I., and Sørensen, J.B. (2014). Synaptotagmin-7 Is an Asynchronous Calcium Sensor for Synaptic Transmission in Neurons Expressing SNAP-23. PLOS ONE *9*, e114033.

Wen, H., Linhoff, M.W., McGinley, M.J., Li, G.-L., Corson, G.M., Mandel, G., and Brehm, P. (2010). Distinct roles for two synaptotagmin isoforms in synchronous and asynchronous transmitter release at zebrafish neuromuscular junction. Proc. Natl. Acad. Sci. U.S.A. *107*, 13906–13911.

Westfall, T.C., Naes, L., Gardner, A., and Yang, C.-L. (2006). Neuropeptide Y induced attenuation of catecholamine synthesis in the rat mesenteric arterial bed. J. Cardiovasc. Pharmacol. *47*, 723–728.

Whim, M.D. (2006). Near Simultaneous Release of Classical and Peptide Cotransmitters from Chromaffin Cells. J Neurosci *26*, 6637–6642.

Wienisch, M., and Klingauf, J. (2006). Vesicular proteins exocytosed and subsequently retrieved by compensatory endocytosis are nonidentical. Nature Neuroscience *9*, 1019.

Wit, J. de, Toonen, R.F., and Verhage, M. (2009). Matrix-Dependent Local Retention of Secretory Vesicle Cargo in Cortical Neurons. J. Neurosci. *29*, 23–37.

de Wit, H., Walter, A.M., Milosevic, I., Gulyás-Kovács, A., Riedel, D., Sørensen, J.B., and Verhage, M. (2009). Synaptotagmin-1 Docks Secretory Vesicles to Syntaxin-1/SNAP-25 Acceptor Complexes. Cell *138*, 935–946.

Wolfes, A.C., and Dean, C. (2020). The diversity of synaptotagmin isoforms. Current Opinion in Neurobiology *63*, 198–209.

Wong, M.Y., Zhou, C., Shakiryanova, D., Lloyd, T.E., Deitcher, D.L., and Levitan, E.S. (2012). Neuropeptide Delivery to Synapses by Long-Range Vesicle Circulation and Sporadic Capture. Cell *148*, 1029–1038.

Wong, Y.-H., Lee, C.-M., Xie, W., Cui, B., and Poo, M. (2015). Activity-dependent BDNF release via endocytic pathways is regulated by synaptotagmin-6 and complexin. PNAS *112*, E4475–E4484.

Wu, D., Bacaj, T., Morishita, W., Goswami, D., Arendt, K.L., Xu, W., Chen, L., Malenka, R.C., and Südhof, T.C. (2017a). Postsynaptic synaptotagmins mediate AMPA receptor exocytosis during LTP. Nature *544*, 316–321.

Wu, Z., Bello, O.D., Thiyagarajan, S., Auclair, S.M., Vennekate, W., Krishnakumar, S.S., O'Shaughnessy, B., and Karatekin, E. (2017b). Dilation of fusion pores by crowding of SNARE proteins. ELife *6*, e22964.

Wu, Z., Dharan, N., Thiyagarajan, S., O'Shaughnessy, B., and Karatekin, E. (2019). The neuronal calcium sensor Synaptotagmin-1 and SNARE proteins cooperate to dilate fusion pores mechanically. BioRxiv 623827.

Xia, X., Lessmann, V., and Martin, T.F.J. (2009). Imaging of evoked dense-core-vesicle exocytosis in hippocampal neurons reveals long latencies and kiss-and-run fusion events. J Cell Sci *122*, 75–82.

Xu, J., Mashimo, T., and Südhof, T.C. (2007). Synaptotagmin-1, -2, and -9: Ca2+ Sensors for Fast Release that Specify Distinct Presynaptic Properties in Subsets of Neurons. Neuron *54*, 567–581.

Xu, J., Pang, Z.P., Shin, O.-H., and Südhof, T.C. (2009). Synaptotagmin-1 functions as the Ca2+-sensor for spontaneous release. Nat Neurosci *12*, 759–766.

Xu, W., Morishita, W., Buckmaster, P.S., Pang, Z.P., Malenka, R.C., and Südhof, T.C. (2012). Distinct Neuronal Coding Schemes in Memory Revealed by Selective Erasure of Fast Synchronous Synaptic Transmission. Neuron *73*, 990–1001.

Xue, R., Gaffaney, J.D., and Chapman, E.R. (2015). Structural elements that underlie Doc2β function during asynchronous synaptic transmission. Proc Natl Acad Sci U S A *112*, E4316–E4325.

Yáñez, M., Gil-Longo, J., and Campos-Toimil, M. (2012). Calcium Binding Proteins. In Calcium Signaling, Md.S. Islam, ed. (Dordrecht: Springer Netherlands), pp. 461–482.

Yao, J., Gaffaney, J.D., Kwon, S.E., and Chapman, E.R. (2011). Doc2 is a Ca2+ sensor required for asynchronous neurotransmitter release. Cell *147*, 666–677.

Yao, J., Kwon, S.E., Gaffaney, J.D., Dunning, F.M., and Chapman, E.R. (2012a). Uncoupling the roles of synaptotagmin I during endo- and exocytosis of synaptic vesicles. Nature Neuroscience *15*, 243.

Yao, L.-H., Rao, Y., Varga, K., Wang, C.-Y., Xiao, P., Lindau, M., and Gong, L.-W. (2012b). Synaptotagmin 1 Is Necessary for the Ca2+ Dependence of Clathrin-Mediated Endocytosis. J. Neurosci. *32*, 3778–3785.

Zaben, M.J., and Gray, W.P. (2013). Neuropeptides and hippocampal neurogenesis. Neuropeptides *47*, 431–438.

Zeisel, A., Muñoz-Manchado, A.B., Codeluppi, S., Lönnerberg, P., Manno, G.L., Juréus, A., Marques, S., Munguba, H., He, L., Betsholtz, C., et al. (2015). Cell types in the mouse cortex and hippocampus revealed by single-cell RNA-seq. Science *347*, 1138–1142.

Zhang, G., Bai, H., Zhang, H., Dean, C., Wu, Q., Li, J., Guariglia, S., Meng, Q., and Cai, D. (2011a). Neuropeptide Exocytosis Involving Synaptotagmin-4 and Oxytocin in Hypothalamic Programming of Body Weight and Energy Balance. Neuron *69*, 523–535.

Zhang, J.Z., Davletov, B.A., Südhof, T.C., and Anderson, R.G.W. (1994). Synaptotagmin I is a high affinity receptor for clathrin AP-2: Implications for membrane recycling. Cell *78*, 751–760.

Zhang, Q., Liu, B., Wu, Q., Liu, B., Li, Y., Sun, S., Wang, Y., Wu, X., Chai, Z., Jiang, X., et al. (2019). Differential Co-release of Two Neurotransmitters from a Vesicle Fusion Pore in Mammalian Adrenal Chromaffin Cells. Neuron *102*, 173-183.e4.

Zhang, X., Rizo, J., and Südhof, T.C. (1998). Mechanism of Phospholipid Binding by the C2A-Domain of Synaptotagmin I. Biochemistry *37*, 12395–12403.

Zhang, Z., Bhalla, A., Dean, C., Chapman, E.R., and Jackson, M.B. (2009). Synaptotagmin IV: a multifunctional regulator of peptidergic nerve terminals. Nat Neurosci *12*, 163–171.

Zhang, Z., Hui, E., Chapman, E.R., and Jackson, M.B. (2010). Regulation of Exocytosis and Fusion Pores by Synaptotagmin-Effector Interactions. Mol Biol Cell *21*, 2821–2831.

Zhang, Z., Wu, Y., Wang, Z., Dunning, F.M., Rehfuss, J., Ramanan, D., Chapman, E.R., and Jackson, M.B. (2011b). Release mode of large and small dense-core vesicles specified by different synaptotagmin isoforms in PC12 cells. Mol Biol Cell *22*, 2324–2336.

Zhao, B., Wang, H.-B., Lu, Y.-J., Hu, J.-W., Bao, L., and Zhang, X. (2011). Transport of receptors, receptor signaling complexes and ion channels via neuropeptide-secretory vesicles. Cell Res *21*, 741–753.

Zhu, D., Zhou, W., Liang, T., Yang, F., Zhang, R.-Y., Wu, Z.-X., and Xu, T. (2007). Synaptotagmin I and IX function redundantly in controlling fusion pore of large dense core vesicles. Biochemical and Biophysical Research Communications *361*, 922–927.

Zucker, R.S., and Fogelson, A.L. (1986). Relationship between transmitter release and presynaptic calcium influx when calcium enters through discrete channels. PNAS *83*, 3032–3036.